Chapter-4

Synthesis, Resolution and Application of Cyclohexanol derivatives in Enantiomeric Recognition

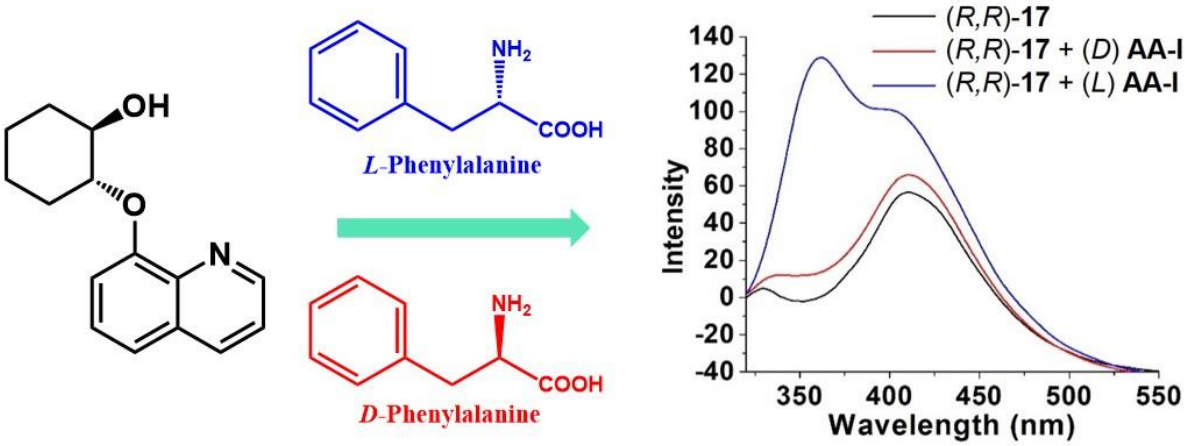

Range of Analytes: 24 examples

NMR: *α-functional acids, Phosphoric acids, Binols*

Fluorescence: *Amino acids and Dipeptides*

4.1 Introduction

An important aspect of chiral synthesis is the determination of the optical purity of chiral molecules which often involves chromatography based separation techniques (HPLC or GC) utilizing special columns with chiral solid phase are employed.[1] The proper determination of optical purity requires precise molecular recognition which is usually substrate specific. Small structural changes in similar type of the analytes result in poor or failure in recognition under comparable conditions. Over the years other techniques such as mass spectrometry,[2] IR & UV spectroscopy,[3] CD & electrophoresis,[4] competitive immunoassay,[5] etc have evolved for accurate determination of the ratio of chiral isomers. These techniques are often time consuming and require costly reagents. The use of nuclear magnetic resonance spectroscopy (NMR) provides an alternate and efficient method for quick and accurate determination. The enantiomers in achiral environment in NMR spectroscopy show indistinguishable set of signals, while the diastereomers may show separate signals. The chiral discrimination by NMR involves the use of chiral lanthanide shift reagent (CLSR),[6] chiral derivatizing agents (CDA) [7] and chiral solvating agent (CSA).[8] The cost and availability of chiral lanthanide shift reagents, while the prior derivatization in case of CDA have led to the rapid development of chiral solvating agents. The design of structure with proper functional groups is the key aspect of chiral solvating agents.

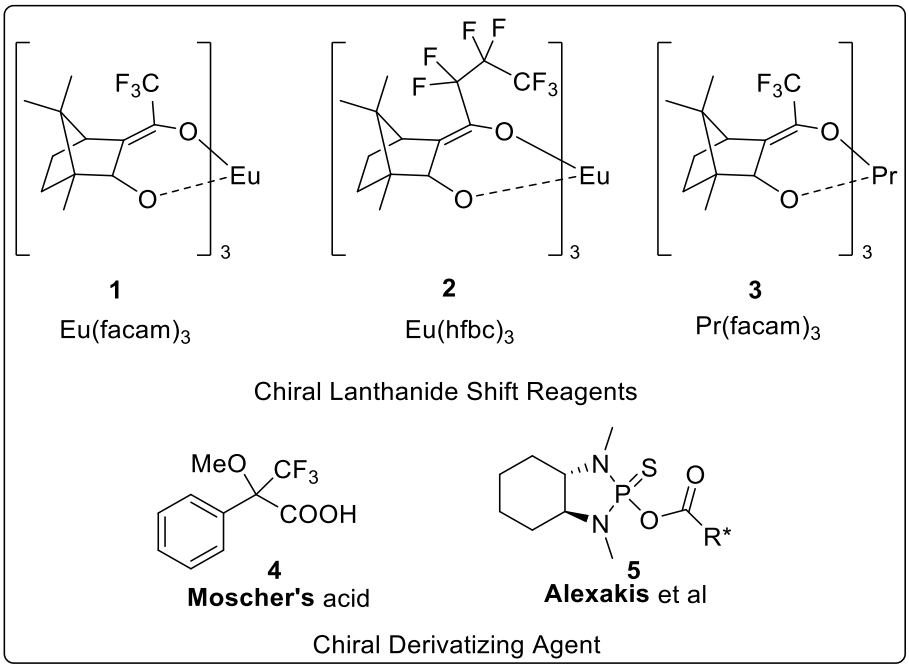

Figure 4.1: Some examples of chiral lanthanide shift reagents and chiral derivatizing agents

Over the last few decades many new chiral solvating agents have been introduced. The most effective chiral solvating agents have been designed with BINOL, proline, phenylethyl amine, amino naphthol, diamino cyclohexane (DACH) etc as their chiral core. The design of CSAs based on cyclohexane have been of prime focus due to their immense success in molecular recognition. Some common examples of cyclohexane based CSAs are presented in Figure 4.2. The choice of cyclohexanol unit in the design of these compounds may be attributed to the rigid backbone of the ring and the favorable orientation attained by *trans*-1,2- substituents leading to effective enantiodiscrimination.

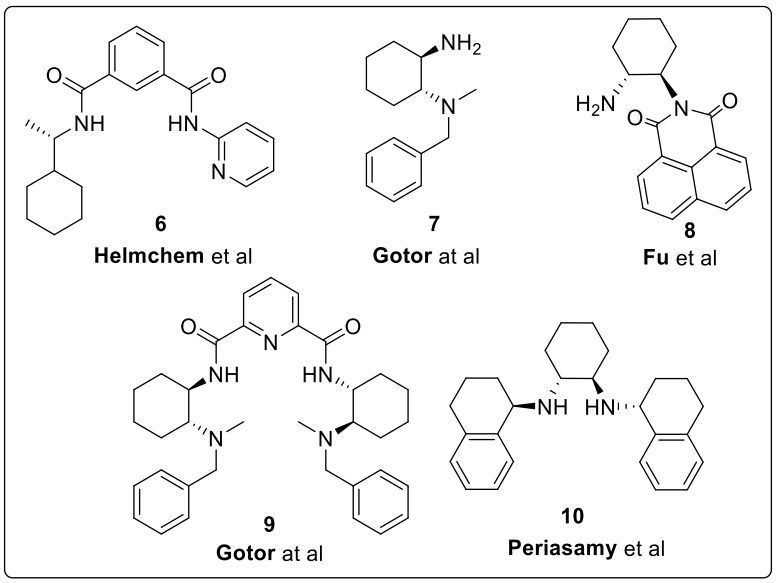

Figure 4.2: Cyclohexane based chiral solvating agent

Gotor et al have incorporated the *trans*-1,2 diamino cyclohexane scaffold in the design of symmetrical and unsymmetrical chiral solvating agents for enantiomeric discrimination of α-functional carboxylic acid derivatives (Figure 4.3). The pinsir type CSA exhibited base line separation in NMR analysis for mandelic acid derivatives on account of its 'U' shaped geometry formed due to double hydrogen bonding between amide N-H and pyridine 'N'.[8i]

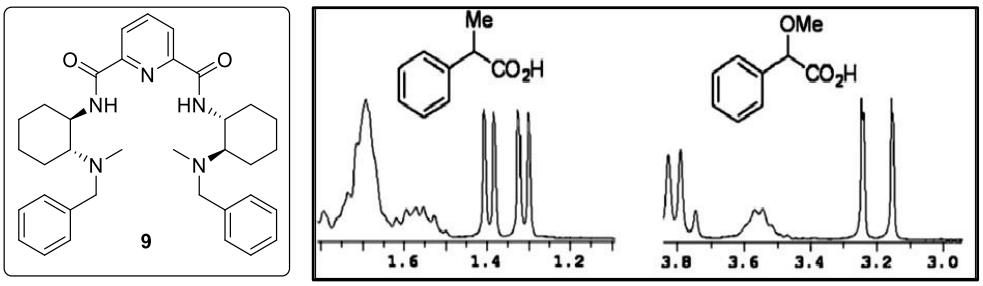

Figure 4.3: Application of *trans*-1,2-diamino cyclohexane derivative as CSA

Amino acids are considered as an important class of compounds as they are the building blocks for many natural products and drug molecules. Quick determination of optical purity of amino acid derivatives is essential from synthetic point of view. Periasamy et al have designed cyclohexane based CSA (*R,R,R,R*)-**10** for successful enantiodiscrimination of N-tosyl-amino acid derivatives (Figure 4.4).[8j]

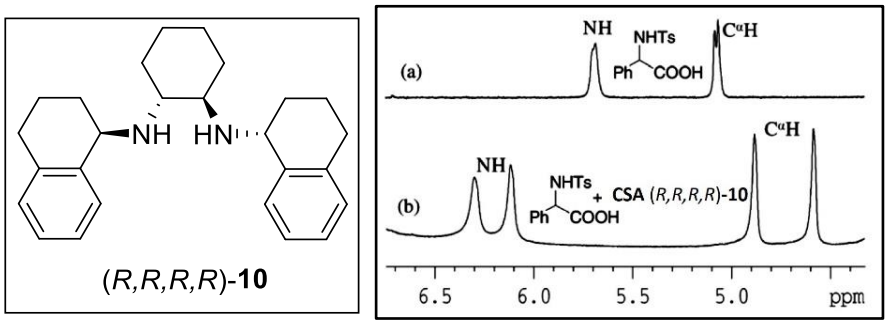

Figure 4.4: Application of (*R,R,R,R*)-**10** as CSA for N-tosyl phenylglycine

In recent times, along with NMR, fluorescence spectroscopy based methods for determination of optical purity have also been developed.[9,10] Fluorescence spectroscopy has been utilized for quick and reliable determination of optical purity.[11] Fluorescent sensors, capable of differentiating the two enantiomers of a chiral substrate should provide a real time technique in the rapid chiral assays with many unique advantages. Considerable work has been done on searching chiral fluorescent sensors, such as natural products like cinchona alkaloid based[10h] or synthetic ones designed from BINOL derivatives,[10i] which are capable of recognizing isomers of optically active analytes.

Chiral fluorescent sensors are generally composed of a fluorophore, a rigid backbone and a binding site, and are incorporated with a signaling mode for the fluorophore in response to chiral recognition process. Enantiomeric recognition by fluorescence spectroscopy involves signaling modes such as enhancement, quenching, excimers, life time, etc. In the last few decades, fluorescent sensors have been extensively designed with 1,1'-binaphthyl skeleton. The restricted rotation of the two naphthyl rings around their 1,1'-bond rendered high configurational stability to these sensors. Moreover, the naphthyl rings also serve as good fluorophores. However, incorporation of *trans*-1,2-amino cyclohexane moiety in combination with naphthyl skeleton has gathered significant interest in recent times resulting in application of cyclohexane based chiral fluorescent sensors in molecular recognition (Figure 4.5).

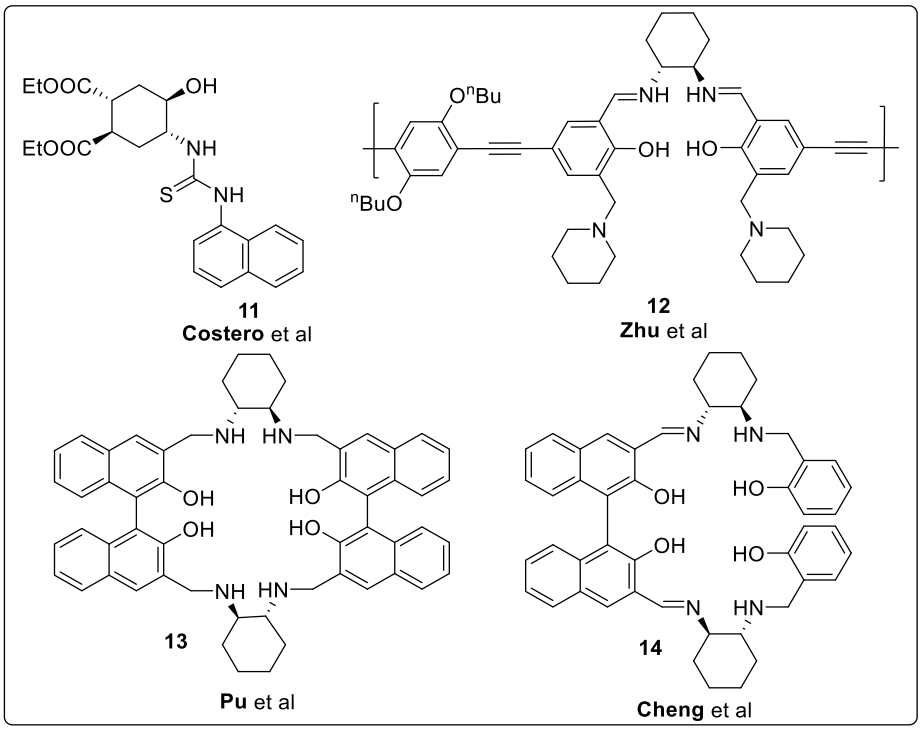

Figure 4.5: Cyclohexane based fluorescent sensors

Cyclohexane 1,2 diamine based binaphthyl sensor (**13**), by **Pu** et al, has been employed for molecular recognition of α-hydroxy carboxylic acids and N-protected amino acids. The fluorescent sensor exhibits highly enantiospecific fluorescent response towards acid analytes (Figure 4.6).[10c]

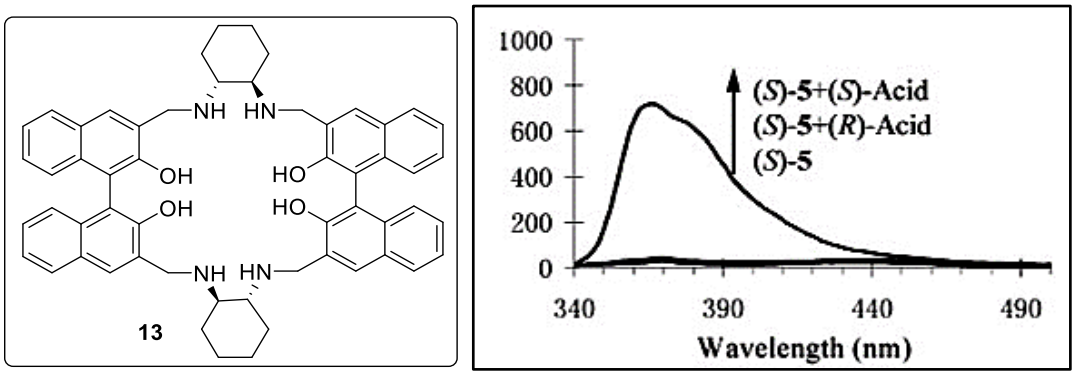

Figure 4.6: *trans*-1,2-cyclohexane diamine based macrocycle as fluorescent sensor

4.2 Result and Discussion:

In this part we report preparation of a simple chiral molecule, 2-(quinolin-8-yloxy)cyclohexan-1-ol, which has three distinct binding sites along with the aromatic quinoline moiety for effective supramolecular interactions as well as being capable of exhibiting good fluorescence response.

4.2.1 Synthesis of 2-(quinolin-8-yloxy)cyclohexan-1-ol (17):

The proposed sensor 2-(quinolin-8-yloxy)cyclohexan-1-ol (**17**) is a derivative of 8-hydroxyquinoline (**16**), which itself is known to show good fluorescence property.[12] The racemic sample of (**17**) was prepared by stereoselective opening of cyclohexene oxide (**15**) (Scheme 4.1).

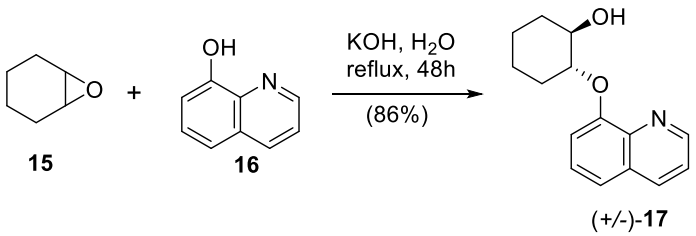

Scheme 4.1. Synthesis of (±)-2-(quinolin-8-yloxy)cyclohexan-1-ol **(17)**

4.2.2 Resolution of 2-(quinolin-8-yloxy)cyclohexan-1-ol (17):

The resolution of 2-(quinolin-8-yloxy)cyclohexan-1-ol (**17**) was carried out by kinetic resolution protocol.[13] Several conditions were investigated for resolution of alcohol (**17**), of which the best condition was when alcohol was treated with 3 eq (w/w) Steapsin lipase in THF with vinyl acetate as acyl donor yielding 37% (>99% ee) acetate derivative (**18**) while around 53% unreacted alcohol was isolated with moderate optical purity (60% ee) (Scheme 4.2). The unreacted alcohol (*S*,*S*)-**17** was further crystallized with hexane-CH_2Cl_2 (9:1) to afford almost optically pure alcohol.

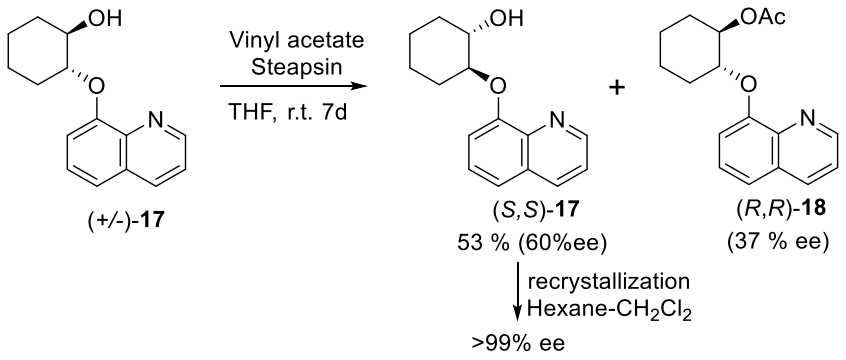

Scheme 4.2. Resolution of (±)-**17**

4.2.3 Determination of Absolute configuration

The absolute configuration of (**17**) was established by making its derivative with compound of known optical configuration. The alcohol (*R*,*R*)-**17**, obtained by hydrolysis of (*R*,*R*)-**18**, was coupled with (*R*)-*O*-acetyl mandelic acid (Scheme 4.3),[14a] while the relative absolute configuration of the ester (*R*,*R*,*R*)-**19** was established by its single crystal X-ray diffraction analysis (Figure 4.7).

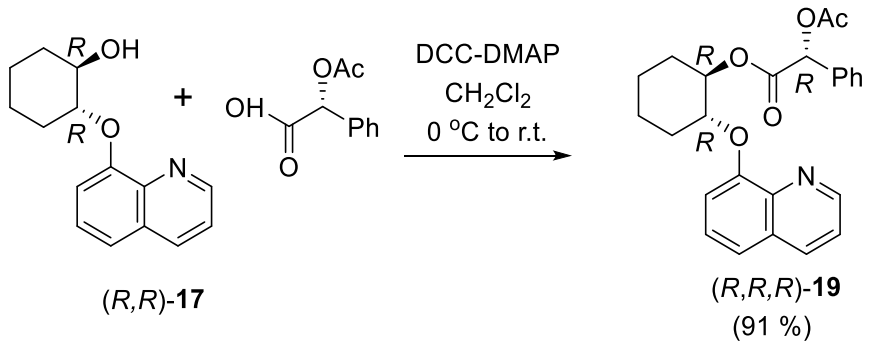

Scheme 4.3: Synthesis of (*R*,*R*,*R*)-**19**

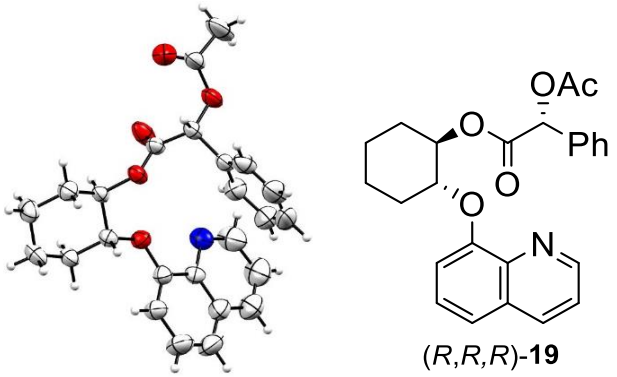

Figure 4.7: Determination of absolute configuration of alcohol and ORTEP diagram of (*R*,*R*,*R*)-**19**

The single crystal x-ray analysis of (*R,R*)-**17** exhibits three point interaction with water molecule via intermolecular hydrogen bonds. The crystal structure one molecule of water being shared between two molecules of (*R,R*)-**17** with three hydrogen bonds between (N···HO) (2.063 Å), (OH···O) (2.023 Å) and (O···HO) (2.981 Å). Additionally the cyclohexyl ring has lateral short interaction with quinoline ring (2.884 Å) constituting a helical assembly with *P*- configuration. The assembly is formed due to interactions of (*R,R*)-**17** with water as well as intermolecular interactions with other molecule of (*R,R*)-**17**. This encouraged us to analyze the crystal of its enantiomer (*S,S*)-**17** which exhibited similar three point interaction between (N···HO) (1.966 Å), (OH···O) (1.996 Å) and (O···HO) (2.969 Å). Moreover it has lateral interaction between cyclohexane ring and

quinoline (2.664 Å) resulting in similar helical assembly with opposite *M*-configuration (Figure 4.8).

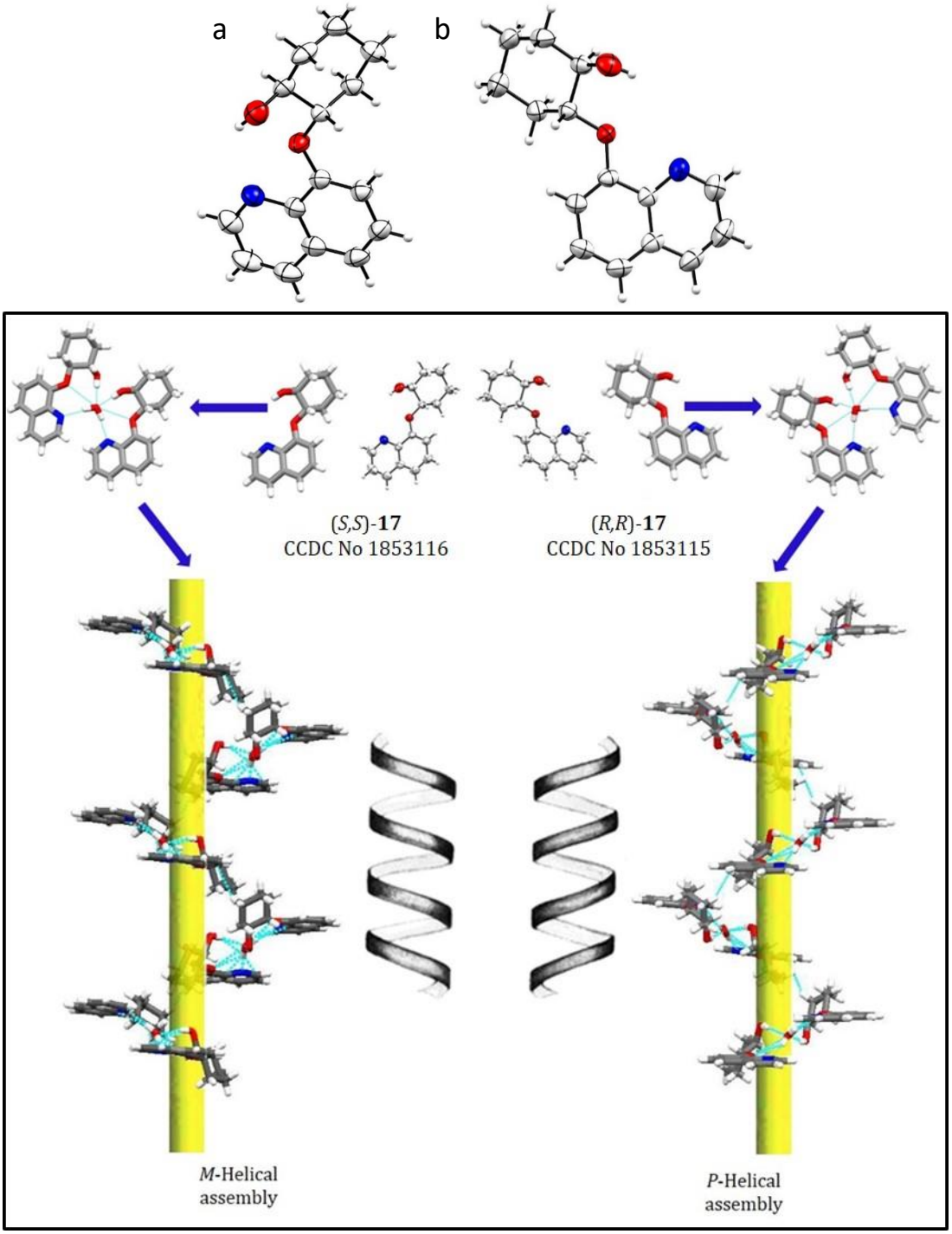

Figure 4.8: ORTEP diagram of the compound (*S*,*S*)-**17 (**CCDC-1853116) (left) and (*R*,*R*)-**17** (CCDC-1853115) (right) (50% probability factor for thermal ellipsoids)

4.2.4 Application as Chiral Solvating Agent:

Having optimized the synthesis and established absolute configuration of (*R*,*R*)-**17**, we tested our hypothesis to screen it as chiral solvating agent for evaluating enantiodiscrimination of signals of optically active acid analytes Type-A-F by NMR

spectroscopy (Figure 4.9). The design of the alcohol (**17**) suggests possibility of three point interaction with acidic substrates like mandelic acid (**A-I**). We envisage protonation of the quinoline 'N', along with two sets of intermolecular hydrogen bonding with the carboxylate. This was checked by ^{1}H NMR of (*R*,*R*)-**17** with racemic **A-I** (20 mM in $CDCl_3$, 400 MHz). The spectra indicates a well resolved signal of C$_\alpha$*H* with a considerable chemical shift non-equivalence (ΔΔδ) (Table 1), salt formation by deprotonation was further supported by FT-IR studies.[15] The ability to detect the molecular recognition of other derivatives of α-substituted phenyl acetic acids (Type **A** and **B**) was further investigated, with moderate to good level of detection (by ^{1}H-NMR & ^{19}F-NMR). Structurally similar acid **C**, an intermediate of Nebivolol, a beta blocker drug[16] was also screened with good separation of signals in ^{19}F-NMR.

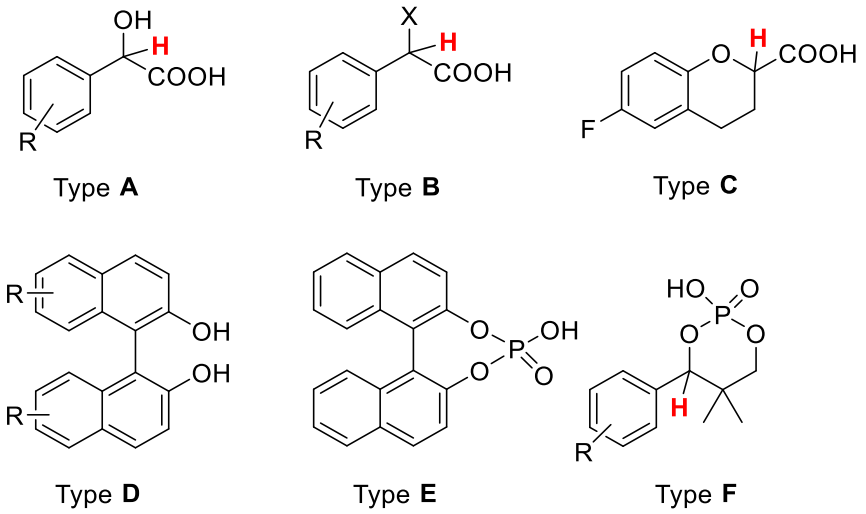

Figure 4.9: List of substrates screened with CSA

To understand the interactions between the (*R*,*R*)-**17** and the isomers of mandelic acid, attempt to grow the crystal of its salt with both isomers of **A-I** was made.[14c] A suitable quality crystal of (*R*,*R*)-**17** and (*R*)-**A-I** could be obtained from acetonitrile, while the other pair resulted in amorphous salt. The single crystal X-ray analysis of (*R*,*R*)-**17**•(*R*)-**A-I** confirmed the three point supramolecular interactions (Figure 4.10). The deprotonation of mandelic acid is further confirmed by shorter bond length of (C–O) bond (1.22-1.28 Å) of carboxylate. The salt shows (NH···O) hydrogen bond (1.789 Å) between protonated quinoline 'NH' and (C–O), and (OH···O) hydrogen bond (2.049 Å) between alcoholic 'OH' and (C-O) of carboxylate of mandelic acid. The mandelic acid shows further (CO···O) interaction (2.889 Å) with ether 'O' of (*R*,*R*)-**17**. In addition, the other 'O' of carboxylate shows strong (CH-O) interaction (2.491 Å) with C-H of quinoline ring. Furthermore the hydroxyl of mandelic acid shows lateral (OH-C)

interaction (2.851 Å) with carbon of cyclohexyl ring and with (O-HC) (2.716 Å) of quinoline ring

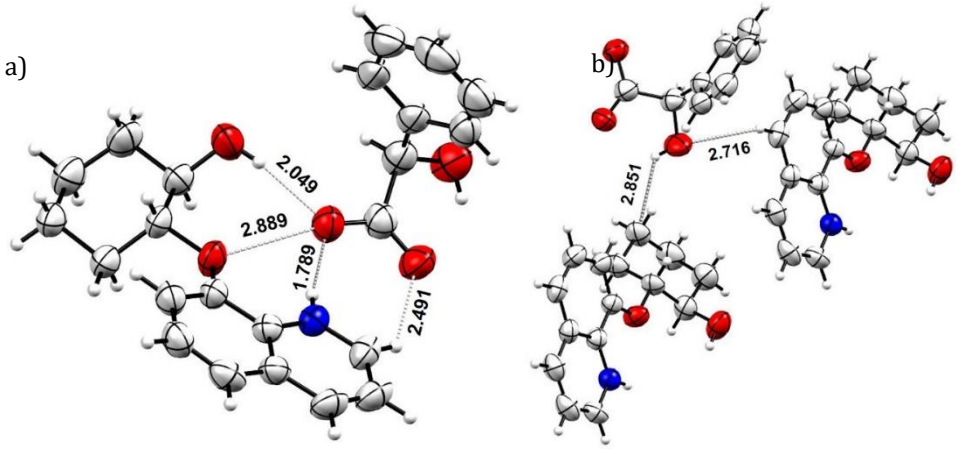

Figure 4.10: ORTEP diagram of the compound (*R,R,*)-**17-**(*R*)-MA (50% probability factor for thermal ellipsoids) CCDC-1853113

The chiral discriminating ability of CSA (**17**) for mandelic acid was further investigated to confirm the stoichiometry between (*R,R*)-**17** and analytes. The Jobs plot between (*R,R*)-**17** and **A-I** shows maxima at 0.5 indicating 1:1 binding for the CSA-analyte complex which is in agreement with the information from single crystal X-ray analysis (Figure 4.11)

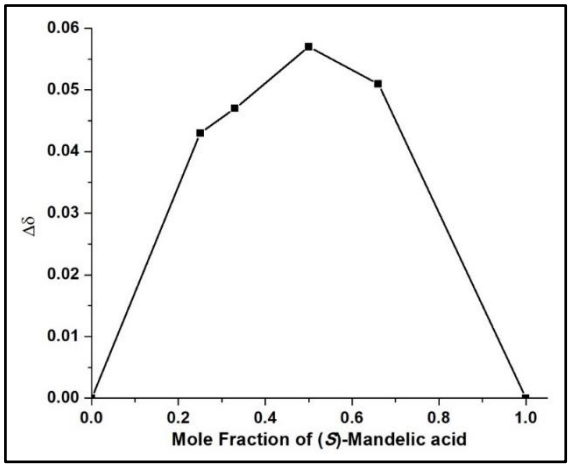

Figure 4.11: Job's Plot with (*S*)-mandelic acid

The effect of ratio of concentration between the CSA (*R,R*)-**17** and **A-I** on the chemical shift non-equivalence (ΔΔδ) were studied by performing NMR experiments with varying concentration of CSA to analyte. The ratio of CSA:analyte was varied gradually and its effect on the separation of signal was monitored. It was observed that the chemical shift non-equivalence was maximum when the ratio was 1:1 (Figure 4.12a). Moreover, the effect of overall concentration of CSA and analyte (10 mM to 30 mM) has also been studied for optimizing the concentrations for further experiments with other analytes. It

was observed that the best separation (0.026 ppm) was observed with 20 mM concentration which remains constant with further increase in concentration (Figure 4.12b).

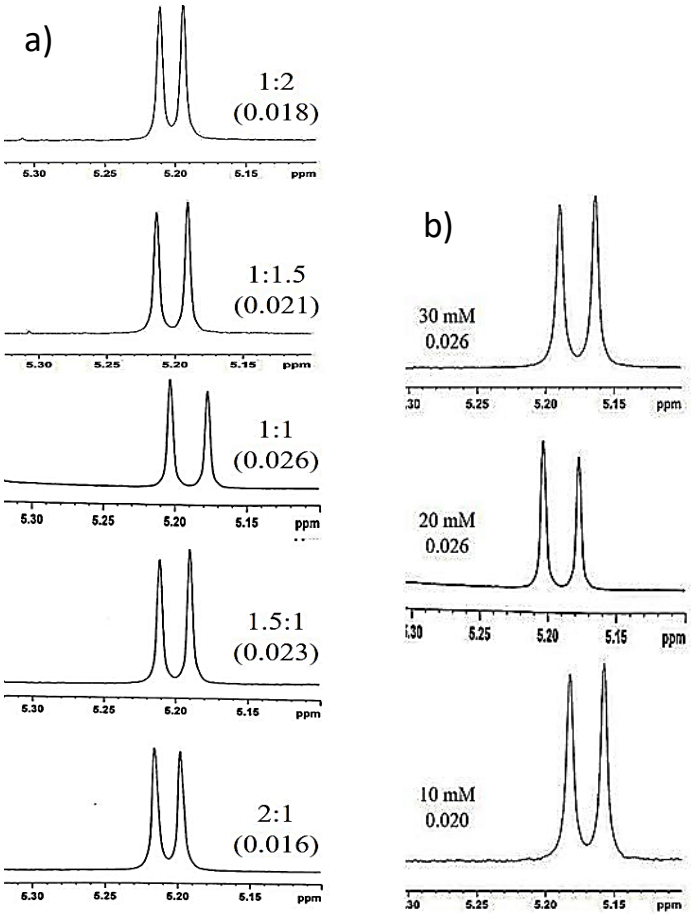

Figure 4.12: (a) Selected region of ^{1}H NMR spectra of varying ratio of concentration of (*R,R*)-**17** with racemic **A-I** (left); (b) Selected region of ^{1}H NMR spectra of (*R,R*)-**17** with A-**I** with increasing concentration of CSA-analyte**.** The value in parenthesis indicates $\Delta\Delta\delta$ in Hz.

The interaction between CSA and analyte is known to be influenced with the polarity of solvent. The role of solvent was further investigated by performing the experiments with different solvents. Four solvents were screened for the enantiodiscrimination of acid **A-I**, wherein C_6D_6 and $CDCl_3$ showed recognition, former being less polar showed better separation (0.034 ppm), while CD_3CN and CD_3OD failed to show any detectable discrimination (Figure 4.13).

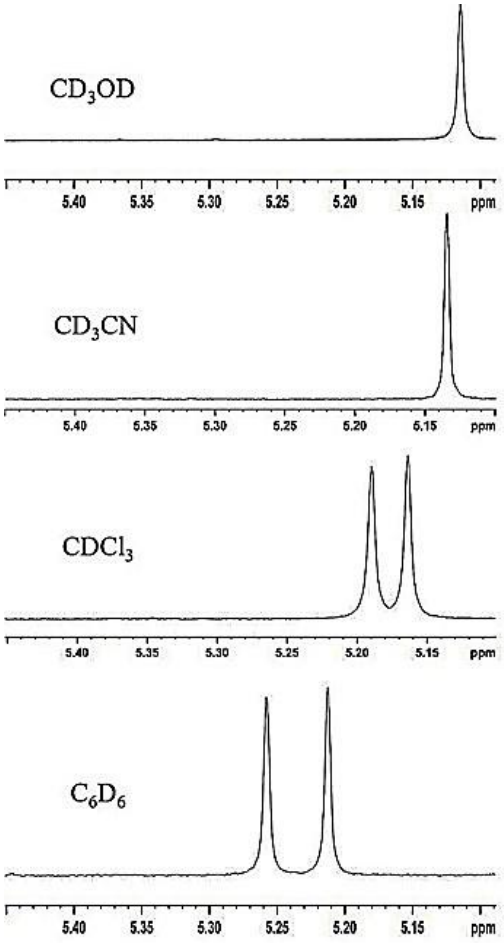

Figure 4.13: Selected region of ^{1}H NMR spectra of (*R,R*)-**17** with racemic **A-I** in different solvents**.**

The practical utility of CSA for determination of optical purity of analytes was investigated by determination of ee of various scalemic samples of **A-I** by integration of ^{1}H signal of **A-I** in ^{1}H NMR. Figure 4.14 indicates that CSA (*R,R*)-**17** maintains resolution for nonracemic samples of **A-I** over a wide range of ee values. The plot of ee values determined by NMR and by gravimetry shows linear relationship with R^2 = *0.9999*. The scalemic samples of **A-I** were prepared by properly mixing accurately weighed quantities of (*S*) and (*R*)-A-I.

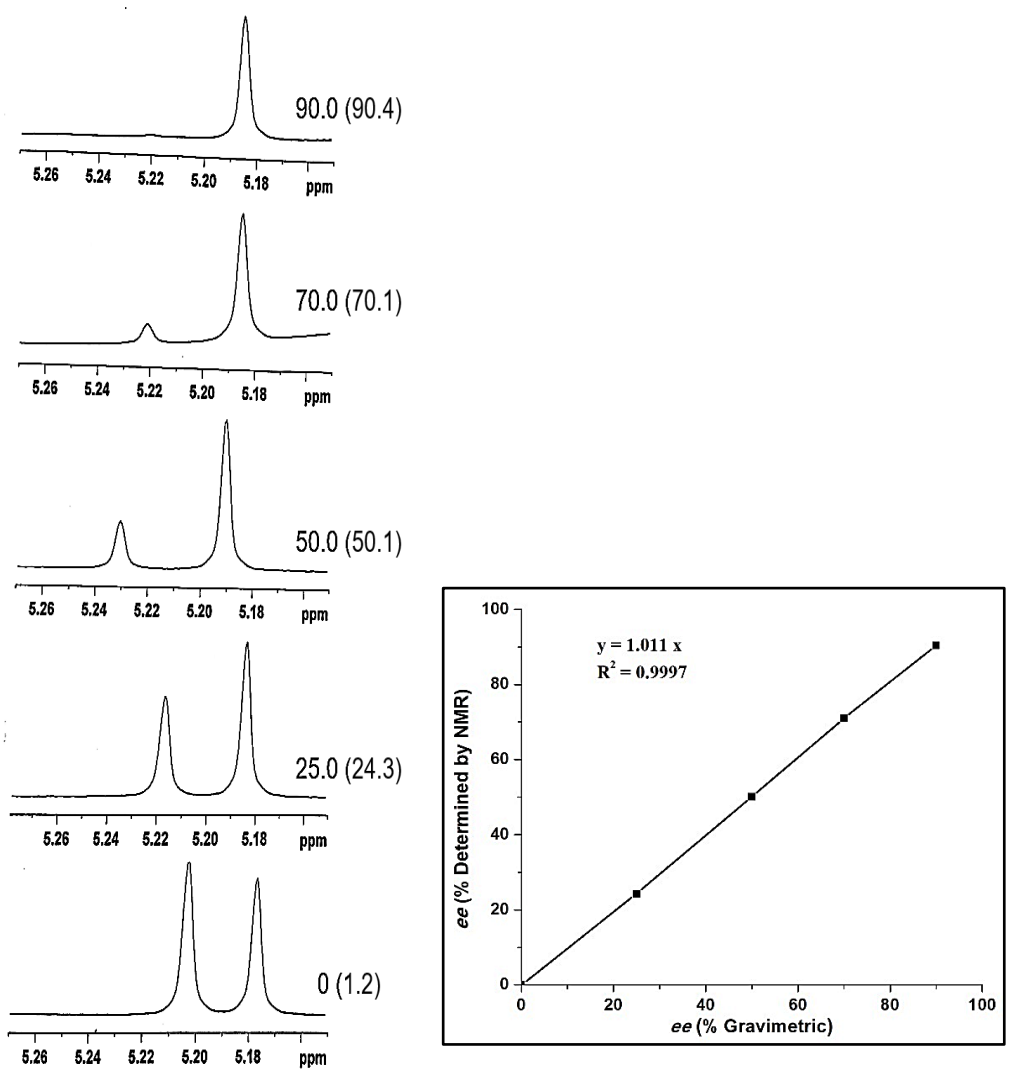

Figure 4.14: Selected region of ^{1}H NMR spectra of scalemic mixture of **A-I** in presence of (*R,R*)**-17** (Left) and its correlation between theoretical and observed % *ee* values (Right).

The derivatives of mandelic acid were further screened with CSA (*R,R*)-**17**. It was observed that 4-bromo derivative exhibited the best separation. The separation in case of 4-CF_3 derivative was almost comparable which also showed good baseline resolution in ^{19}F NMR. Along with mandelic acid derivatives, other α-halo phenylacetic acid derivatives were also used as analytes. The α-bromo phenylacetic acid derivative gave the best result while the separation was lesser for the α -chloro analogue. However, the 4-CF_3 derivative of α -chloro phenylacetic acid showed separation in both ^{1}H and ^{19}F NMR.

Table 4.1. Application of (*R*,*R*)-17 as Chiral Solvating Agent for discrimination of signals of α-substituted carboxylic acids by NMR

No	Analyte	R =	ΔΔδ[a] (^{1}H)	ΔΔδ[a,] (^{19}F)
1	A-I	H	0.026	--
2	A-II	4-CF_3	0.032	0.036
3	A-III	2-Cl	0.019	--
4	A-IV	3,4-O-CH_2-O	0.029	--
5	A-V	4-Br	0.033	--
6	B-I	R = H; X-Br	0.030	--
7	B-II	R = H; X-Cl	0.016	--
8	B-III	R = 2-Cl; X-Cl	0.024	--
9	B-IV	R = 4-CF_3; X-Cl	0.014	0.026
10	C	--	--[b]	0.033

[a]Chemical Shift non-equivalence (ΔΔδ) in ppm. [b]Not resolved completely.

The scope of (*R*,*R*)-**17** was further explored for detecting the discrimination of isomers of BINOL (Type-**D**), 1,1'-binaphthyl-2,2'-diyl hydrogenphosphate (Type **E**) and cyclic phosphoric acids (Type **F**) (Table 4.2). Due to considerable interest in the applications of these molecules in asymmetric synthesis, it is crucial to develop an efficient method for establishing their optical purity.[17] For this study ^{1}H NMR of **D-I** with (*R*,*R*)-**17**, exhibited excellent separation for two hydrogens (H6 and H8) (Figure 4.15), whereas **D-II** showed moderate separation (H5). In the case of **E** the resolution of signals in ^{1}H NMR could not be detected due to overlap, however the ^{31}P NMR indicated a good base line separation (Figure 4.15). The cyclic phosphoric acid analogues (Type F), which have not been commonly analyzed for such molecular recognition[18] resulted in good separation of signals, in both ^{1}H and ^{31}P NMR spectroscopy. In general, the presence of electron withdrawing substituent resulted in better separation, probably due to increased acidic nature (**F-II** and **F-III**).

Table 4.2. Application of (*R*,*R*)-17 as CSA for discrimination of signals of BINOLs and phosphoric acids by NMR spectroscopy

No	Analyte	R	$\Delta\Delta\delta^a$ (^{1}H)	$\Delta\Delta\delta^b$ (^{31}P)
1	D-I	--	0.058 (H8)	--
			0.038 (H6)	
2	D-II	--	0.016 (H5)	
3	E	--	--	0.56
4	F-I	H	0.020 (C*H*)	0.37
5	F-II	4-Cl	0.042 (C*H*)	0.39
6	F-III	4-NO_2	0.043 (C*H*)	0.35
7	F-IV	4-OMe	0.047 (C*H*)	--[b]
			0.011 (OCH_3)	

[a]Chemical shift non-equivalence ($\Delta\Delta\delta$) in ppm. [b]Not resolved completely.

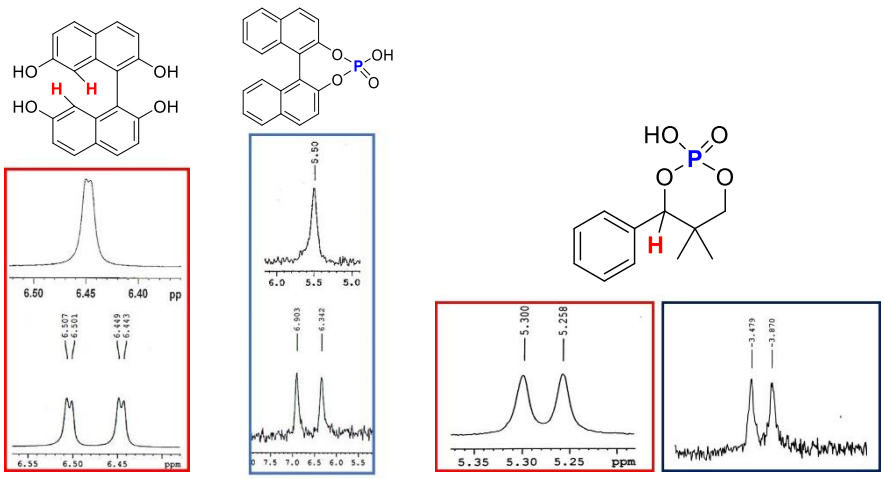

Figure 4.15: ^{1}H NMR spectra of **D-I** with (*R*,*R*)-**17** (left); ^{31}P NMR spectra of **E** with (*R*,*R*)-**17** (right)

4.2.5 Application as Fluorescent sensor

One of the objectives of the design of (*R*,*R*)-**17** was to explore the fluorescence property of 8-hydroxyquinoline in tandem with structural rigidity and hydrogen bonding ability of cyclohexanol moiety. Amino acids, essentially utilized in optically pure form, are generally analyzed by HPLC on chiral columns.[18] While there are some reports of fluorescence spectroscopy based analytical methods, involving prior *N*-protection or involving the use of complex sensors.[19] At the same time few reports are available where

amino acids are directly analyzed,[20] hence we examined our sensor (*R*,*R*)-**17** for fluorescence recognition of amino acids **AA** (Figure 4.16).

Fluorescence recognition of **AA-I** to **AA-IV** with (*R*,*R*)-**17** in EtOH showed significant enhancement indicating selectivity towards one enantiomer. The fluorescence spectra of (*R*,*R*)-**17** in presence of **AA-I** resulted in marked enhancement at short wavelength emission with *L*-isomer, while insignificant change was seen with the other isomer. Similar experiment with isomers of **A-I** did not result in any marked difference in fluorescence, indicating essential role of amino group. The sensor exhibited highly enantioselective fluorescence recognition towards **AA-I** (*ef* = 14.4). The nitrogen of quinoline ring of the sensor interacts with acid due to protonation, thereby making the lone pair unavailable for PIET leading to the enhancement in fluorescence. The binding of (*L*)-**AA-I** with the sensor (*R,R*)-**17** must be stronger then (*D*)-**AA-I** due to favourable hydrogen bonding and π–π interactions.[21] Furthermore, the other isomer of sensor (*S,S*)-**17** when screened with **AA-I** exhibited fluorescence enhancement for the other isomer (*D*)-**AA-I** thus confirming the mirror image relationship.

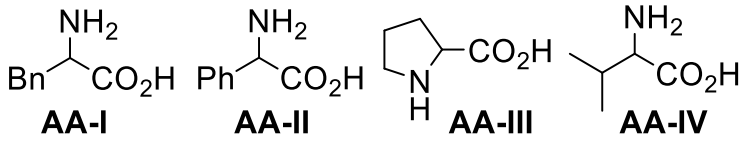

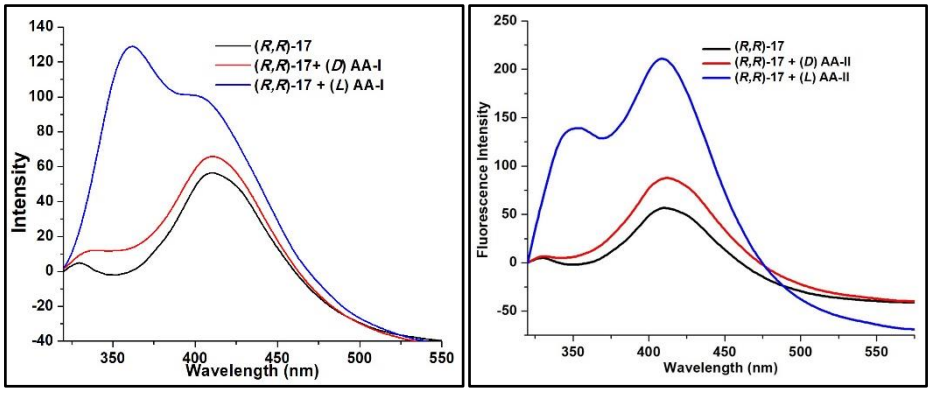

Figure 4.16: Fluorescence spectra of (*R*,*R*)-**17** (1.0 X10^{-5} M in EtOH) in the presence of *D*- and *L*-phenyl alanine (AA-**I**) (1.0 X 10^{-3} M in EtOH) (bottom left) (λ_{ex} 300 nm) (left); Fluorescence Spectra of **(*R*,*R*)-17** (1 x 10^{-5} M), **(*D*)-**AA-**II** and **(*L*)-AA-II** (1 x 10^{-3} M) in presence of **(*R*,*R*)-17** in EtOH (λ_{ex} = 300 nm).

Similar behavior was observed for **AA-II**, but for the aliphatic analogues **AA-III** and **AA-IV**, the *D*-isomer showed higher fluorescence enhancement. This perhaps indicates towards a favorable π–π interaction between the aromatic ring of *L*-amino acid and

quinoline unit of the sensor in case of **AA-I** and **AA-II**, which will be lacking in the other cases (Figure 4.17).

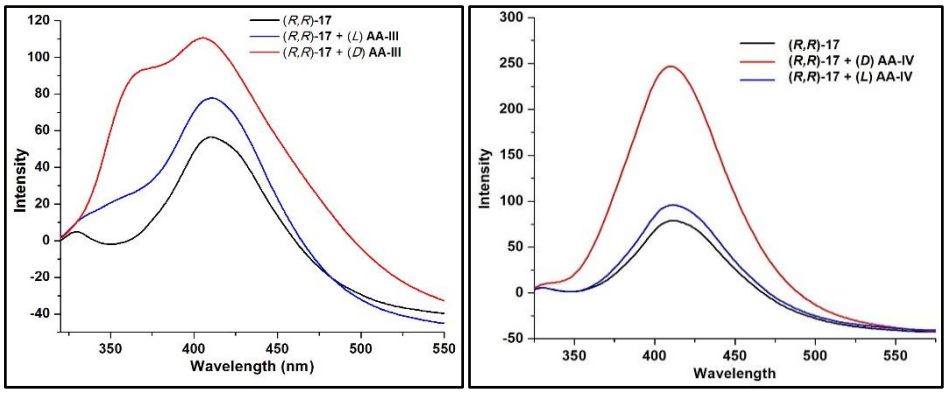

Figure 4.17: Fluorescence spectra of (*R*,*R*)-**17** (1.0 X10^{-5} M in EtOH) in the presence of (*D*)-AA-**III** and (*L*)-AA-**III** (1.0 X 10^{-3} M in EtOH) (bottom left) (λ_{ex} 300 nm) (left); Fluorescence Spectra of **(***R*,*R***)-17** (1 x 10^{-5} M), **(***D***)-**AA-**IV** and **(***L***)-AA-IV** (1 x 10^{-3} M) in presence of **(***R*,*R***)-17** in EtOH (λ_{ex} = 300 nm).

The enantioselective fluorescence response of sensor towards amino acids has been discussed (Table 4.3). To establish this hypothesis the sensor was treated with **AA-I** with the varying concentrations and it followed the Benesi-Hildebrand equation (Figure 4.18).[9h]

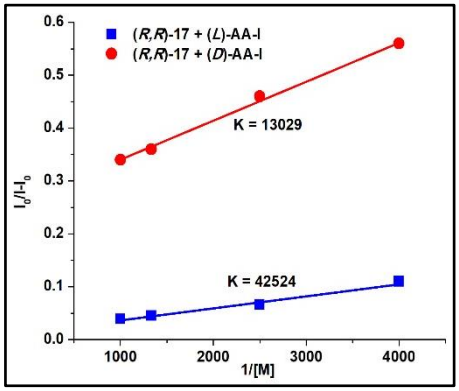

Figure 4.18: Benesi-Hildebrand plot of (*R*,*R*)-**17** (1.0 X10^{-5} M in EtOH) in the presence of *D*- and *L*-phenyl alanine (AA-I).

For establishing the practical applications of (*R*,*R*)-**17** as a tool to determine optical purity of chiral analytes, it is essential to follow linear enantioselective response. This ability of quantitative determination of ee of samples of optically active analytes was established by NMR analysis of scalemic mixture of mandelic acid. However, such study of establishing optical purity by florescence spectroscopy is not widely reported in the literature.[10b,10e,10h]

We explored sensor (*R*,*R*)-**17** for determining the ee of **AA-I** by recording its fluorescence spectra with different samples of enantiomeric purity (Figure 4.19). The optical purity of samples of **AA-I** was determined from the plot of I/I_o vs %ee of *L*-**AA-I**, from this % ee was obtained and compared with actual values. A linear relationship was observed between the actual and experimental values of ee. Furthermore two samples of unknown purity were analyzed in the same way and their ee was validated with the actual and the SOR values.

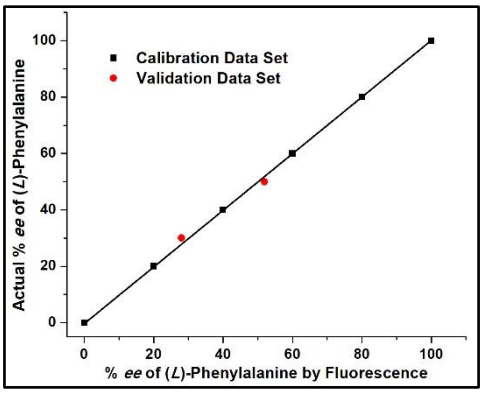

Figure 4.19: Plot of fluorescence response of (*R*,*R*)-**17** (1.0 $X10^{-5}$ M in EtOH) in the presence of **AA-I** (1.0 $X\ 10^{-3}$ M in EtOH) with varying ee ratio.

To the best of our knowledge there are no reports of molecular recognition of peptides using chiral fluorescence sensors, although some studies on fluorescence markers for peptides and proteins are known.[21] With the aim to further explore the possibility of using (*R*,*R*)-**17** for determining fluorescence response with isomers of peptides and its subsequent use as marker with other biomolecules, we investigated few dipeptides as analytes for this study (**DP-I** to **DP-III**, Figure 4.20). The fluorescence study of (*R*,*R*)-**17** with isomers of **DP-I** showed greater enhancement for *L*-**DP-I**, showing selective recognition. This behavior was similar in case of both dipeptides (**DP-I** and **DP-II**) containing amino acids with aromatic groups, and which was consistent with observation for amino acid series (**AA-I** and **AA-II**).

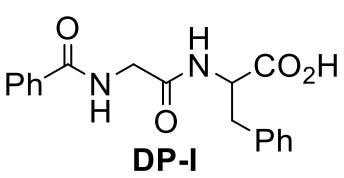

DP-I

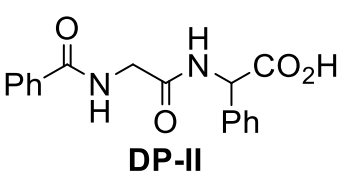

DP-II

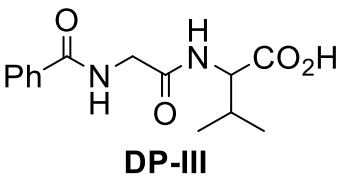

DP-III

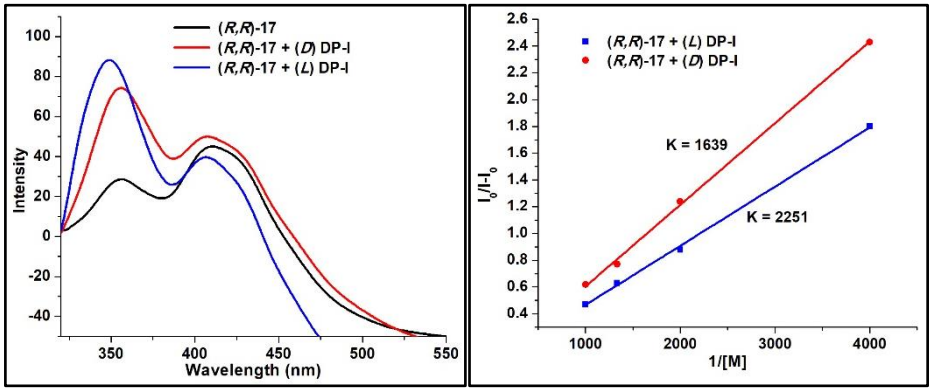

Figure 4.20: Dipeptides investigated as analytes for the fluorescence response with of (*R*,*R*)-**17** (left). Fluorescence spectra of (*R*,*R*)-**17** (5.0 X10^{-6} M in EtOH) in the presence of *D*- and *L*-**DP-I** (1.0 X 10^{-3} M in EtOH) [λ_{ex} 300 nm] (bottom left). Benesi-Hildebrand plot of (*R*,*R*)-**17** (5.0 X10^{-6} M in EtOH) in the presence of *D*- and *L* **DP-I** (right)

The comparison of molecular recognition data for amino acids and dipeptides is summarized in Table 4.3. The behavior of these analytes containing aromatic side chains supports the role of π–π interactions with quinoline unit of sensor **1**. At the same time the response for aliphatic side chain containing analytes was similar.

Table 4.3. Enantioselective fluorescence response and association constant of (*R*,*R*)-17 with AA (I to IV) and DP (I & II)

No	Analyte	Enantioselective fluorescence (*ef*)	K_L/K_D	K_D/K_L
1	AA-I	14.4	3.26	--
2	AA-II	6.9	1.86	--
3	AA-III	3.5	--	2.22
4	AA-IV	4.8	--	6.86
5	DP-I	1.3	1.38	--
6	DP-II	1.5	1.53	--
7	DP-III	1.6	--	--

4.2.6 Synthesis of aminoalcohol (21):

The role of amino alcohols in the field of asymmetric synthesis as chiral ligands and chiral auxiliaries is immense. They are most commonly derived from natural sources. A wide variety of amino alcohols have been derivatized and employed in enantiodiscrimination of chiral compounds using NMR spectroscopy and fluorescence spectroscopy. In this part we wish to synthesize, resolve and employ cyclohexane based

amino alcohol for molecular recognition. Amino alcohol (**21**) was synthesized by ring opening of *meso* cyclohexenoxide (1eq) with N-methyl aniline (1eq) in presence of $Cu(OTf)_2$ in dry ether (Scheme 4.4).

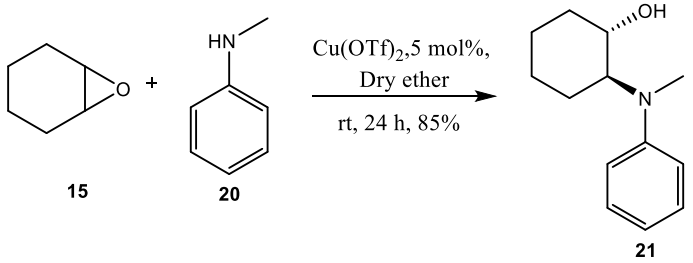

Scheme 4.4: Synthesis of amino alcohol (**21**)[23]

4.2.7 Enzymatic resolution of amino alcohol

The resolution of amino alcohol (**21**) has been reported by Sekar et al. However the resolution process involves prior conversion to acetate derivative which is subjected to hydrolysis using pig level esterase as enzyme. Moreover the ee of unreacted acetate was observed to be around 80%. In order to overcome this limitation and further improve the optical purity of both the compounds, we decided to subject the alcohol (**21**) to enzymatic resolution with CAL B enzyme in THF using vinyl acetate as acyl donor (Scheme 4.5). The initial results indicated high selectivity for acetate derivative (**22**) but the conversion was observed to be poor. To improve the conversion the amount of acyl donor was increased indicating better chemical yield without loss of optical purity however increasing the amount of lipase resulted in reduced chemical yield as well as purity. Further changing the enzyme from CAL B to steapsin the chemical yield as well as optical purity was slightly improved further. Additionally, increasing the amount of enzyme and acyl donor led to increasing the conversion to almost 47% with nearly optically pure acetate derivative. Also the unreacted alcohol was isolated with good yield and better optical purity. The best result was obtained with 3eq (w/w) Steapsin and vinyl acetate (10 eq.) affording not just acetate in optically pure form in good yield but also unreacted alcohol (**21**) in high yield (47%) and chiral purity (95%) (Table 4.4).

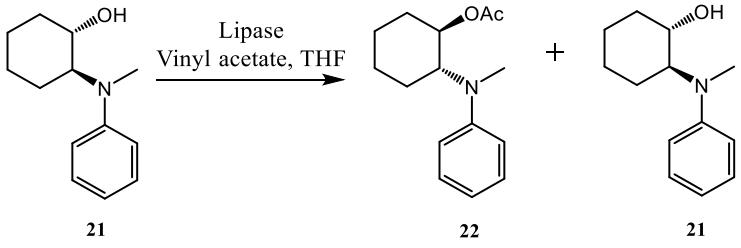

Scheme 4.5: Enzymatic resolution of amino alcohol (**21**)

Table 4.4: Conditions for enzymatic resolution of aminoalcohol (**21**):

No	Lipase (% w/w)	Acyl donor (eq.)	Solvent	Enantiomeric excess		C
				Acetate (**22**) (% *ee*)	Alcohol (**21**) (% *ee*)	
1	CAL-B (30)	VA (2.5)	THF	>99	7	10
2	CAL-B (30)	VA (10)	THF	>99	10	11
3	CAL-B (60)	VA (5)	THF	97	20	10
4	Steapsin (100)	VA (5)	THF	>99	34	28
5	Steapsin (200)	VA (10)	THF	>99	80	42
6	Steapsin (250)	VA (10)	THF	>99	90	45
6	**Steapsin (300)**	**VA (10)**	**THF**	**>99**	**95**	**47**

The absolute stereochemistry of resolved alcohol was determined by comparing the optical rotation values with the literature data.[24b] The SOR data indicated that the configuration of alcohol which underwent acylation was observed to be '*S*,*S*'.

The optically pure alcohol (**21**) obtained by careful hydrolysis of acetate derivative was then converted to its amino ester derivative by treatment with pyridine-2,6-dicarboxylic acid in presence of DCC and DMAP resulting in the formation of amino ester (**23**) (Scheme 4.6).

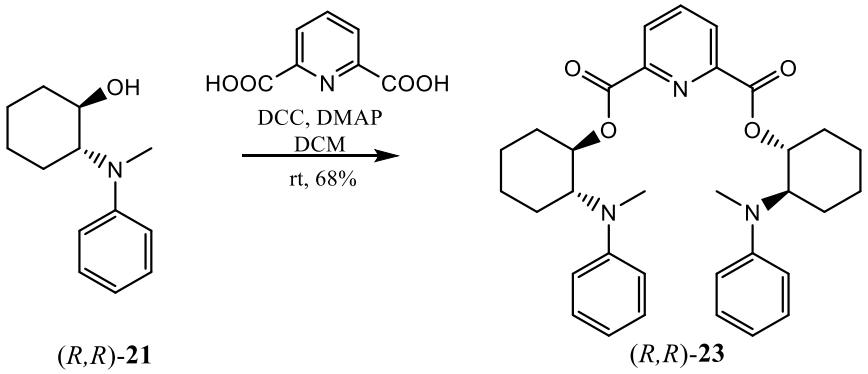

Scheme 4.6: Synthesis of amino ester (**23**)

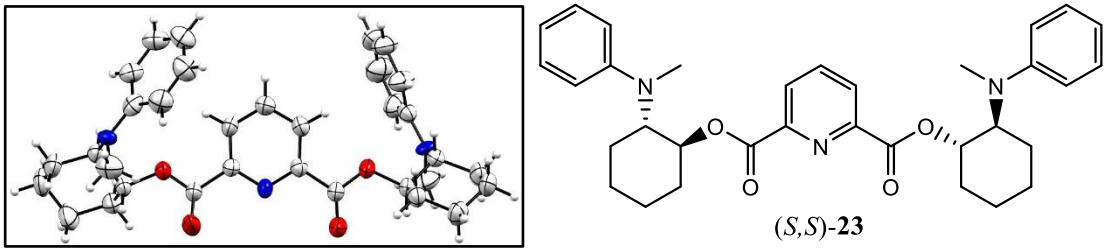

Figure 4.21: Single crystal X-ray analysis of amino ester; ORTEP diagram of (*S*,*S*)-**23** (CCDC1883255)

This amino ester (**23**) has been screened as CSA for mandelic acid and binaphthyl phosphoric acid derivatives. The preliminary results of CSA experiments indicate low to moderate degree of separation of signals (Figure 4.22).

This may be attributed to steric factor, as the phenyl ring being directly attached to amine 'N' blocks the non-covalent interactions and electronic factors as the nucleophilicity of the amine is reduced due to aromatic ring being directly attached. This result also suggest that the phenyl ring attached to amine 'N' in the form of benzyl group as observed in previous case is more favorable as compared to the current scenario.

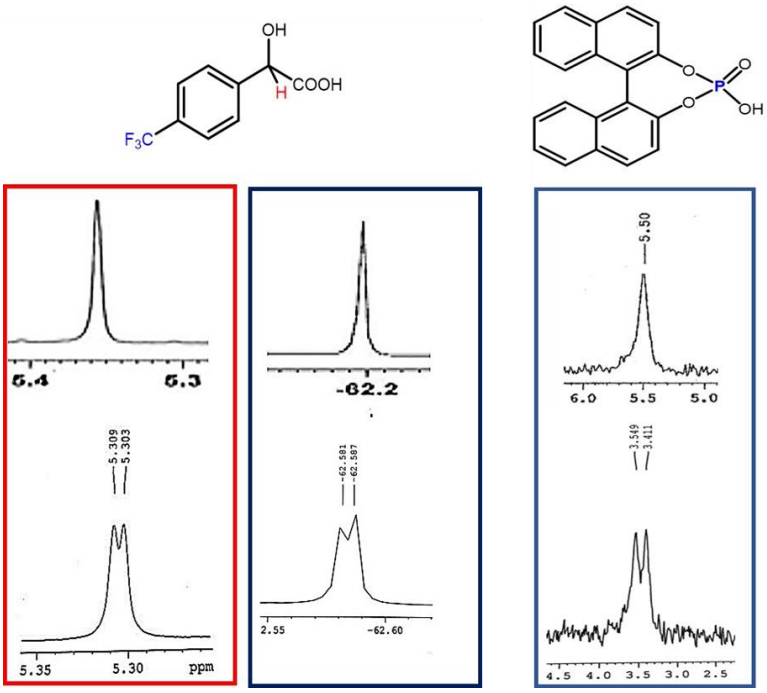

Figure 4.22: ^{1}H and ^{19}F NMR spectra of **A-II** with (*R*,*R*)-**23** (left); ^{31}P NMR spectra of **E** with (*R*,*R*,)-**23** (right)

4.3 Conclusion:

In conclusion, we have presented design, synthesis and resolution of 2-(quinolin-8-yloxy)cyclohexan-1-ol, a potential candidate for molecular recognition studies.

2-(quinolin-8-yloxy)cyclohexan-1-ol (**17**) has been successfully screened as chiral solvating agent by NMR spectroscopy for series of acid analytes ranging from α-substituted acids, binol derivatives and cyclic phosphoric acid analgues.

Study of single crystal X-ray analysis indicates the possible mode of molecular recognition, while the practical utility was confirmed by performing controlled experiments to determine the ee of scalemic samples of mandelic acid **A-I**.

Furthermore, the utility of 2-(quinolin-8-yloxy)cyclohexan-1-ol (**17**) as a chiral fluorescent sensor has been explored establishing the role of (*R,R*)-**17** as chiral sensor for the recognition of amino acid derivatives and dipeptide derivatives.

Moreover its practical application for determination of optical purity by fluorescence spectroscopy has also been studied and extended for determination of ee of samples of unknown purity. This establishes the dual mode of detecting the degree of molecular recognition the sensor for a number of diverse analytes.

The amino alcohol (**21**) obtained by ring opening by *N*-methyl aniline has been subjected to enzymatic resolution with improved ee for both alcohol and acyl derivative as compared to previously reported method.

The chiral amino alcohol derivative was converted to amino ester derivatives and screened for enantiomeric discrimination of acid derivatives.

The CSA experiments indicate lesser separation of signal due to presence of aryl group attached to amine nitrogen making it less efficient for molecular recognition studies. The poor ability of this compound as CSA could be attributed to the low nucleophilicity of amine nitrogen as well as the open structure as compared to aza-macrocycles.

4.4 Experimental procedure:

^{1}H, ^{13}C and ^{31}P NMR spectra are recorded on a 400 MHz Bruker Avance 400 Spectrometer (100 MHz for ^{13}C and 162 MHz for ^{31}P respectively) spectrometer with $CDCl_3$ as solvent and TMS as internal standard. Signal multiplicity is denoted as singlet (s), doublet (d), doublet of doublet of doublets (ddd), triplet (t), doublet of triplet (dt), quartet (q) and multiplet (m). Mass spectra were recorded on Thermo-Fischer DSQ II GCMS instrument. IR spectra were recorded on a Perkin-Elmer FTIR RXI spectrometer as KBr pallets or neat in case of liquids. UV-Vis spectra were recorded on Perkin-Elmer λ–35. Fluorescence spectra were recorded on Jasco FP-6300 Spectrofluorometer. All ^{1}H, ^{19}F and ^{31}P CSA NMRs were recorded by mixing 1equiv (20 mmol) of *(R,R)*-**17** and 1 equiv (20mmol) of hosts (**A**-**F**) in 0.6ml $CDCl_3$.

Synthesis of 2-(quinolin-8-yloxy)cyclohexan-1-ol **(17)**

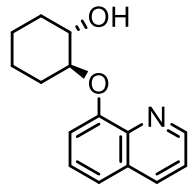

In a solution containing potassium hydroxide (0.386 g, 6.89 mmol) in water (16 mL) in two neck round bottom flask, was added 8-hydroxy quinoline (1.0 g, 6.89 mmol) and heated at 100 ^{o}C. To this solution, cyclohexene oxide (0.81 g, (0.81 mL) 8.2 mmol) was added after 30 mins. The reaction was allowed to reflux for 18 h. The mixture was then and extracted with ethyl acetate 3 x 50 mL. The combined extracts were then dried over sodium sulphate and evaporated under vacuum. The crude reaction mixture was then subjected to column chromatography on silica gel. The desired alcohol was eluted with 50 % ethyl acetate/ petroleum ether. (1.43 g, 86%).[1] M.p = 106 ^{o}C.

^{1}H NMR ($CDCl_3$, 400 MHz): δ ppm 8.89-8.87 (dd, *J* = 8.0, 1.6 Hz, 1H), 8.21-8.19 (dd, *J* = 7.6, 1.6 Hz, 1H), 7.57-7.55 (dd, *J* = 8.0, 1.2 Hz, 1H), 7.50-7.48 (d, *J* = 7.6 Hz, 1H), 7.47-7.43 (m, 2H), 7.36-7.34 (dd, *J* = 7.6, 1.6 Hz, 1H), 6.94 (s, broad 1H –O*H*), 3.98-3.92 (m, 1H), 3.89-3.83 (m, 1H), 2.34-2.33 (m, 1H), 2.19-2.16 (m, 1H), 1.80-1.72 (m, 2H), 1.67-1.64 (m, 1H), 1.37-1.26 (m, 3H).

^{13}C NMR ($CDCl_3$, 100 MHz): δ ppm 154.2, 149.0, 141.6, 136.9, 129.9, 126.9, 122.6, 121.6, 118.7, 88.6, 73.4, 33.2, 31.0, 24.5, 23.9.

IR (KBr) υ cm^{-1}: 3352, 3045, 2934, 1617, 1468, 1380, 1106, 1081, 735.

Mass (ESI): m/z 244 M (100%), 242.1, 225.1, 146.1.

HRMS (ESI): calcd for $C_{15}H_{18}NO_2$ $[M+H]^+$ 244.1335 found 244.1338.

Enzymatic resolution of 2-(quinolin-8-yloxy)cyclohexan-1-ol **(17)**

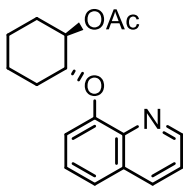

To a solution of racemic alcohol (**17**) (0.30 g, 1.2 mmol) in dry THF (5 mL), lipase (0.9 g, 300% w/w, Steapsin) and vinyl acetate (0.57 mL, 6.1 mmol) were added and the reaction mixture was stirred for 6d at 30 ^{o}C. The material was filtered and the filtrate was concentrated under vacuum. The crude mixture was separated by column chromatography on silica gel using ethyl acetate/ petroleum ether as eluent. The acetate (*R*,*R*)-**18** was eluted with 30% ethyl acetate. (0.13 g, 37%). $[\boldsymbol{\alpha}]_{\boldsymbol{D}}^{\mathbf{25}}$ = (-23.16) (c = 1, $CHCl_3$)

^{1}H NMR ($CDCl_3$, 400 MHz): δ ppm 8.91-8.07 (m, 1H), 8.09-8.07 (d, *J* = 8.4 Hz, 1H), 7.45-7.40 (m, 1H), 7.39-7.35 (m, 2H), 7.27-7.25 (d, *J* = 7.2 Hz, 1H), 5.22-5.07 (m, -C*H*OAc, 1H), 4.60-4.55 (m, -C*H*OAr,1H), 2.70-2.35 (m, 1H), 2.16-2.13 (m, 1H), 1.85-1.82 (m, 2H), 1.79-1.72 (m, 4H, -COCH_3 included), 1.46-1.35 (m, 3H).

^{13}C NMR ($CDCl_3$, 100 MHz): δ ppm 170.3, 154.6, 149.3, 141.1, 135.8, 129.6, 126.5, 121.4, 120.3, 112.5, 79.4, 74.8, 30.1, 29.9, 23.4, 23.1, 21.1.

IR (KBr) υ cm^{-1}: 3039, 2940, 1736, 1639, 1596, 1468, 1373, 1102, 1038, 731.

Mass (ESI): m/z 309 M+Na (100%).

HRMS (ESI): calcd for $C_{17}H_{20}NO_2$ $[M+H]^+$ 286.1443 found 286.1456.

HPLC condition: Lux Amylose column, 30% iso-propanol in hexane, flow rate 1.0 mL/min, UV 254 nm, retention time 18.5 min for (*S*,*S*)-isomer, 21.5 min for (*R*,*R*)-isomer.

The unreacted alcohol was eluted with 50 % ethyl acetate in petroleum ether. (0.16 g, 53%). $[\boldsymbol{\alpha}]_{\boldsymbol{D}}^{\mathbf{25}}$ = (160.5) (c = 1, $CHCl_3$)

HPLC condition: Chiralcel OD-H column, 30% iso-propanol in hexane, flow rate 1.0 mL/min, UV 254 nm, retention time 4.94 min for (*R*,*R*)-isomer, 7.74 min for (*S*,*S*)-isomer.

Determination of Absolute Configuration: Synthesis of (*R*,*R*,*R*)-**19**

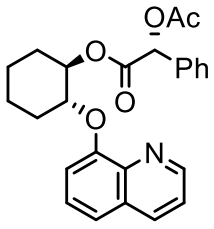

Alcohol (*R*,*R*)-**17** (0.10 g, 4.1 mmol), DCC (0.084 g, 4.1 mmol) and DMAP (0.010 g 0.8 mmol) were placed in two-necked flask under nitrogen atmosphere, were dissolved in dry dichloromethane (10 mL) and cooled to 0 ^{o}C. A solution of (R)-O-acyl mandelic acid (0.079 g, 4.1 mmol) in dichloromethane (5 mL) was then added drop wise. The reaction mixture was stirred at rt for 4h.athe reaction mixture was then filtered through Celite bed, washed with dichloromethane and purified by column chromatography over silica gel (30% ethyl

acetate/petroleum ether) affording white solid (0.13 g, 76%) M.p = 92 °C. $[\boldsymbol{\alpha}]_{\boldsymbol{D}}^{\mathbf{25}}$ = -118.9 (c = 1, $CHCl_3$)

^{1}H NMR ($CDCl_3$, 400 MHz): δ ppm 8.88-8.87 (dd, *J* = 4.0, 1.2 Hz, 1H), 8.11-8.09 (dd, *J* = 8.0, 2.4 Hz, 1H), 7.42-7.40 (dd, *J* = 8.4, 3.2, 1H), 7.36-7.33 (dd, *J* = 8.4, 4.0 Hz, 2H), 7.20-7.18 (m, 2H), 7.03-7.00 (m, 1H), 6.92-6.89 (m, 1H), 6.81-6.78 (t, *J* = 7.6 Hz, 2H), 5.85 (s, -C*H*OAc, 1H), 5.31-5.27 (m, -C*H*OCO, 1H), 4.52-4.48 (m, -C*H*OAr, 1H), 2.27-2.26 (m, 1H), 2.13 (s, 3H), 2.09-2.01 (m, 1H), 1.87-1.81 (m, 1H), 1.79-1.74 (m, 2H), 1.57-1.27 (m, 4H).

^{13}C NMR ($CDCl_3$, 100 MHz): δ ppm 170.4, 168.1, 153.8, 149.0, 140.7, 135.7, 133.3, 129.6, 128.5, 128.0, 127.3, 126.5, 121.4, 119.7, 110.3, 75.5, 74.5, 29.6, 29.4, 23.1, 23.0, 20.7.

IR (KBr) υ cm^{-1}: 3046, 2939, 1759, 1738, 1564, 1464, 1372, 1104, 1053, 758.

Mass (ESI): m/z 443.1 (M+Na) (100%).

HRMS (ESI): calcd for $C_{25}H_{26}NO_5$ $[M+H]^+$ 420.1811 found 420.1807.

Synthesis of *trans*-2-(*N*-Methyl-*N*-phenylamino)cyclohexanol (**21**):

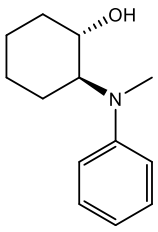

A solution of an cyclohexenoxide (0.5 g, 5.0 mmol) and *N*-methyl aniline (0.7 g, 6.6 mmol) in anhydrous ether (15 mL) was treated with $Cu(OTf)_2$ (5 mol %) and stirred for 24 h at room temperature. The solvent was then removed on a rotary evaporator, and the crude product was purified over silica gel by column chromatography to provide pure amino alcohol (**21**) as colorless oil. (1.2 g, 86%). $[\boldsymbol{\alpha}]_{\boldsymbol{D}}^{\mathbf{25}}$ = (-77.3) (c = 5, CH_2Cl_2)[24b]

^{1}H NMR ($CDCl_3$, 400MHz): δ 7.27-7.23 (m, 2H), 6.95-6.93 (m, 2H), 6.83-6.79 (m, 1H), 3.66-3.62 (dt, *J* = 10.2, 4.8 Hz, 1H, -C*H*OH), 3.43-3.39 (m, 1H, -C*H*NMe), 2.78-2.75 (m, 4H, -N*CH*$_3$ signal merged), 2.23-2.11 (m, 1H), 1.77-1.72 (m, 3H), 1.42-1.38 (m, 2H), 1.29-1.26 (m, 2H).[23]

IR (neat): 3434, 3026, 2932, 1598, 1501, 1451, 1393, 1073, 859 cm^{-1}.

Enzymatic Resolution of *trans*-2-(*N*-Methyl-*N*-phenylamino)cyclohexanol (**21**):

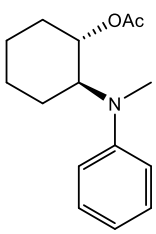

To a solution of racemic alcohol (**21**) (0.30 g, 1.5 mmol) in dry THF (5 mL), lipase (0.9 g, 300% w/w, Steapsin) and vinyl acetate (1.41 mL, 15 mmol) were added and the reaction mixture was stirred for 9 d at rt. The material was filtered and the filtrate was concentrated under vacuum. The crude mixture was separated by column chromatography on silica gel

using ethyl acetate/ petroleum ether as eluent. The acetate (*R*,*R*)-**22** was eluted with 5% ethyl acetate as colorless oil. (0.17 g, 47%). $[\boldsymbol{\alpha}]_{\boldsymbol{D}}^{\mathbf{25}}$ = (148.0) (c = 1, $CHCl_3$).

^{1}H NMR ($CDCl_3$, 400MHz): δ7.25-7.21 (m, 2H), 6.84-6.82 (m, 2H), 6.73-6.69 (m, 1H), 5.02-5.00 (dt, *J* = 10.2, 4.8 Hz, 1H, -C*H*OAc), 3.72-3.69 (m, 1H, -C*H*NMe), 2.73 (s, 3H, -NC*H*$_3$), 2.11-2.07 (m, 1H), 1.84-1.71 (m, 3H), 1.61 (s, 3H), 1.57-1.41 (m, 2H), 1.36-1.24 (m, 2H). [24]

IR (neat): 3026, 2936, 1734, 1598, 1451, 1368, 1242, 1040, 994 cm^{-1}.

HPLC condition: Chiralcel OD H column, 5% iso-propanol in hexane, flow rate 0.5 mL/min, UV 254 nm, retention time 9.1 min for (R,R)-isomer, 10.2 min for (S,S)-isomer.

The unreacted alcohol was eluted with 50 % ethyl acetate in petroleum ether. (0.16 g, 53%). $[\boldsymbol{\alpha}]_{\boldsymbol{D}}^{\mathbf{25}}$ = (160.5) (c = 1, $CHCl_3$)

HPLC condition: Chiralcel OD H column, 5% iso-propanol in hexane, flow rate 0.5 mL/min, UV 254 nm, retention time 17.7 min for (S,S)-isomer, 19.2 min for (R,R)-isomer.

Synthesis of aminoester (**23**).

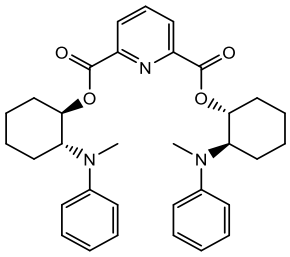

Alcohol (*S*,*S*)-**21** (0.50 g, 2.4 mmol), DCC (0.6 g, 2.9 mmol) and DMAP (0.06 g 0.5 mmol) were placed in two-necked flask under nitrogen atmosphere, were dissolved in dry dichloromethane (10 mL) and cooled to 0 ^{o}C. A solution of pyridine-2,6-dicarboxylic acid (0.49 g, 2.9 mmol) in dichloromethane (5 mL) was then added drop wise. The reaction mixture was stirred at rt for 12 h.athe reaction mixture was then filtered through Celite bed, washed with dichloromethane and purified by column chromatography over silica gel (20% ethyl acetate/petroleum ether) affording white solid. (0.45 g, 68%) %). $[\boldsymbol{\alpha}]_{\boldsymbol{D}}^{\mathbf{25}}$ = (-14.5) (c = 1, $CHCl_3$)

^{1}H NMR ($CDCl_3$, 400 MHz): δ7.44-7.40 (m, 1H), 7.32-7.30 (m, 2H), 7.15-7.11 (m, 4H), 6.83-6.81 (d, *J* = 8.0 Hz, 4H), 6.57-6.62 (t, *J* = 7.2 Hz, 2H), 5.32-5.24 (m, 2H, -C*H*OCO-), 3.97-3.90 (m, 2H, -C*H*NMe), 2.74 (s, 6H, -NC*H*$_3$), 2.28-2.25 (m, 2H), 1.95-1.92 (m, 2H), 1.88-1.79 (m, 4H), 1.75-1.65 (m, 2H)1.61-51 (m, 2H), 1.47-1.39 (m, 4H).

IR (neat): 3083, 3058, 1746, 1597, 1502, 1448, 1353, 1237, 1142 cm^{-1}.

4.5.1 Spectral Data

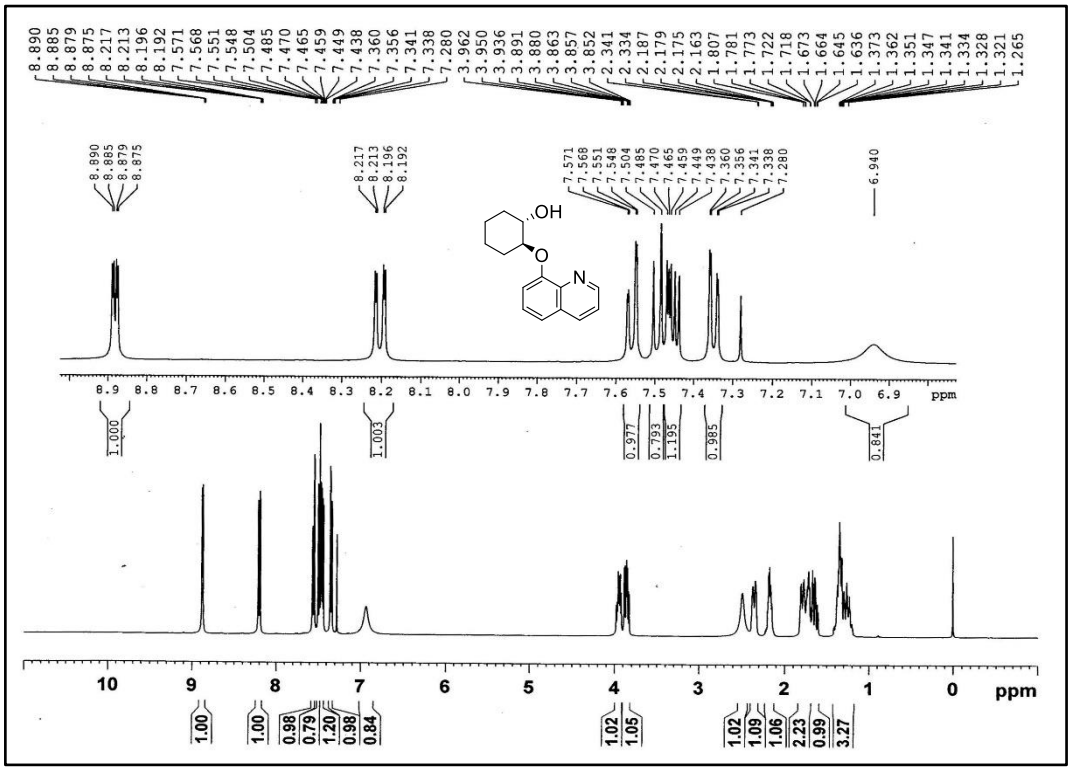

^{1}H NMR Spectra of Compound (**17**)

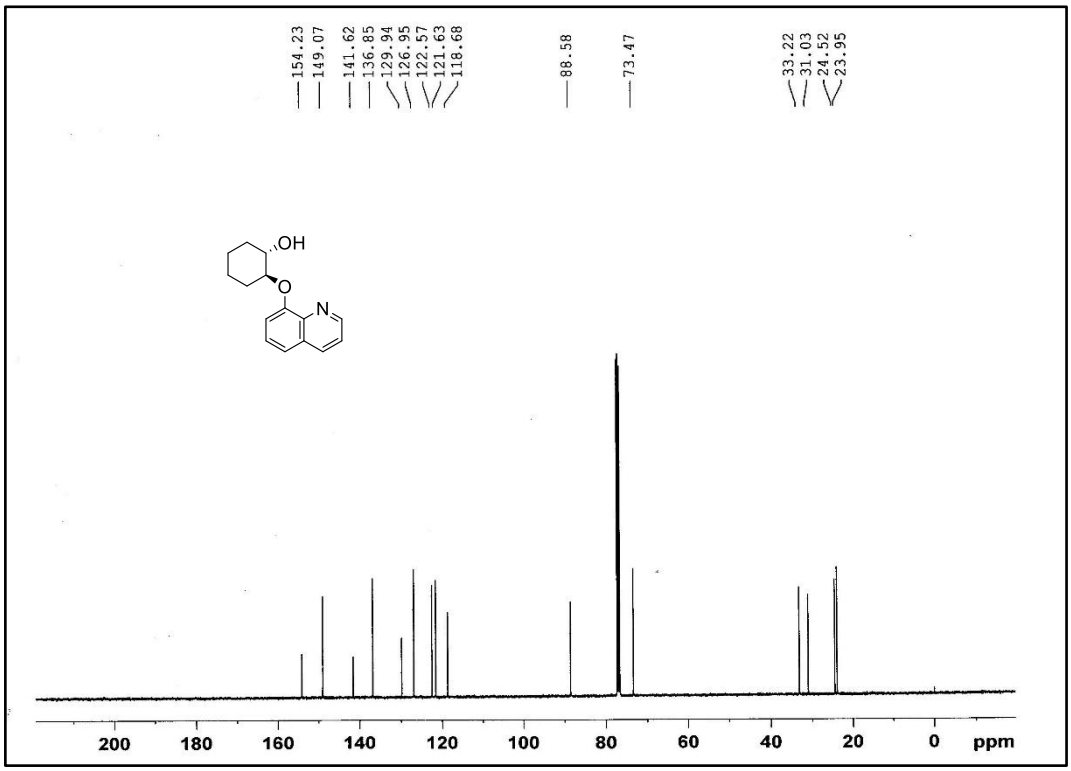

^{13}C NMR Spectra of Compound (**17**)

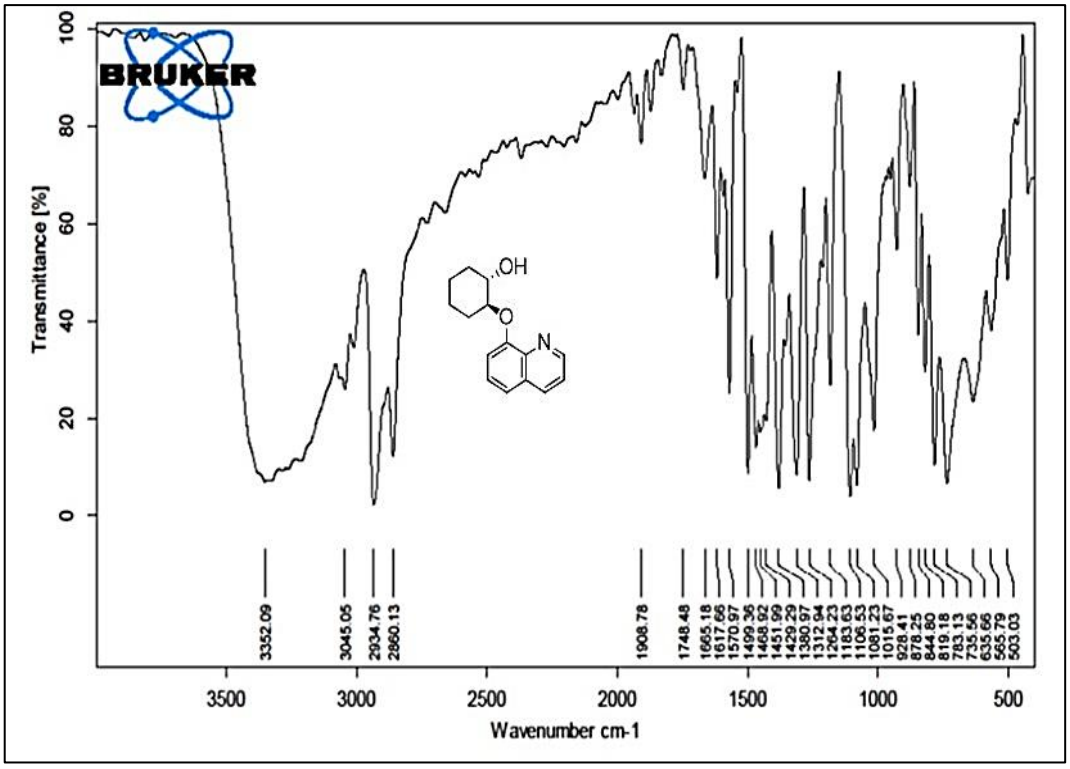

IR Spectra of Compound (**17**)

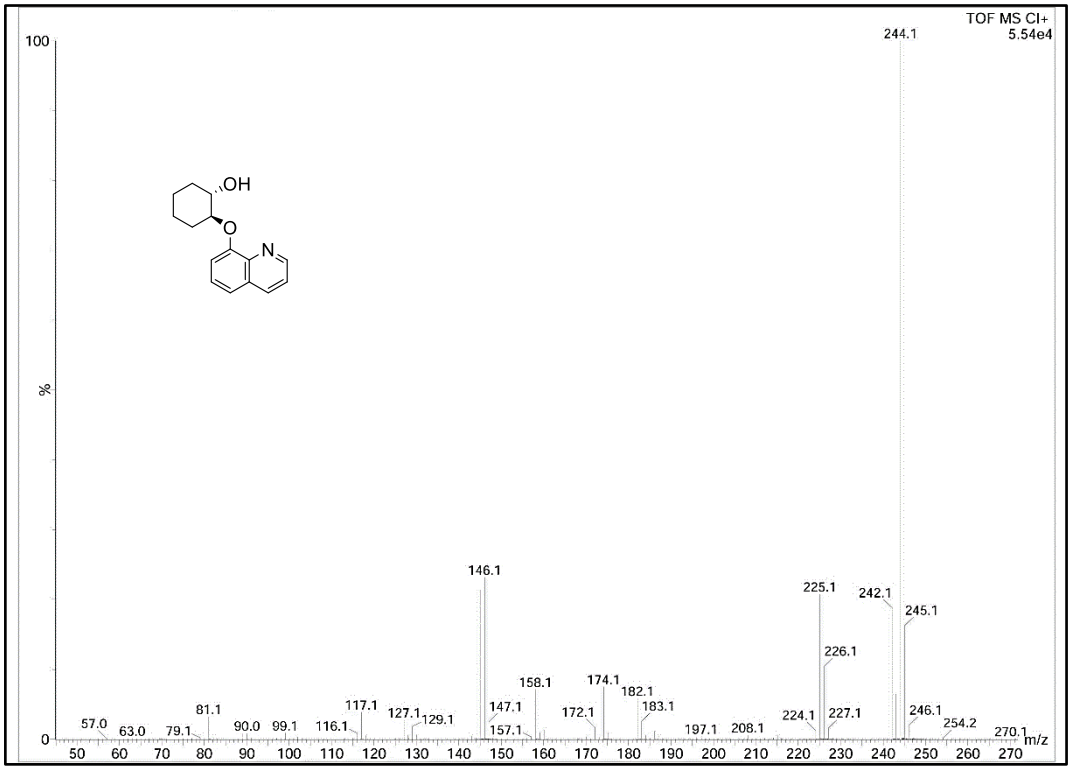

MS Spectra of Compound (**17**)

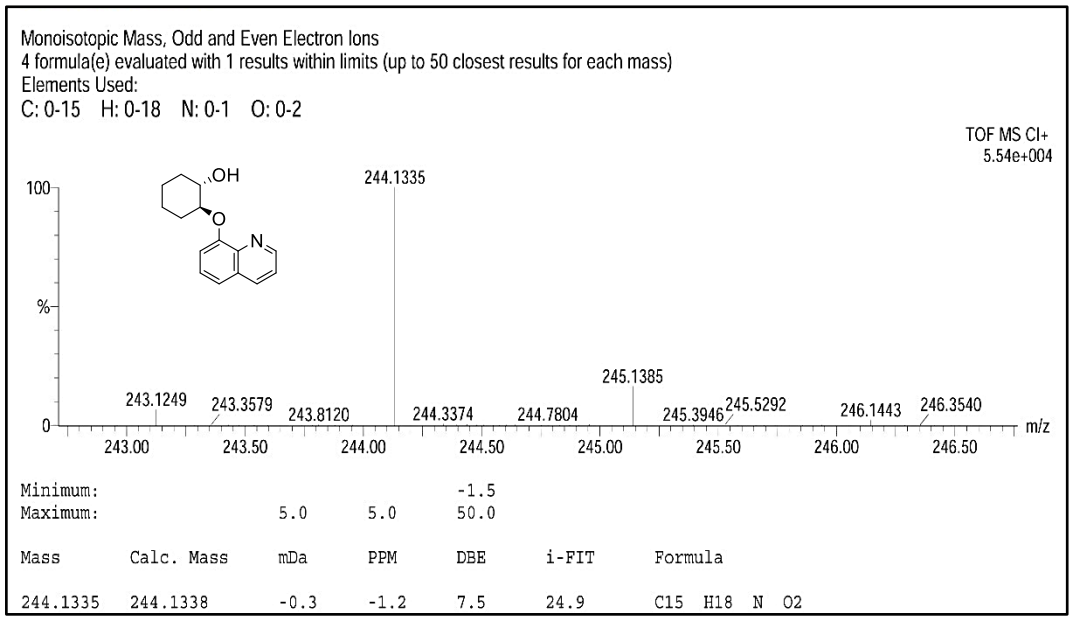

HRMS Spectra of Compound (**17**)

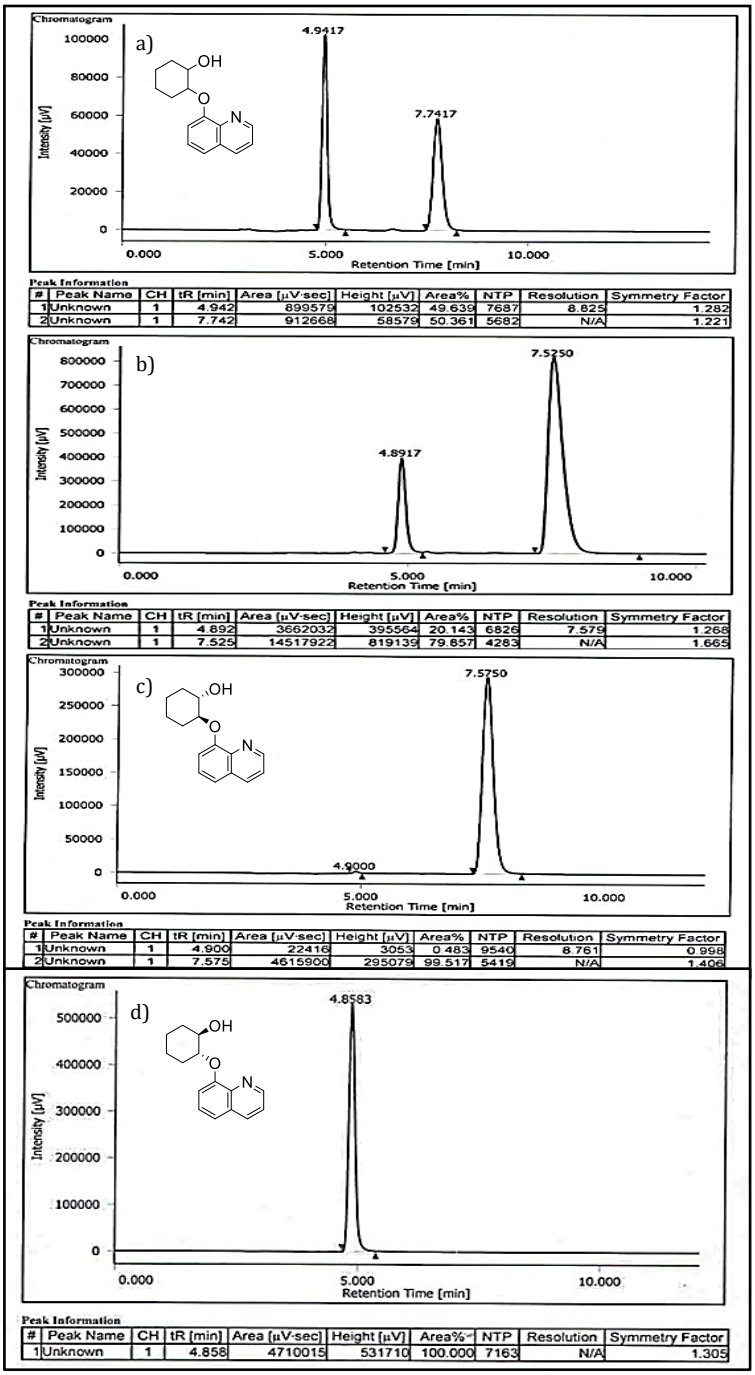

HPLC Chromatogram of a) *rac*-**17**, b) (*S*,*S*)-**17** before crystallization (60 %*ee*), c) (*S*,*S*)-**17** after crystallization and d) (*R*,*R*)-**17** after hydrolysis.
Chiralcel-OD-H column: 30% Isopropyl alcohol-Hexane,
UV=254 nm, Flow= 1.0mL/min.
R_t = 4.9 min (1st Peak) and R_t= 7.7 min (2nd Peak)

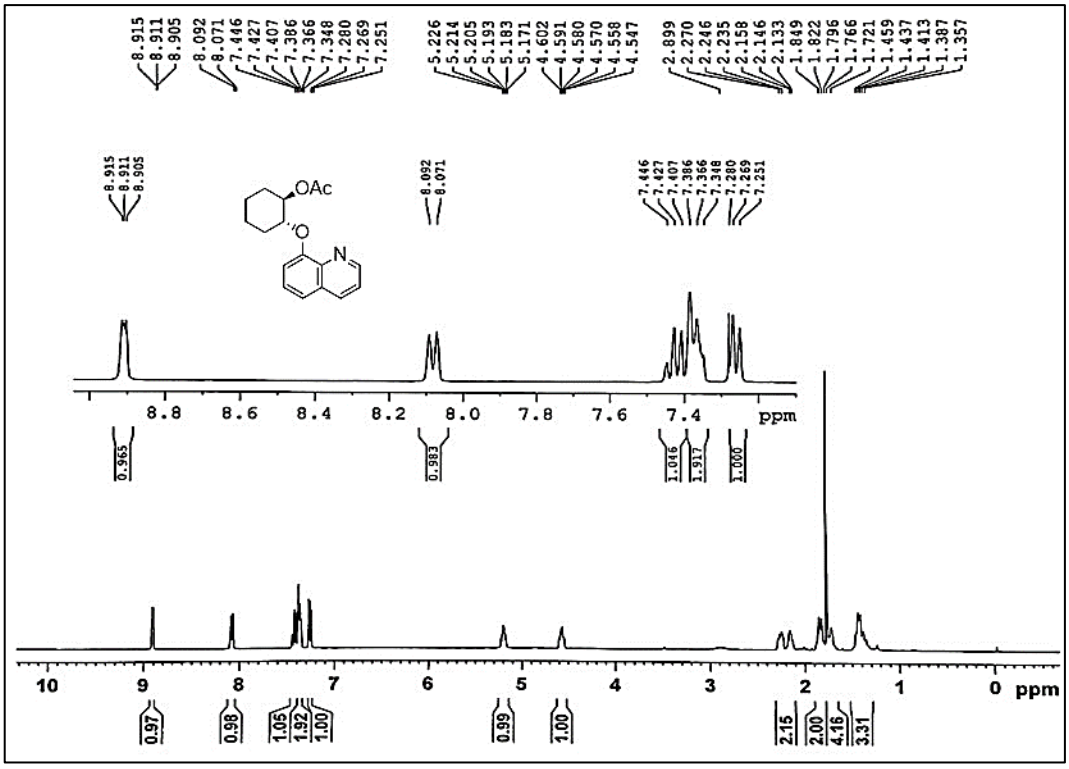

^{1}H NMR Spectra of Compound (**18**)

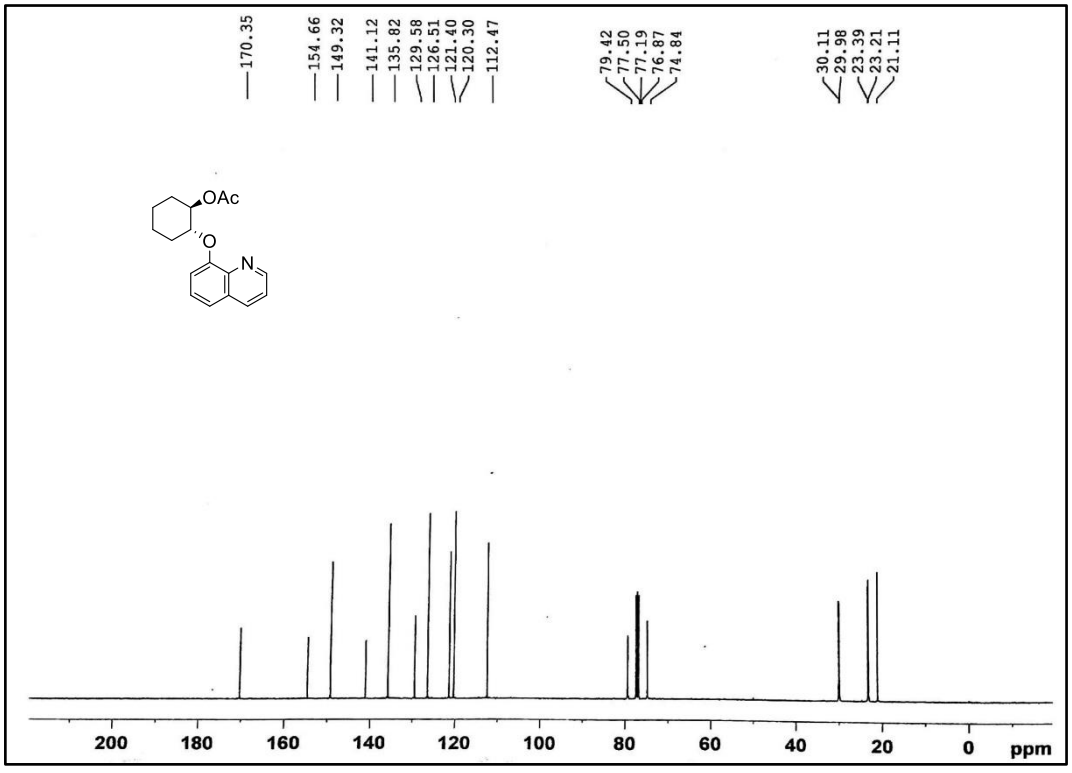

^{13}C NMR Spectra of Compound (**18**)

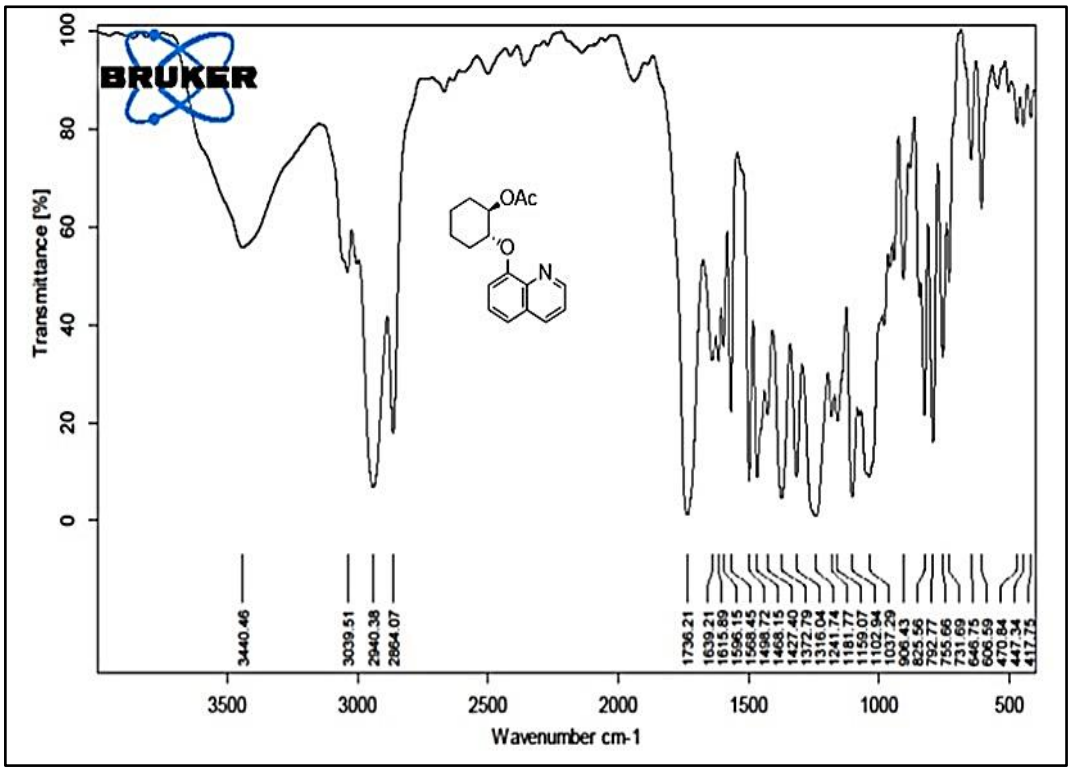

IR Spectra of Compound (**18**)

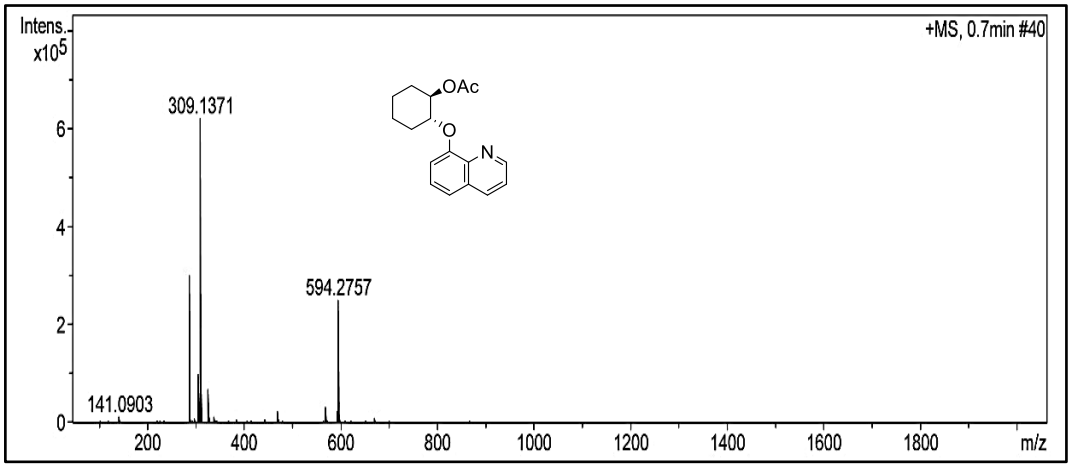

MS Spectra of Compound (**18**)

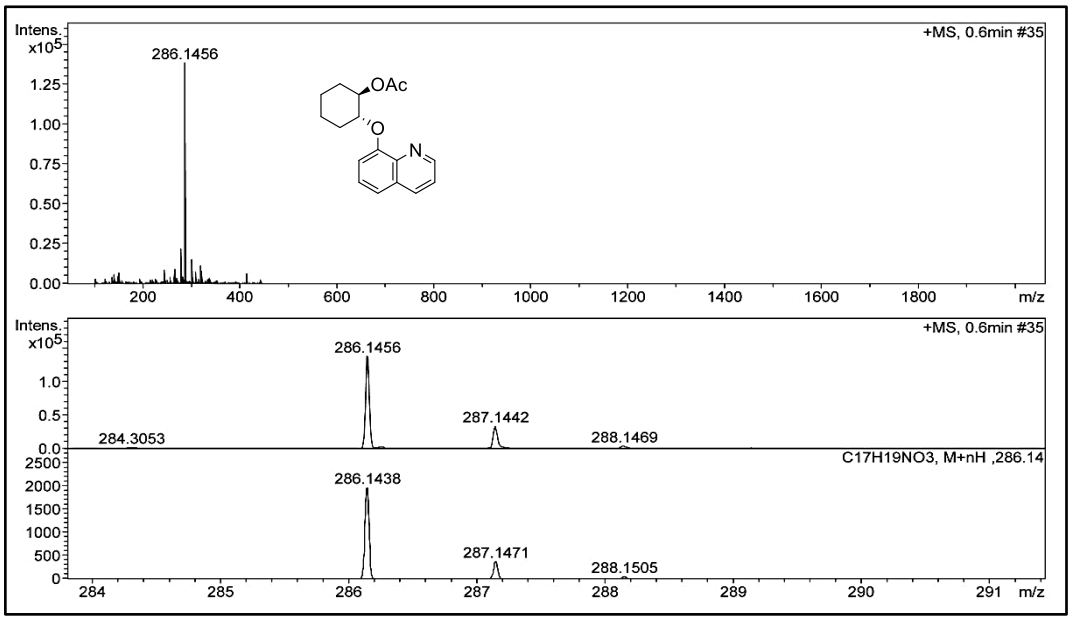

HRMS Spectra of Compound (**18**)

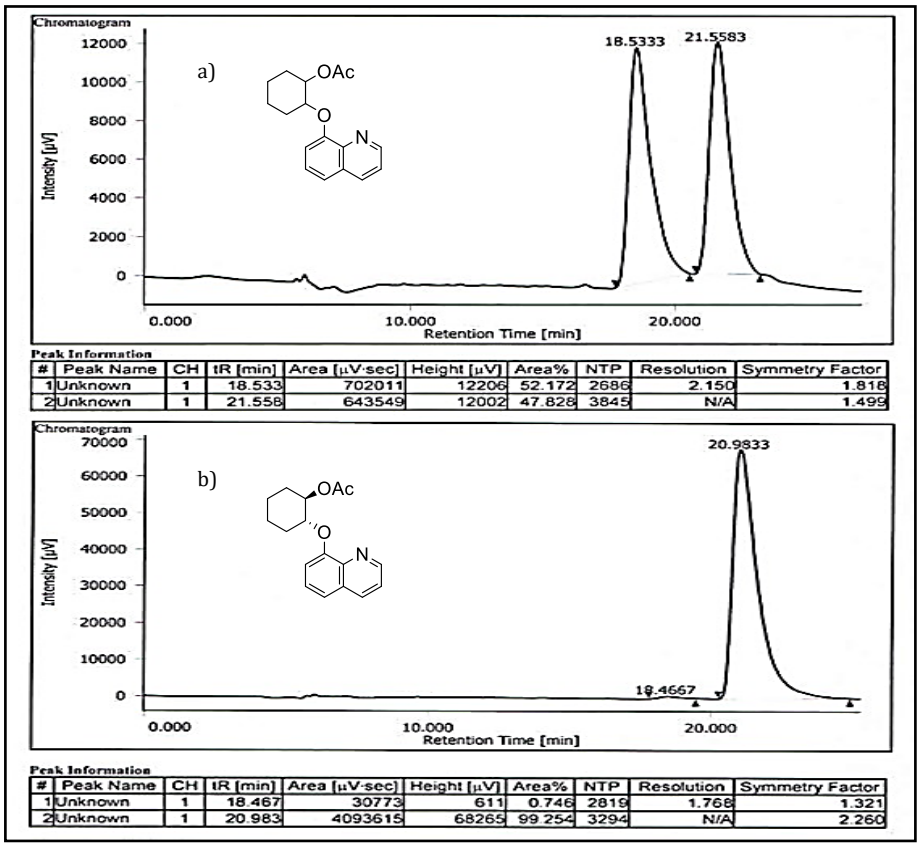

HPLC Chromatogram of a) *rac*-**18** and b) (*R*,*R*)-**18**
Lux Amylose column: 30% Isopropyl alcohol-Hexane,
UV=254 nm, Flow= 1.0 mL/min.
R_t = 18.5 min (1st Peak) and R_t= 21.5 min (2nd Peak)

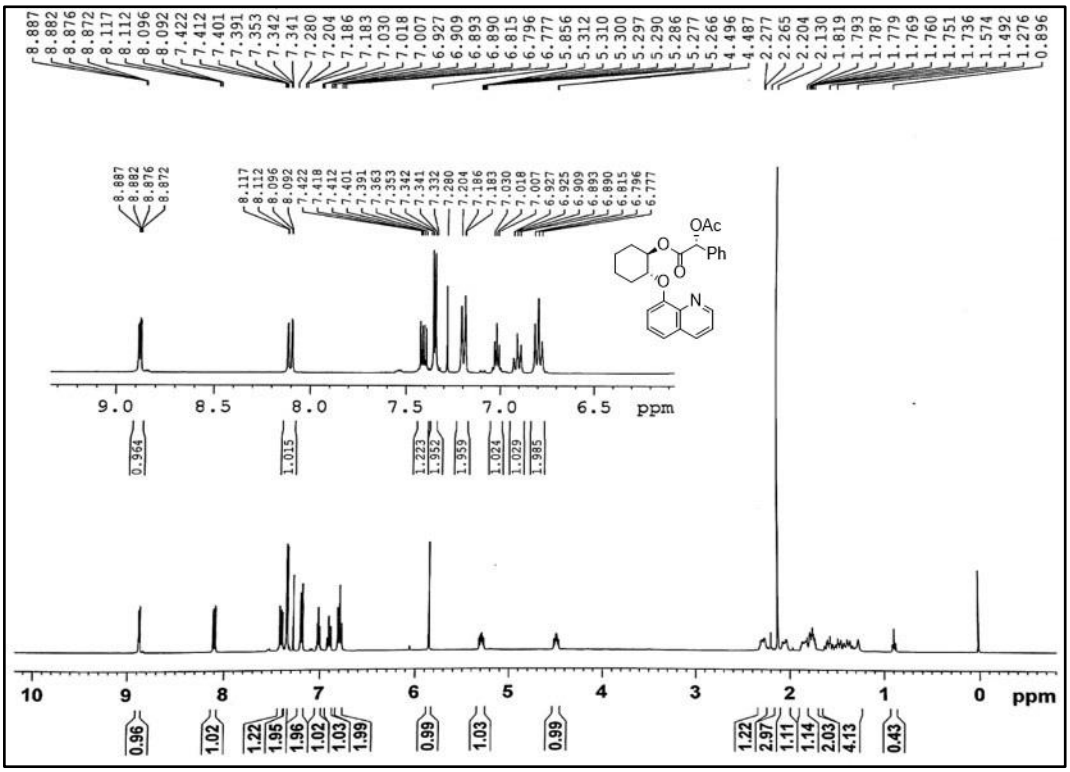

^{1}H NMR Spectra of Compound (**19**)

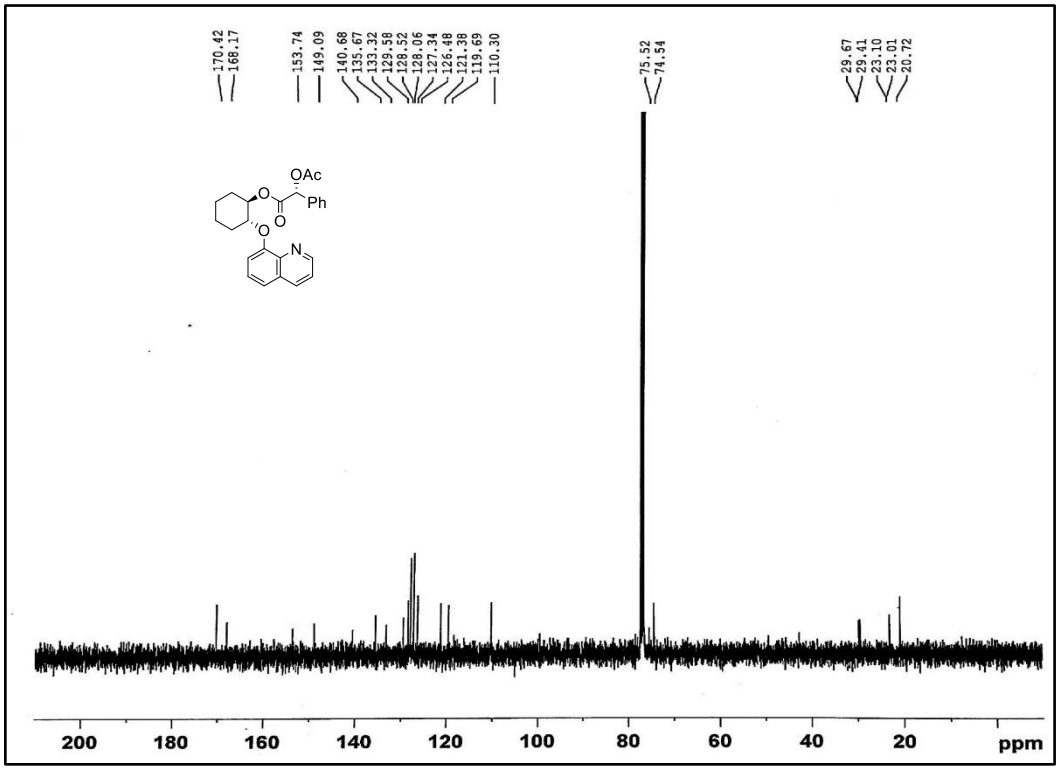

^{13}C NMR Spectra of Compound (**19**)

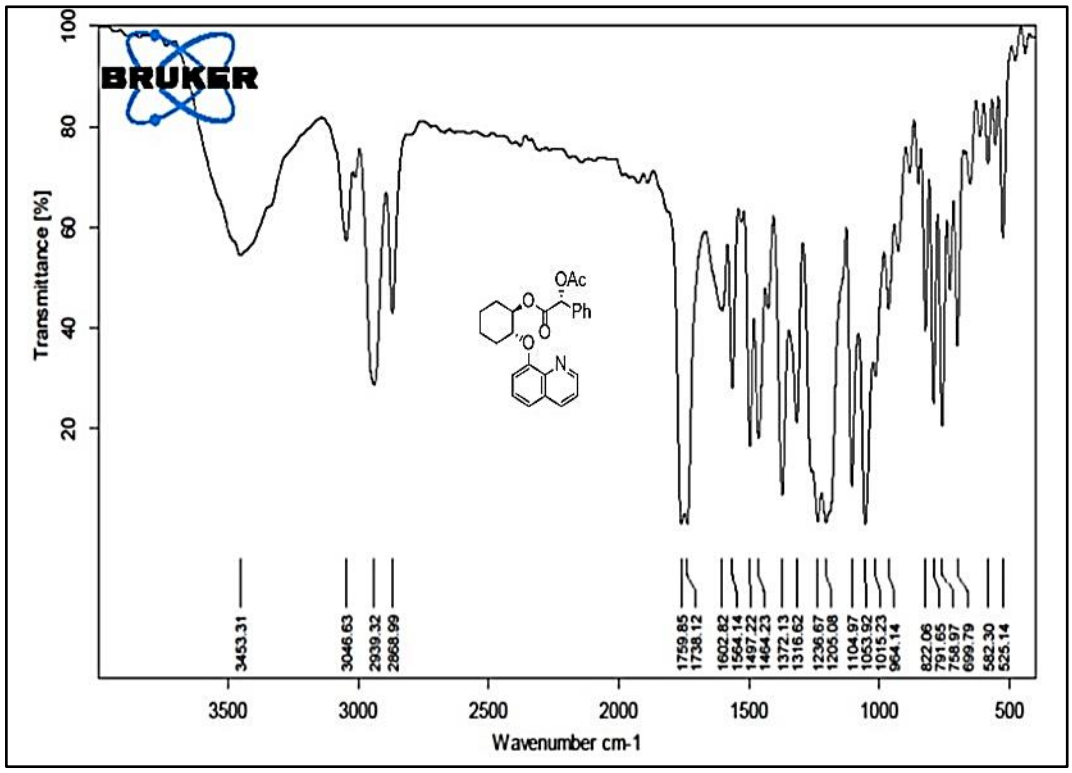

IR Spectra of Compound (**19**)

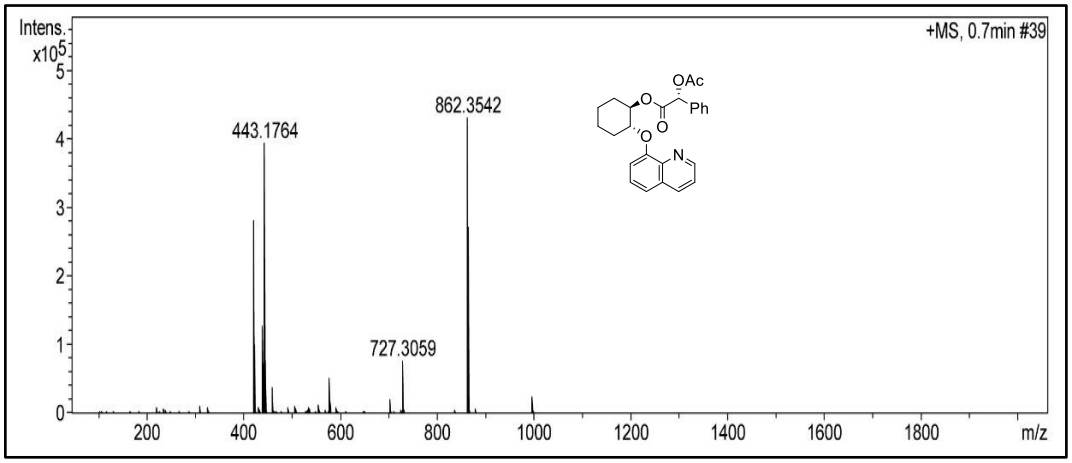

MS Spectra of Compound (**19**)

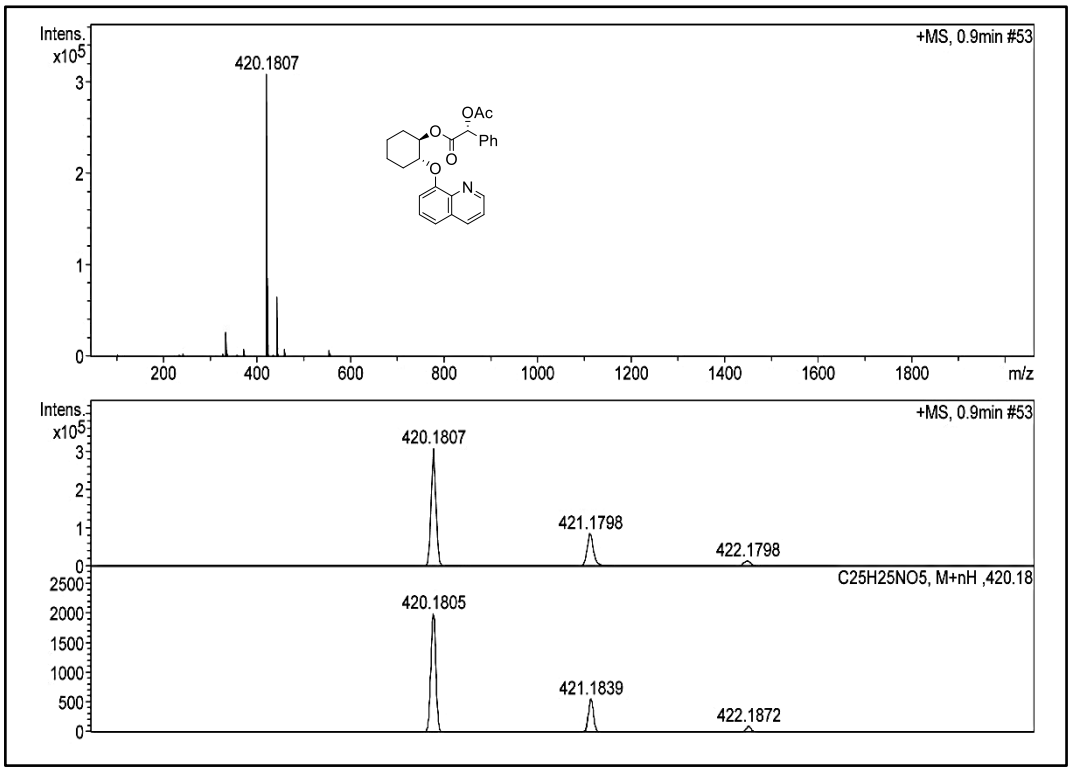

HRMS Spectra of Compound (**19**)

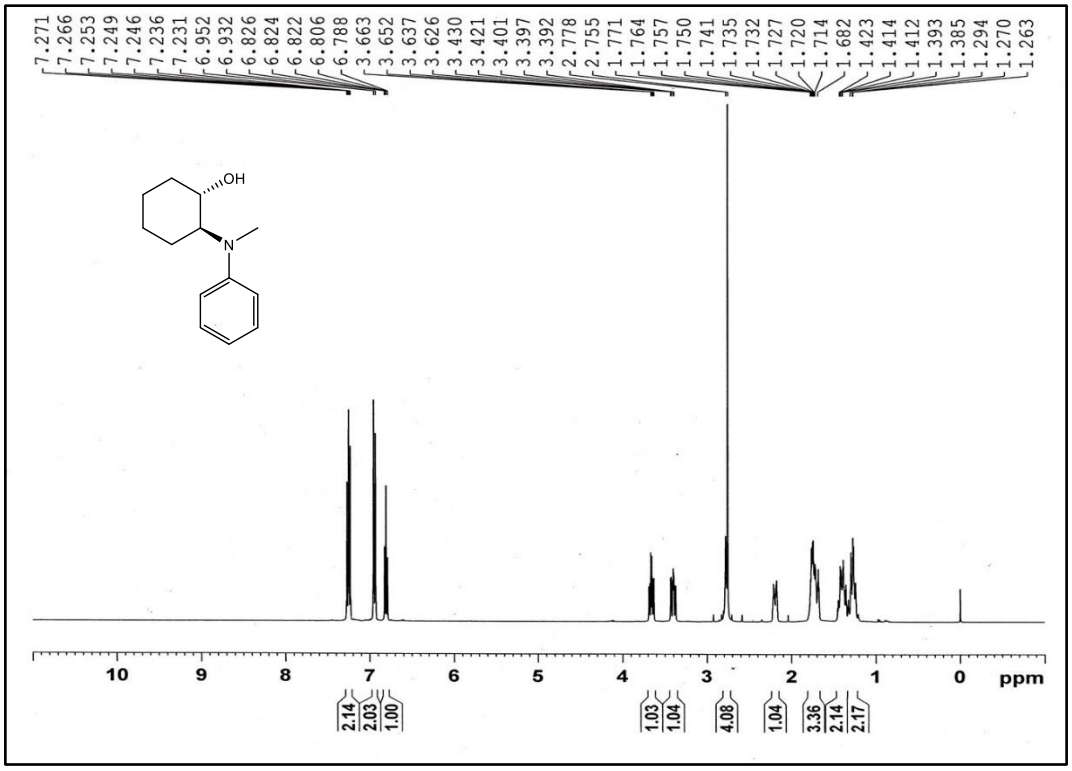

^{1}H NMR Spectra of Compound (**21**)

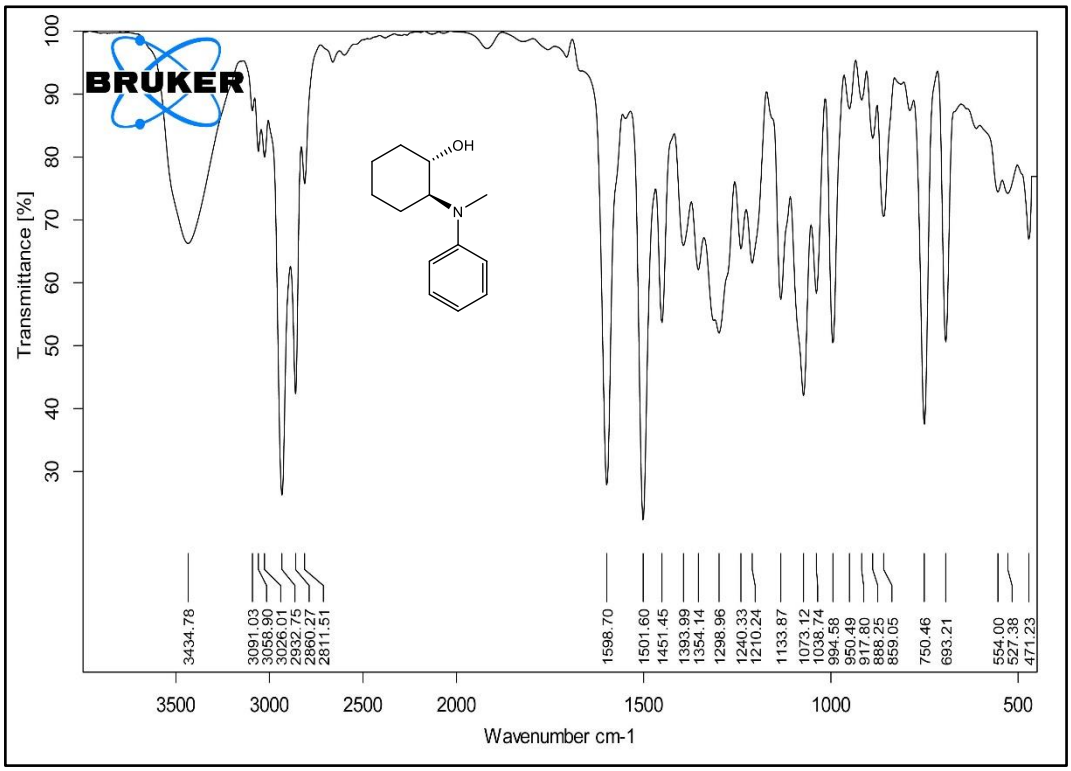

IR Spectra of Compound (**21**)

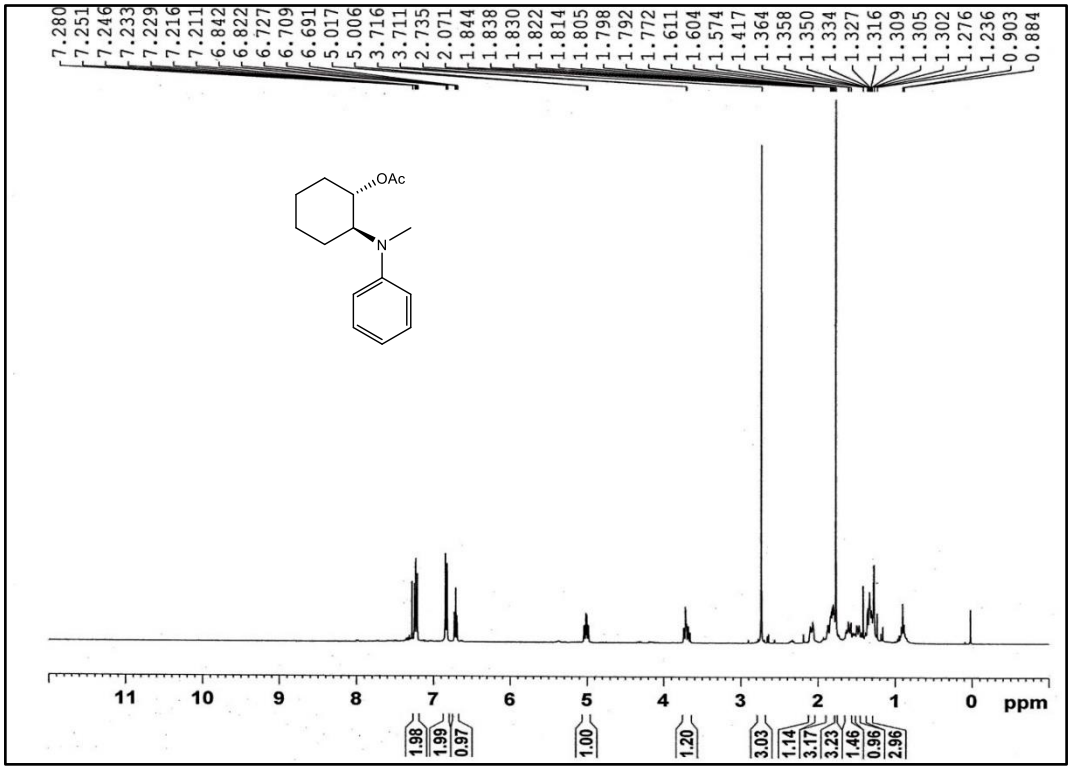

^{1}H NMR Spectra of Compound (**22**)

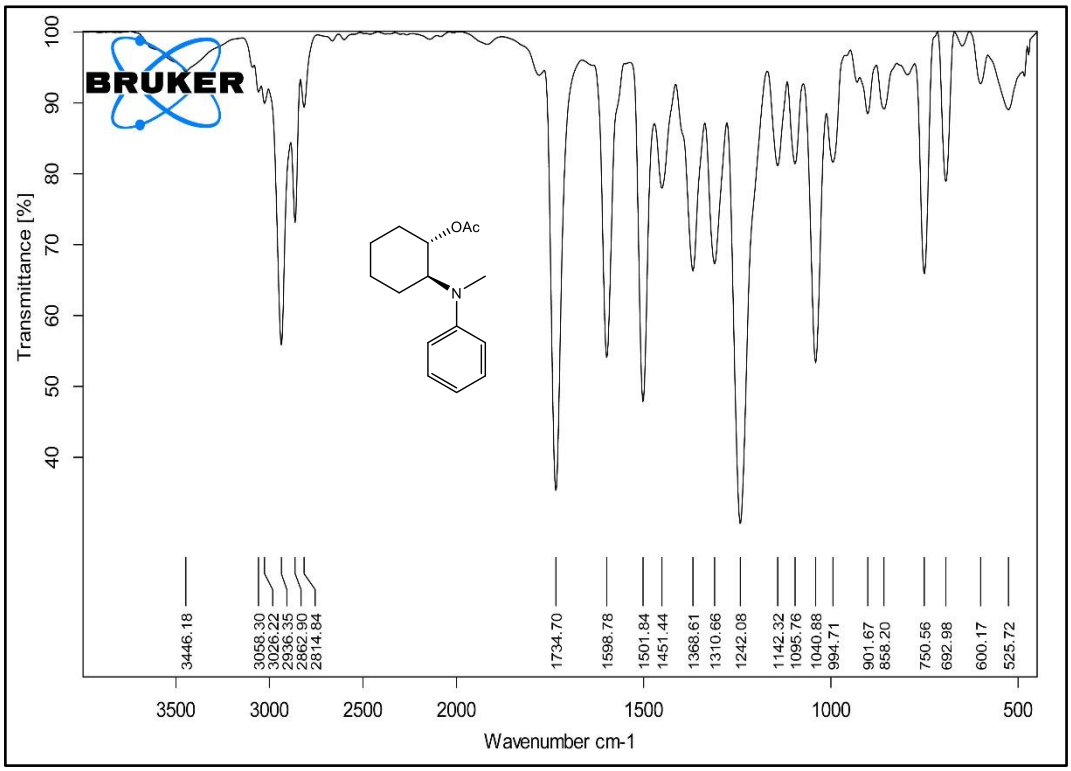

IR Spectra of Compound (**22**)

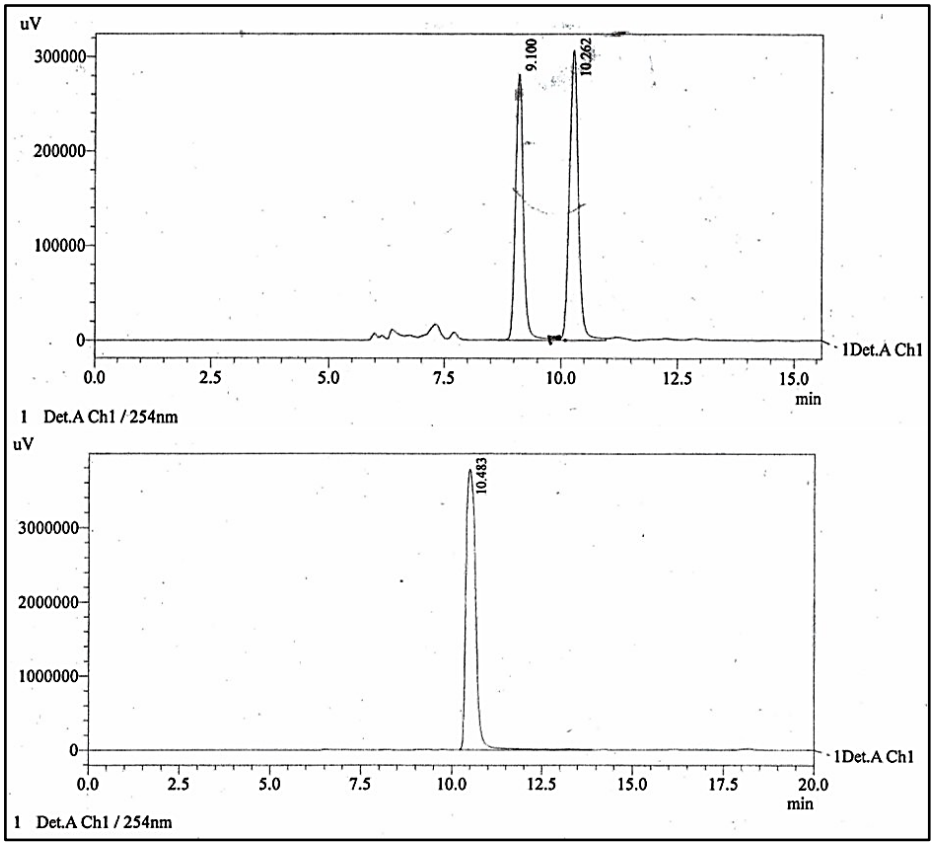

HPLC Chromatogram of Compound (**22**) racemic top; (*R*,*R*)-**22** bottom

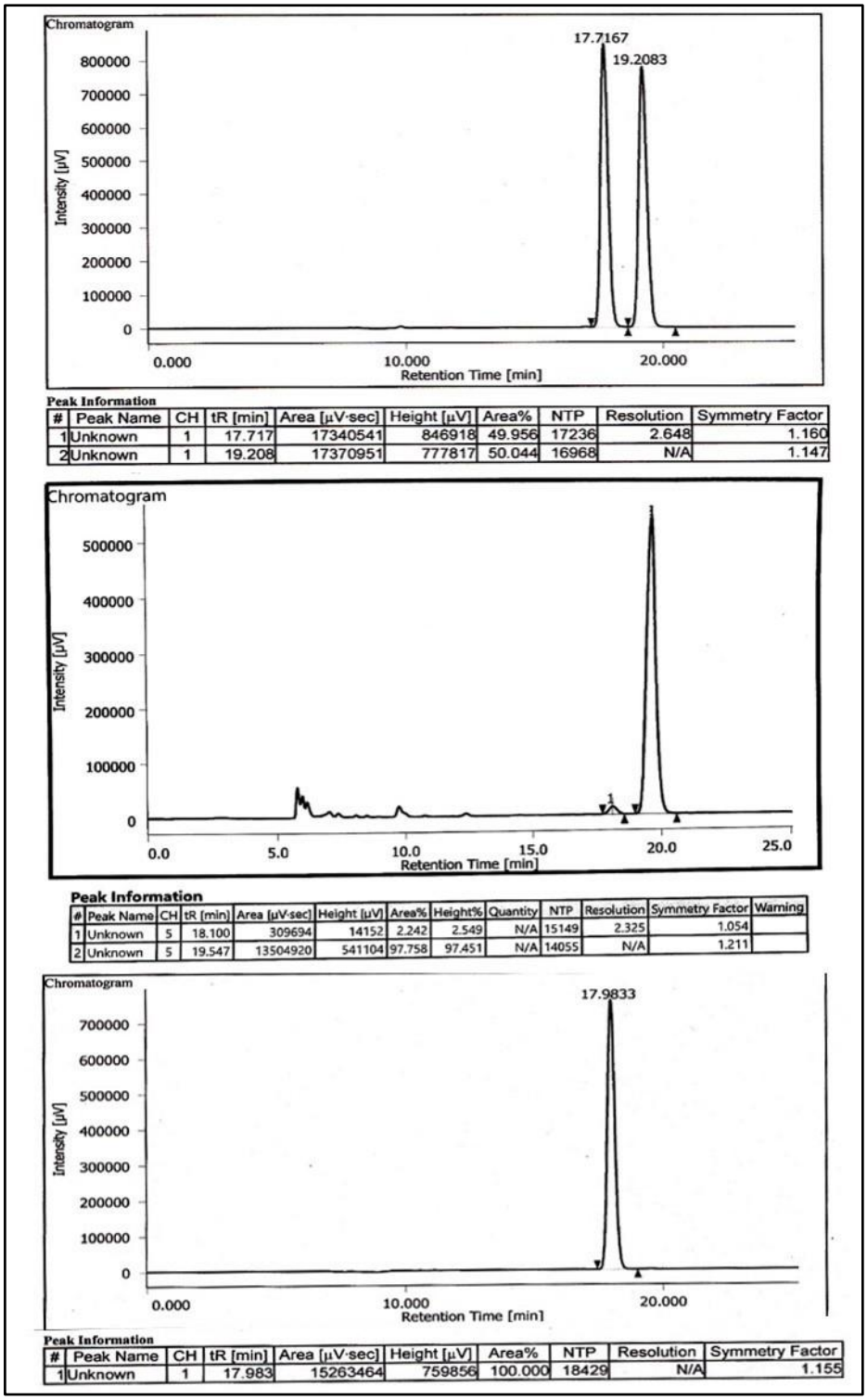

Peak Information

#	Peak Name	CH	tR [min]	Area [μV·sec]	Height [μV]	Area%	NTP	Resolution	Symmetry Factor
1	Unknown	1	17.717	17340541	846918	49.956	17236	2.648	1.160
2	Unknown	1	19.208	17370951	777817	50.044	16968	N/A	1.147

Peak Information

#	Peak Name	CH	tR [min]	Area [μV·sec]	Height [μV]	Area%	Height%	Quantity	NTP	Resolution	Symmetry Factor	Warning
1	Unknown	5	18.100	309694	14152	2.242	2.549	N/A	15149	2.325	1.054	
2	Unknown	5	19.547	13504920	541104	97.758	97.451	N/A	14055	N/A	1.211	

Peak Information

#	Peak Name	CH	tR [min]	Area [μV·sec]	Height [μV]	Area%	NTP	Resolution	Symmetry Factor
1	Unknown	1	17.983	15263464	759856	100.000	18429	N/A	1.155

HPLC Chromatogram of Compound (**21**) racemic top; (*S*,*S*)-**21** middle; (*R*,*R*)-**21** bottom

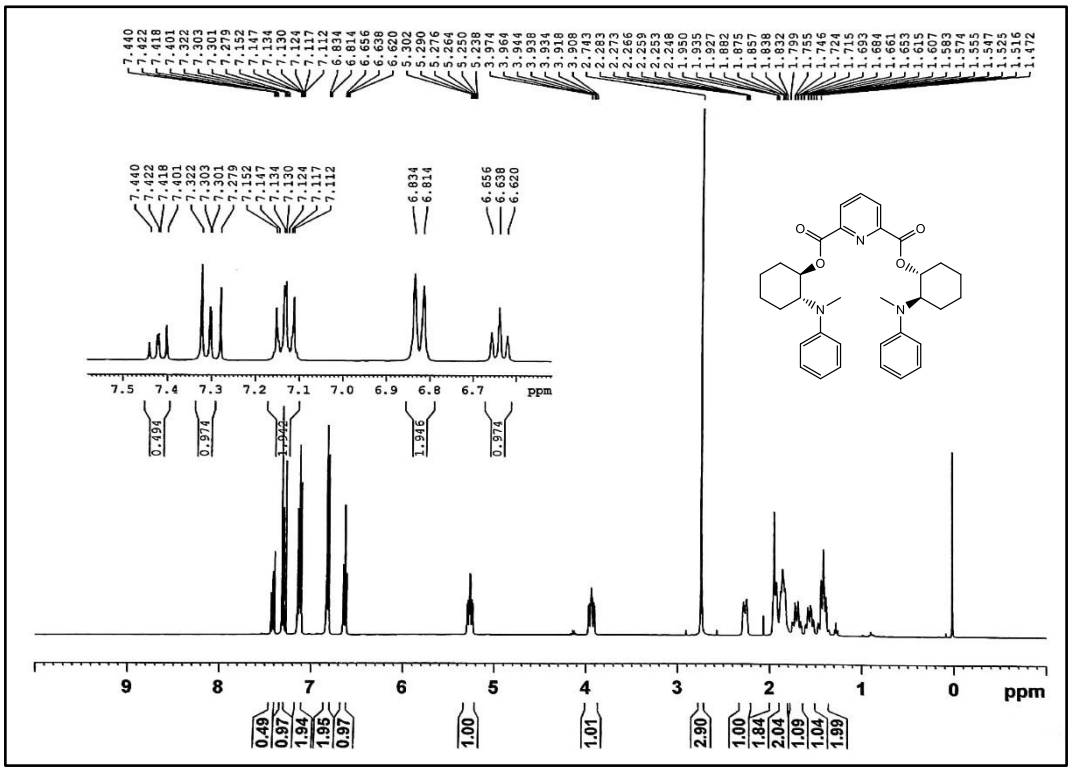

^{1}H NMR Spectra of Compound (**23**)

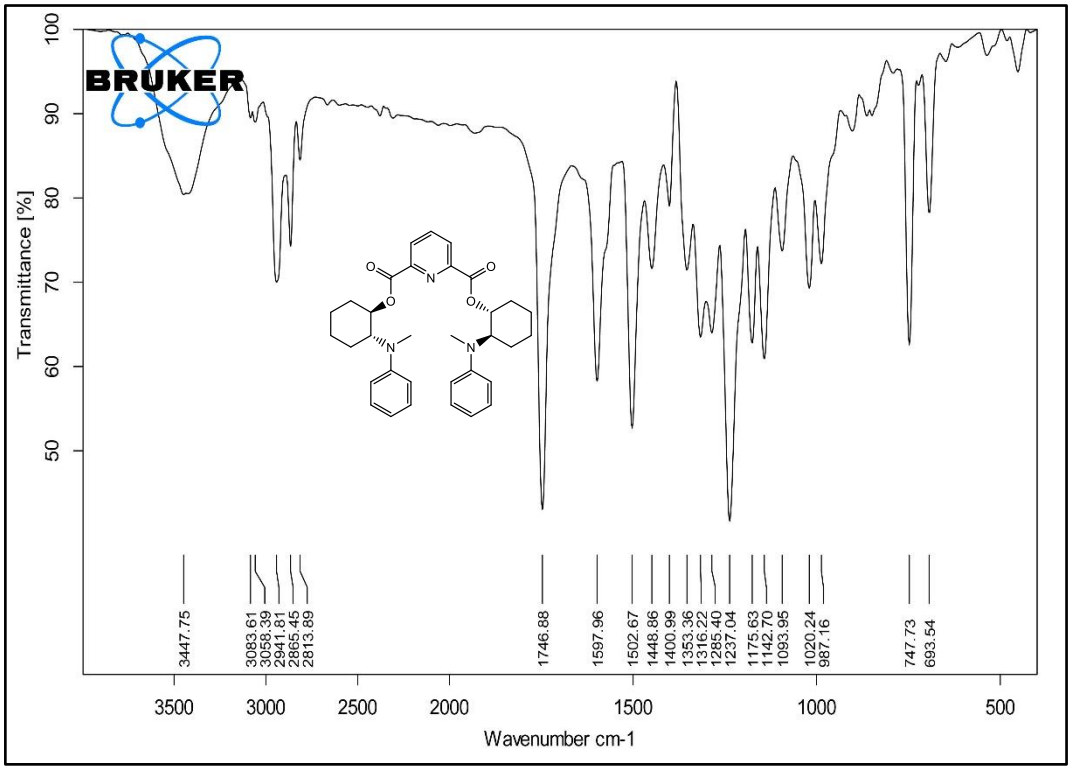

IR Spectra of Compound (**23**)

4.5.2 CSA Spectras

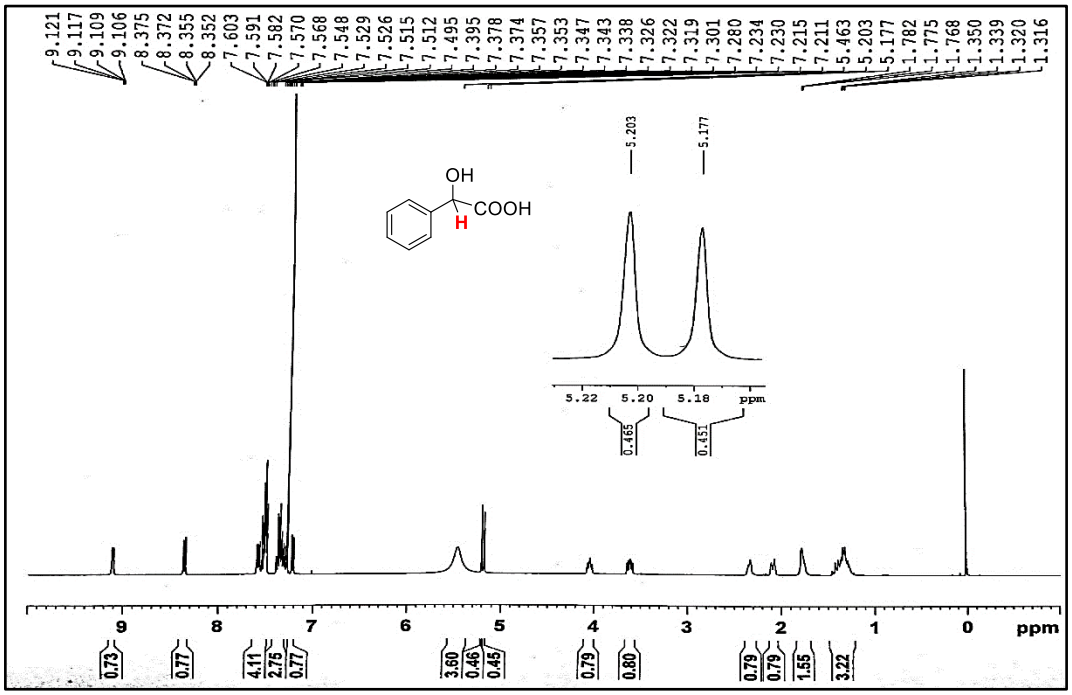

^{1}H NMR Spectra of Mandelic acid (**A-I**) with (*R,R*)-**17**

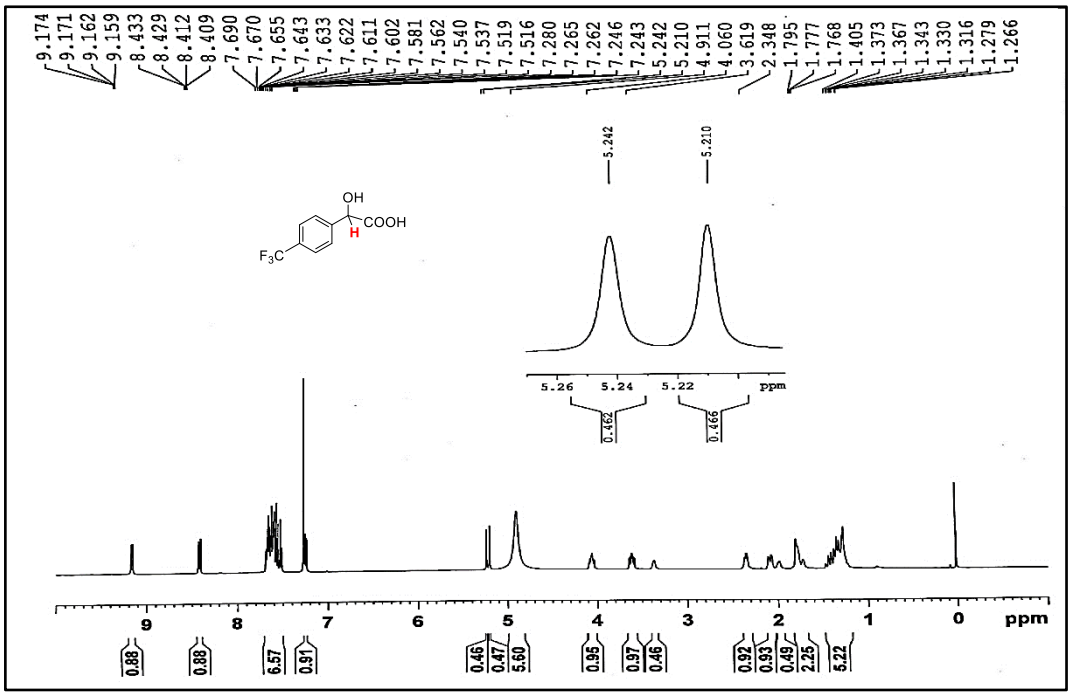

^{1}H NMR Spectra of 4-trifluoromethyl-mandelic acid (**A-II**) with (*R,R*)-**17**

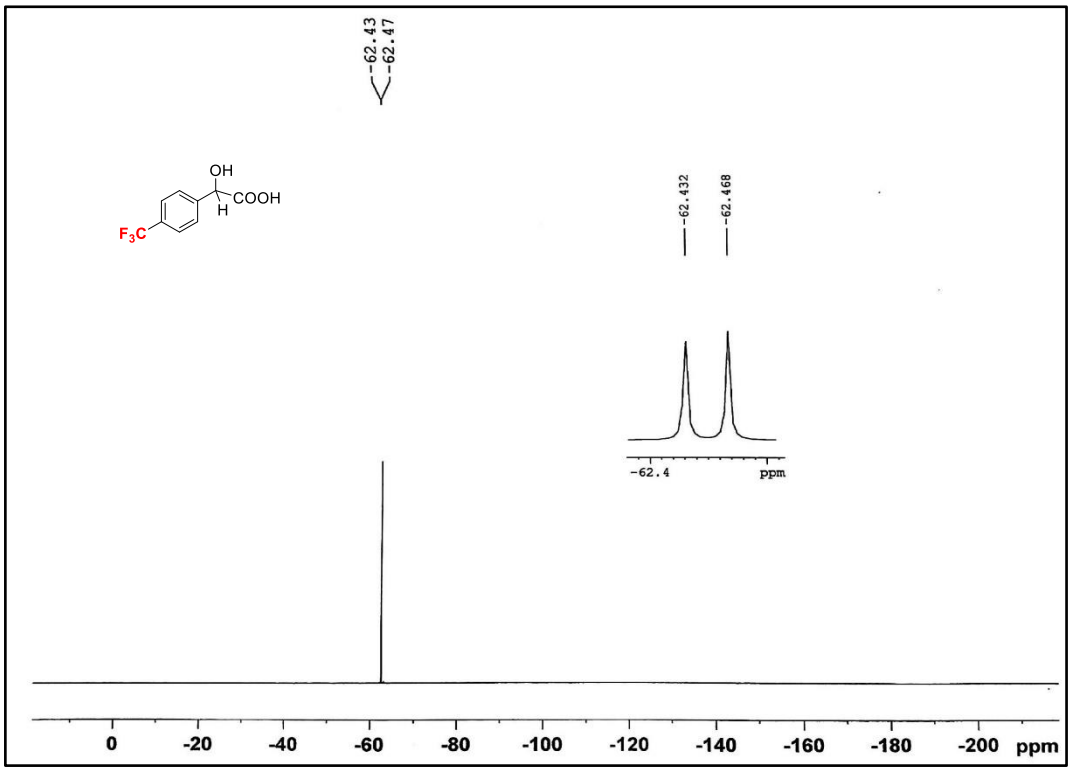

^{19}F NMR Spectra of 4-trifluoromethyl-mandelic acid (**A-II**) with (*R,R*)-**17**

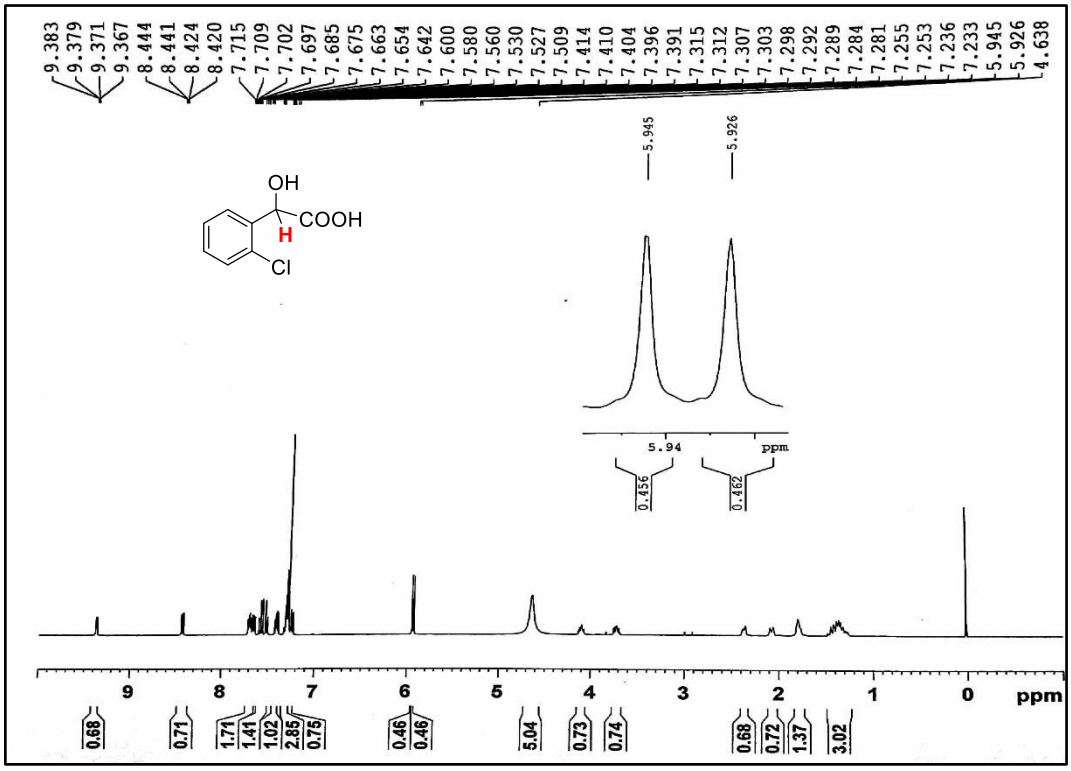

^{1}H NMR Spectra of 2-chloro-mandelic acid (**A-III**) with (*R,R*)-**17**

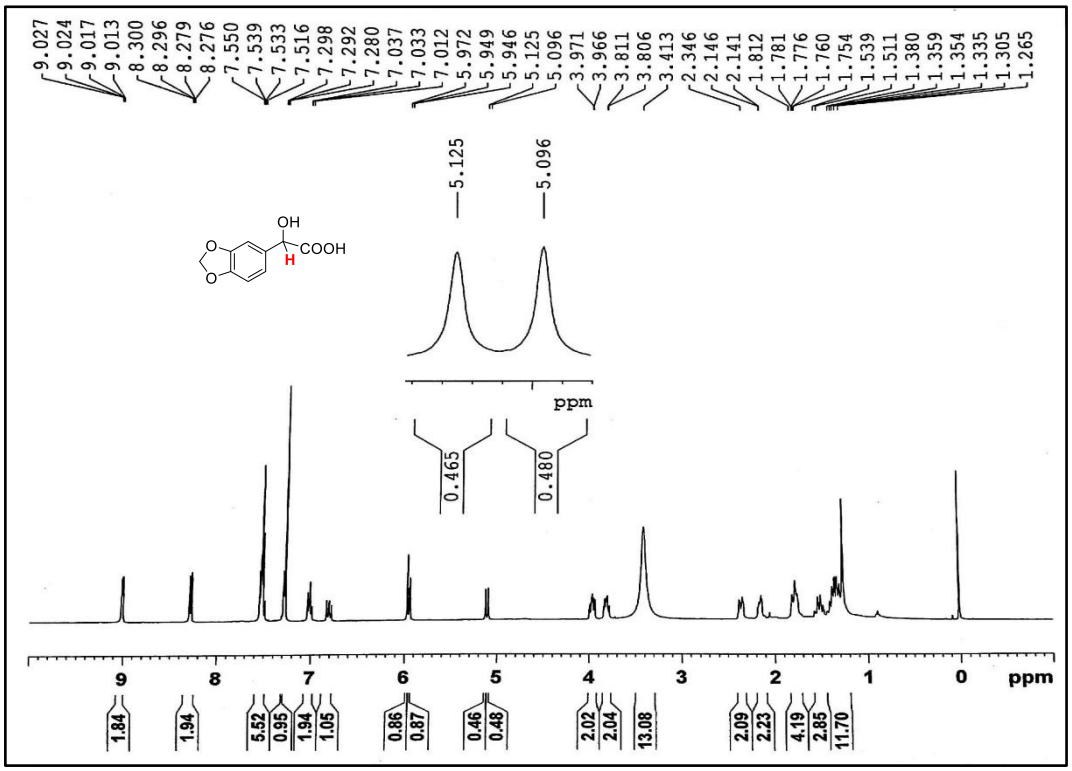

^{1}H NMR Spectra of 3,4-methylene-dioxo-mandelic acid (**A-IV**) with (*R,R*)-**17**

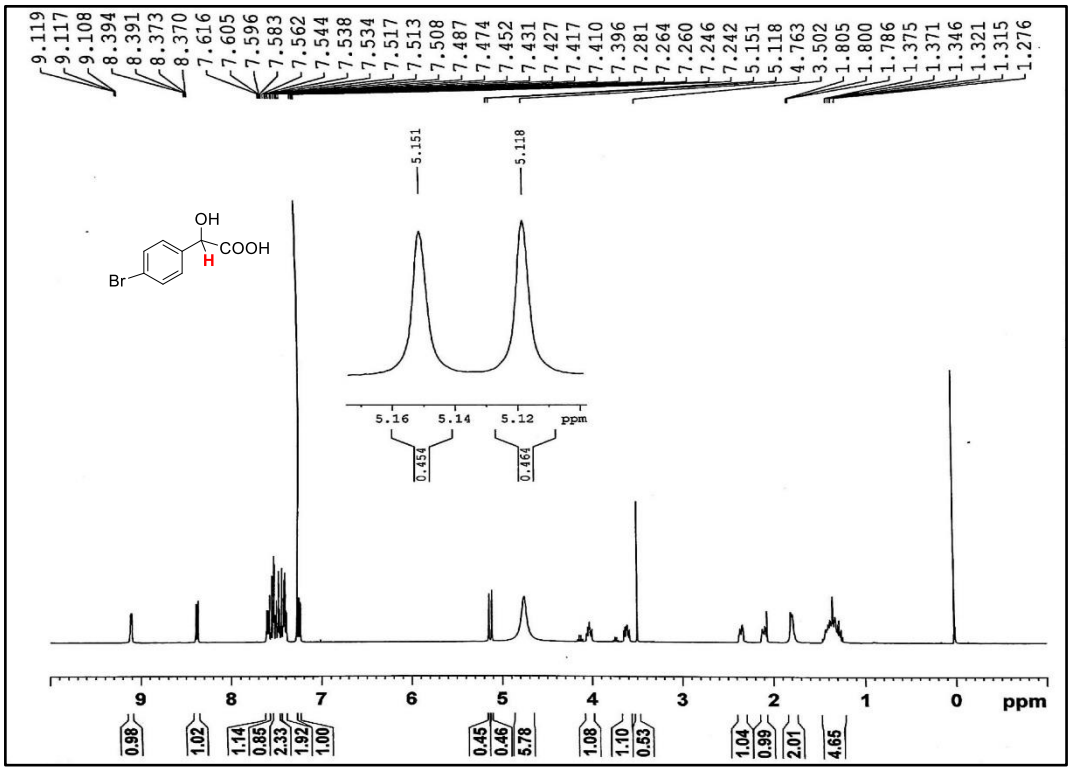

^{1}H NMR Spectra of 4-bromo-mandelic acid (**A-V**) with (*R,R*)-**17**

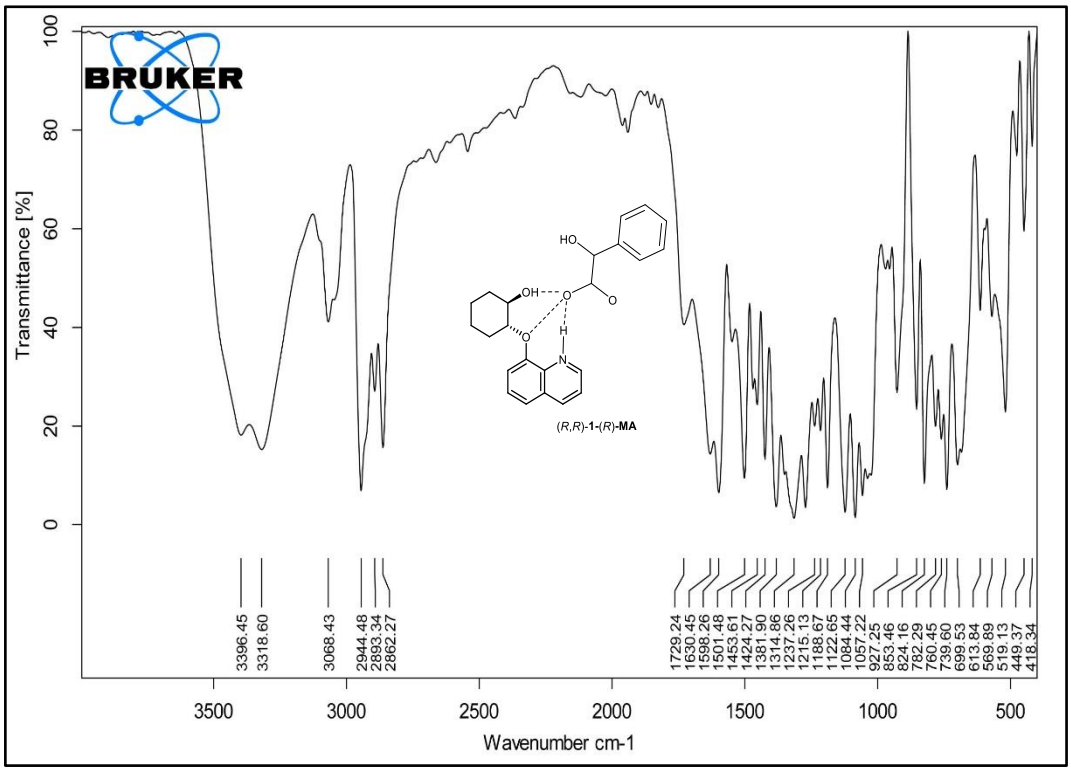

IR Spectra of salt of (*R*,*R*)-**17**-(*R*)-MA

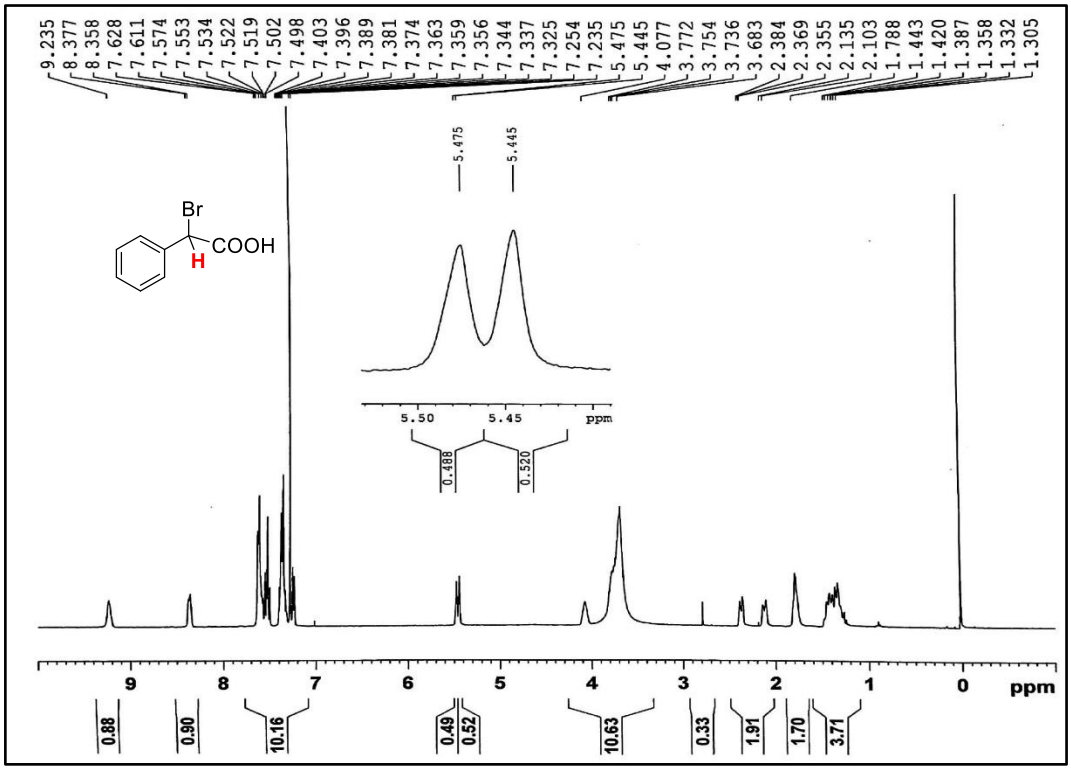

^{1}H NMR Spectra of 2-bromo-2-phenylacetic acid (**B-I**) with (*R*,*R*)-**17**

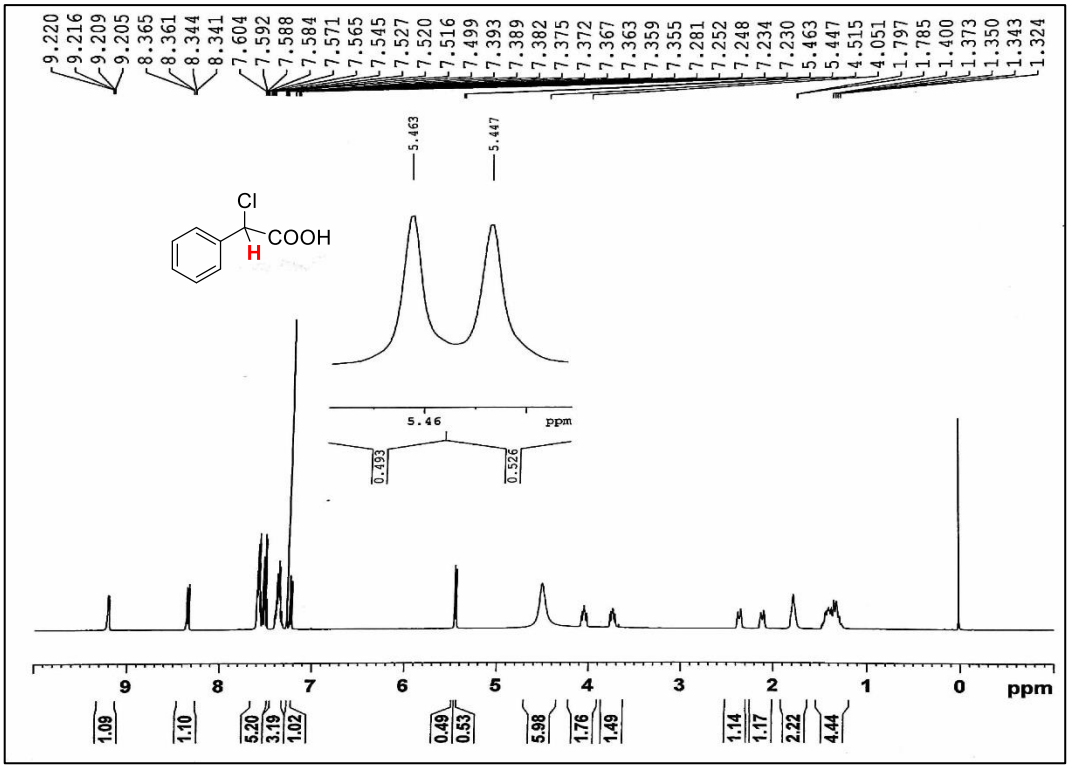

^{1}H NMR Spectra of 2-chloro-2-phenylacetic acid (**B-II**) with (*R,R*)-**17**

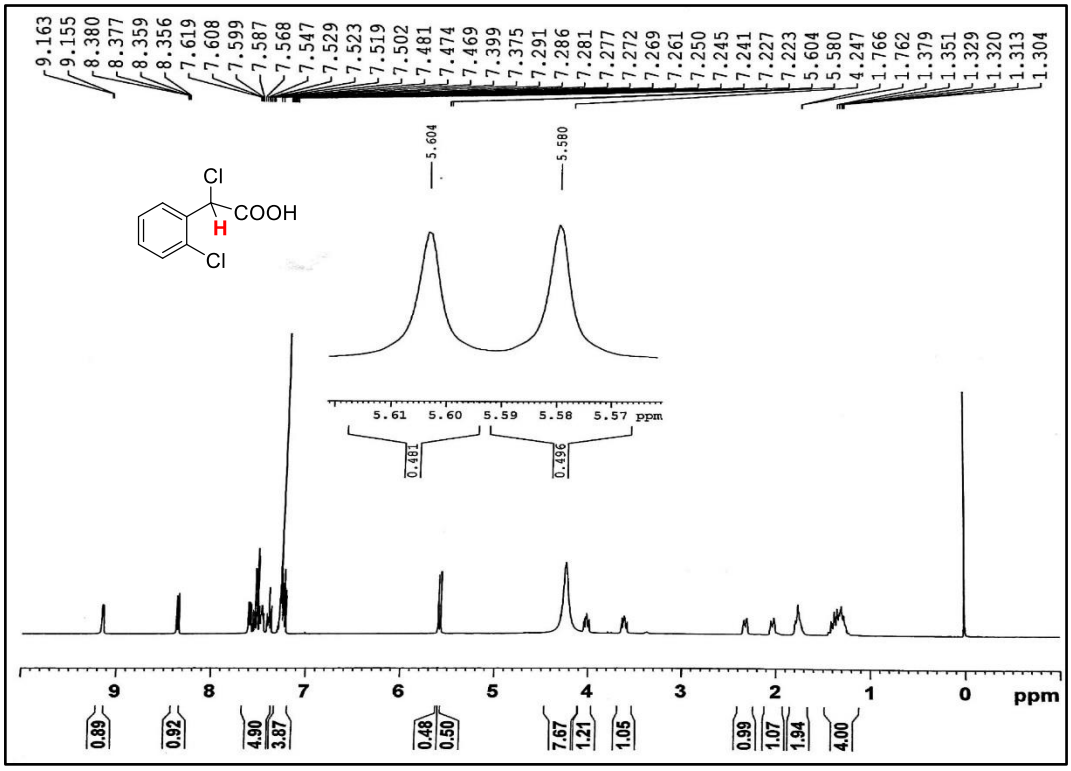

^{1}H NMR Spectra of 2-chloro-2-(2chlorophenyl) acetic acid (**B-III**) with(*R,R*)-**17**

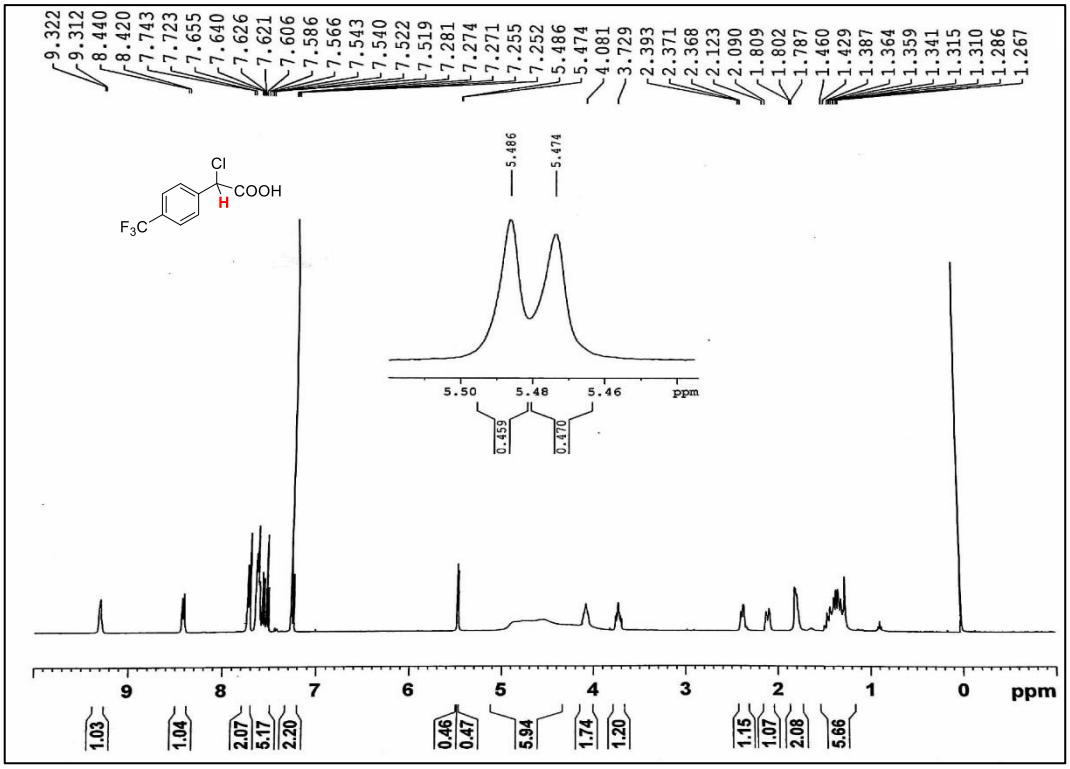

^{1}H NMR Spectra of 2-chloro-2-(4-trifluoromethyl-phenyl)acetic acid (**B-IV**) with (*R*,*R*)-**17**

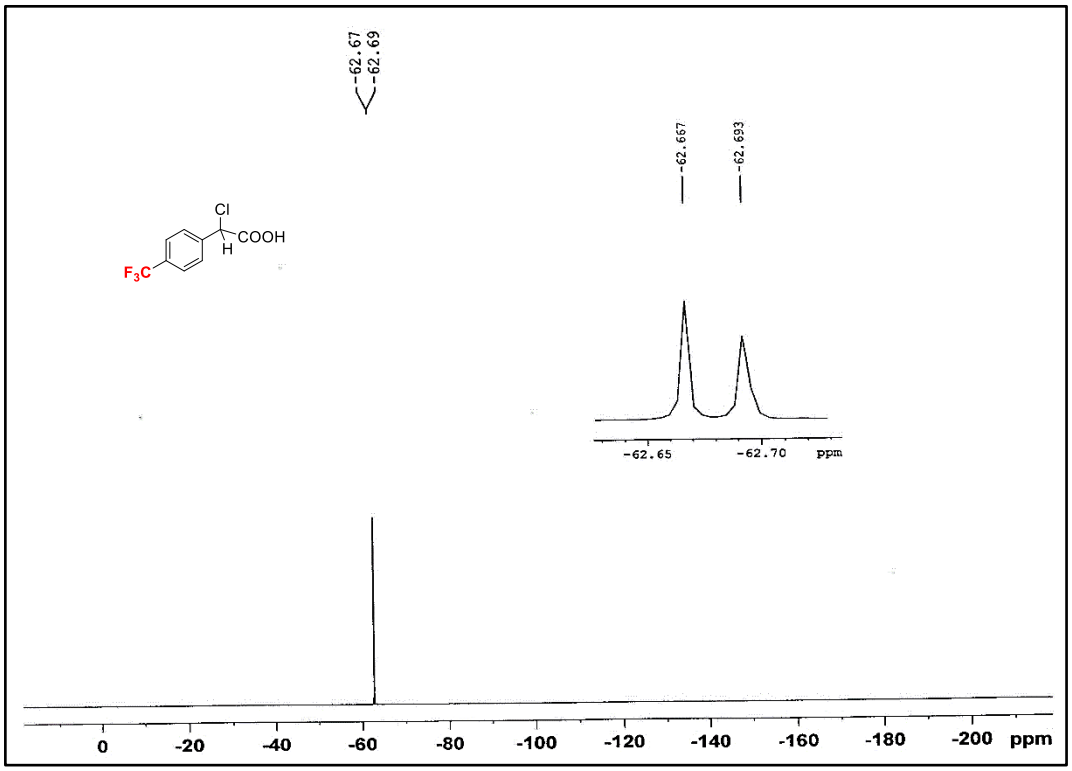

^{19}F NMR Spectra of 2-chloro-2-(4-trifluoromethyl-phenyl)acetic acid (**B-IV**) with (*R*,*R*)-**17**

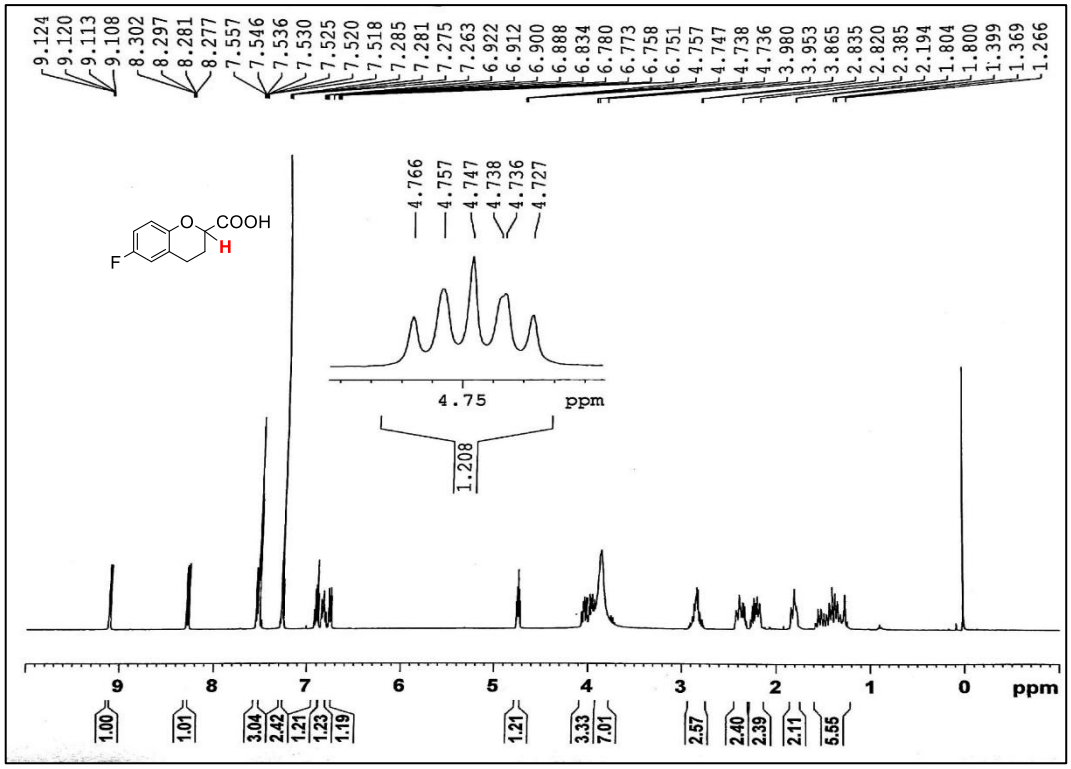

^{1}H NMR Spectra of **C** with (*R*,*R*)-**17**

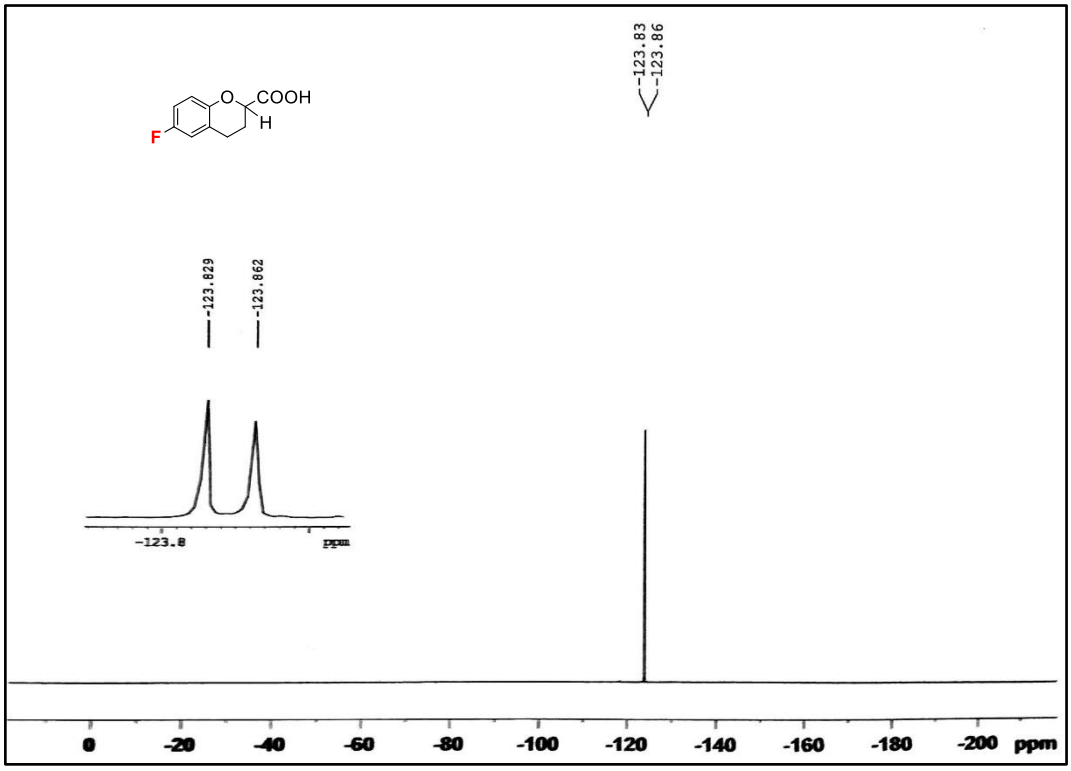

^{19}F NMR Spectra of **C** with (*R*,*R*)-**17**

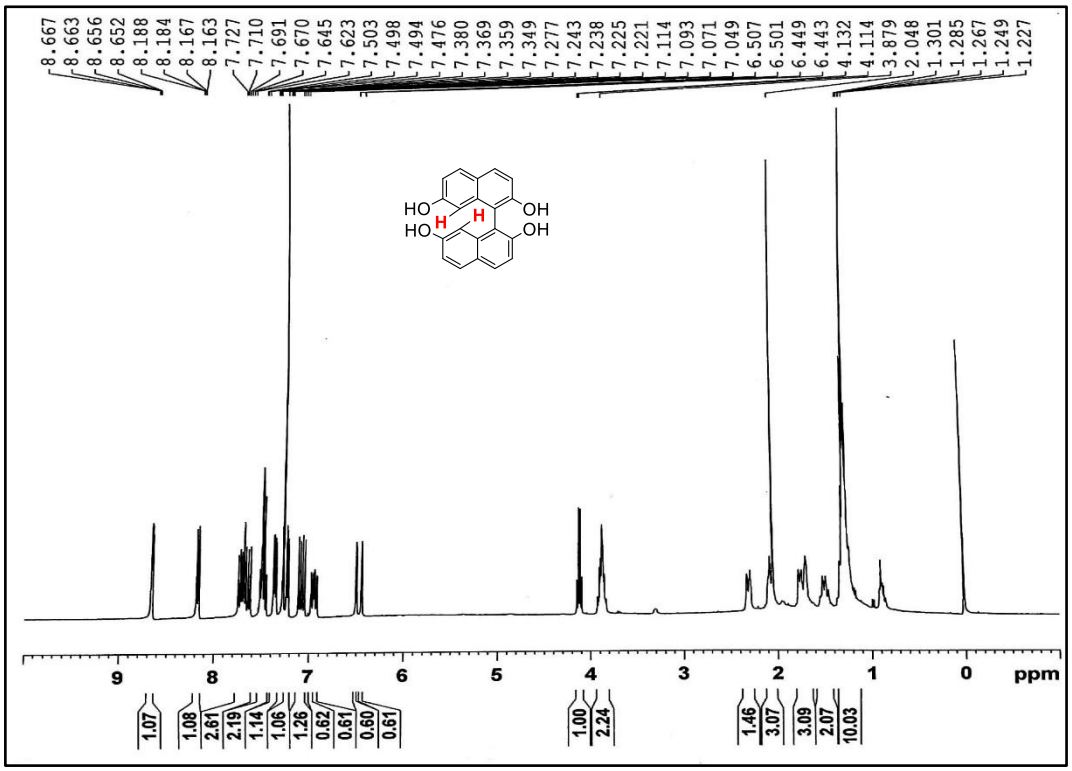

^{1}H NMR Spectra of Tetrol (**D-I**) with (*R*,*R*)-**17**

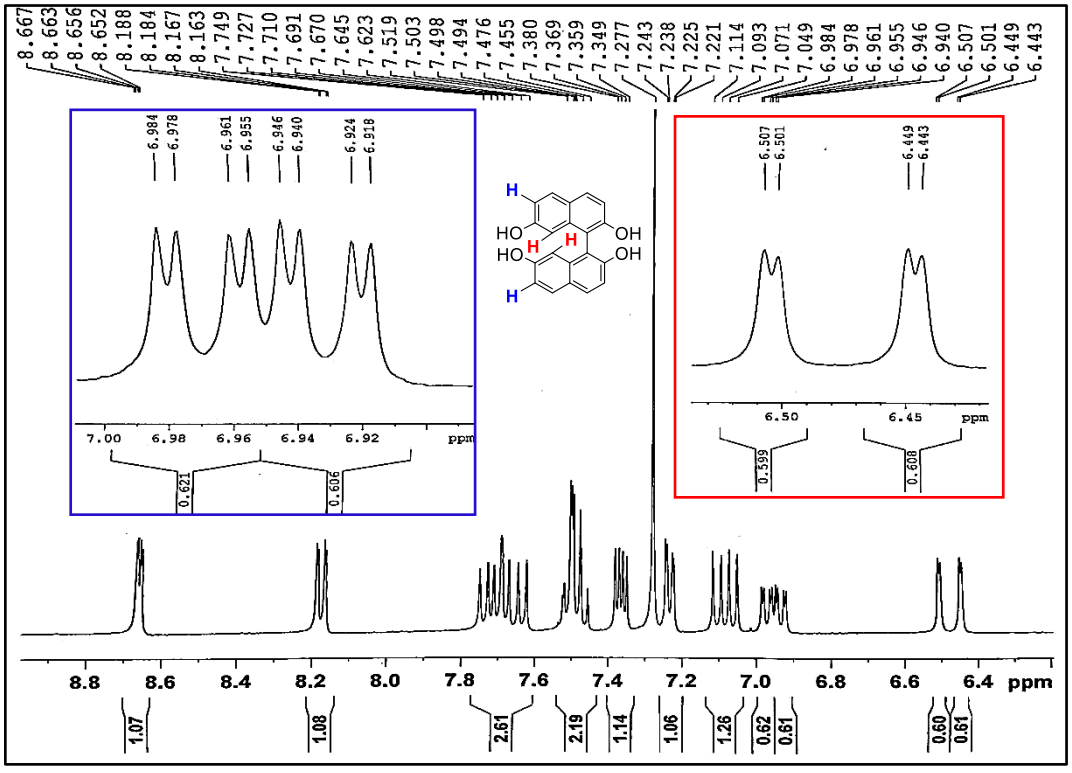

^{1}H NMR enlarged Spectra of Tetrol (**D-I**) with (*R*,*R*)-**17**

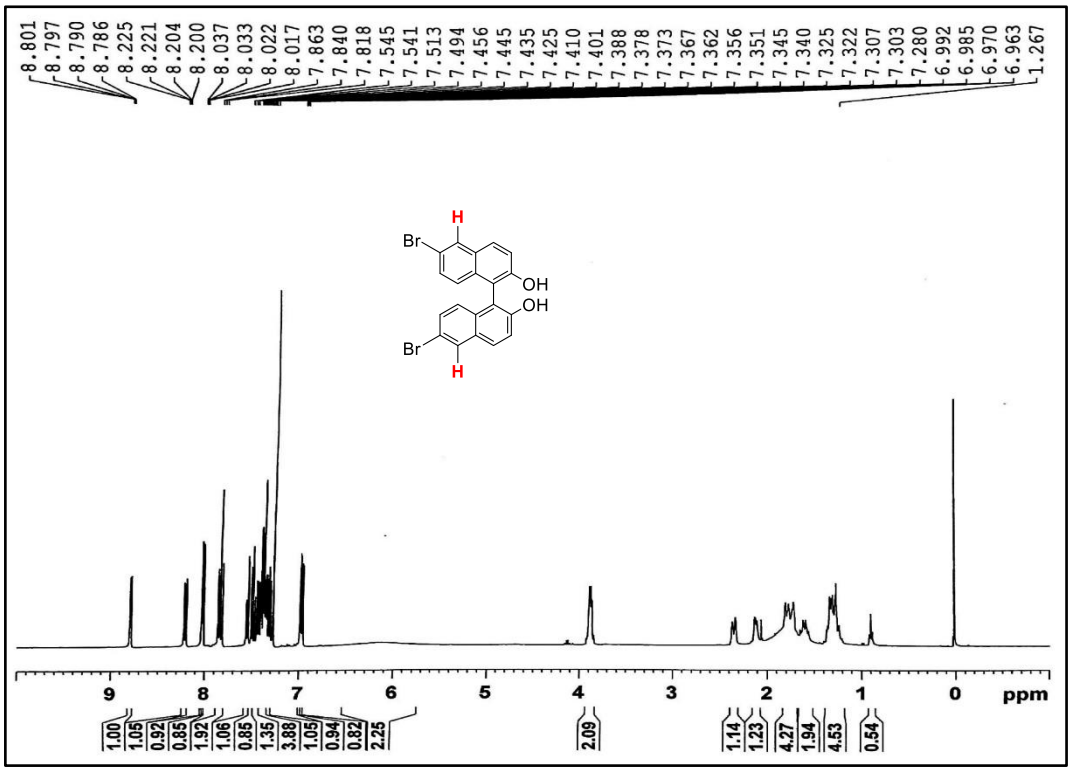

^{1}H NMR Spectra of Dibromo-binol (**D-II**) with (*R*,*R*)-**17**

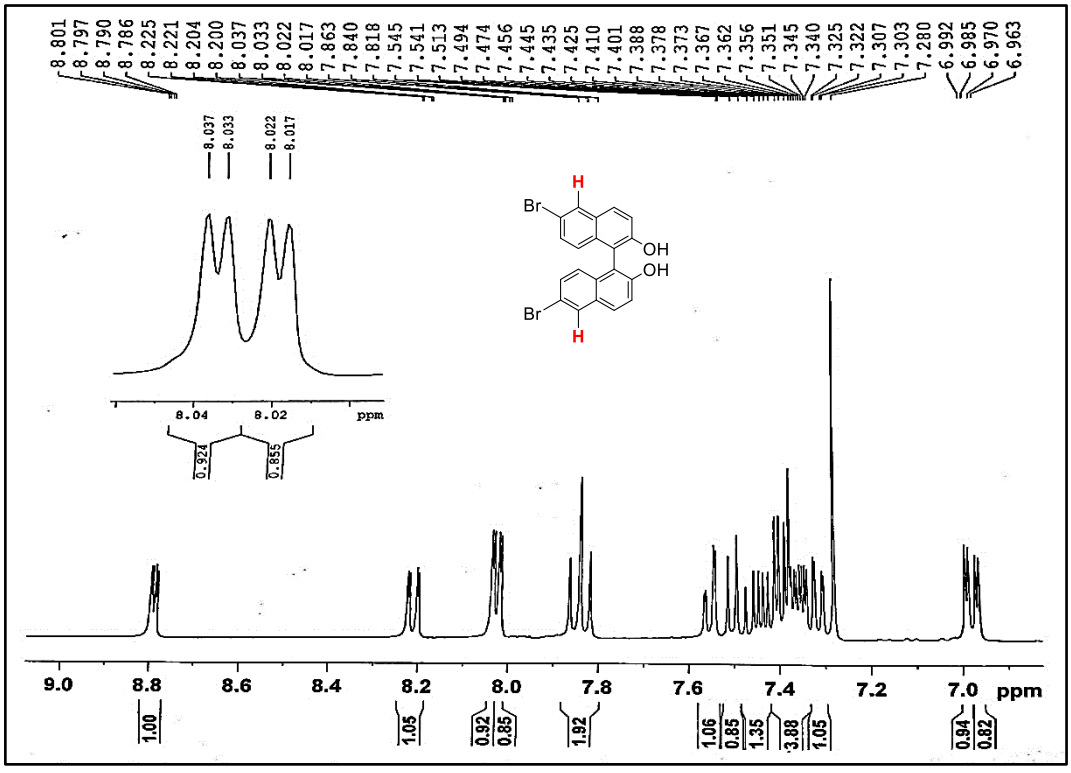

^{1}H NMR enlarged Spectra of Dibromo-binol (**D-II**) with (*R*,*R*)-**17**

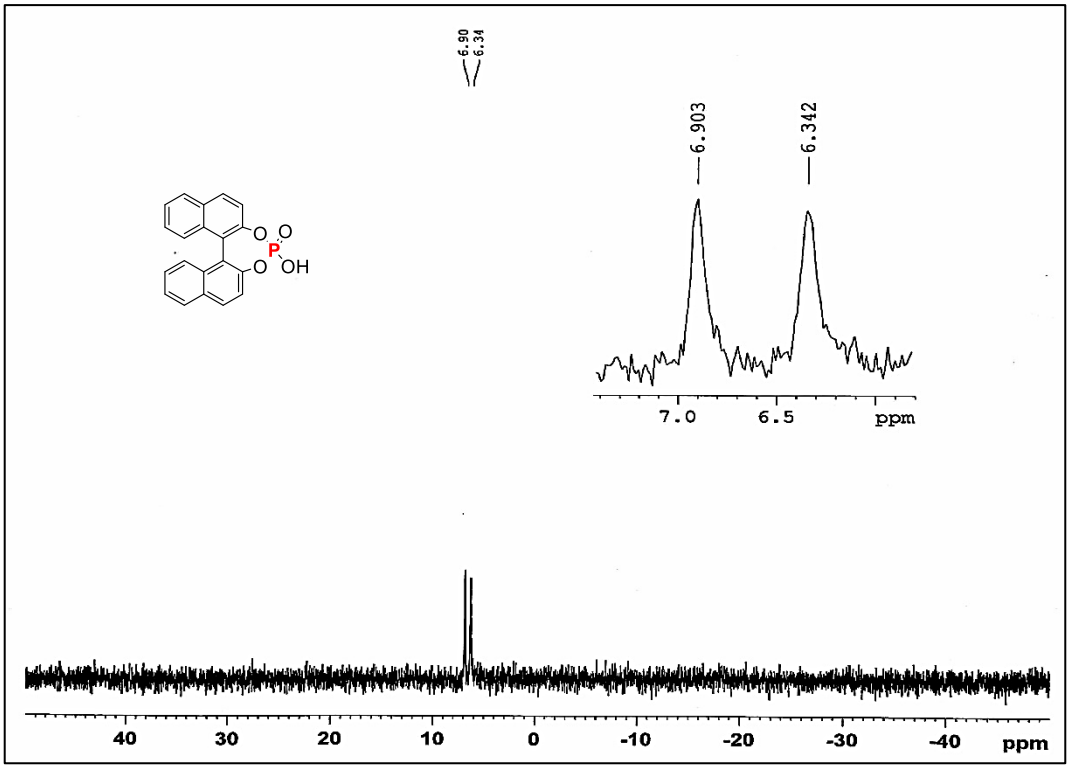

^{31}P NMR Spectra of Binaphthyl phosphoric acid (**E**) with (*R*,*R*)-**17**

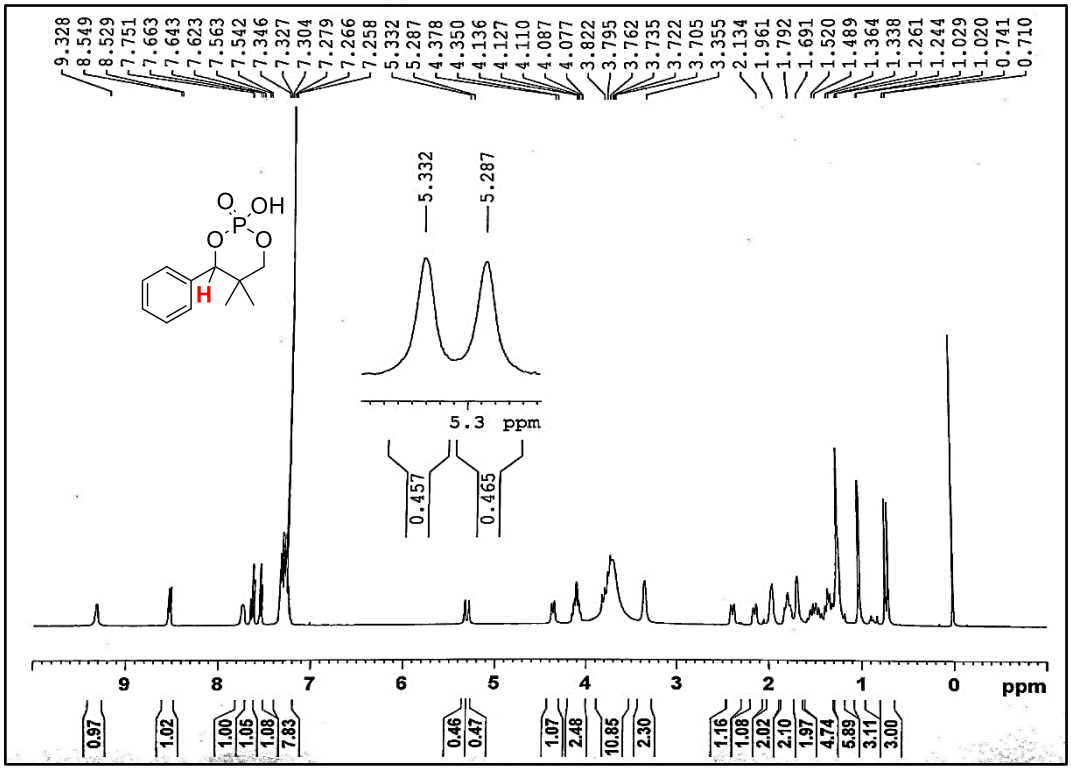

^{1}H NMR Spectra of (**F**-**I**) with (*R*,*R*)-**17**

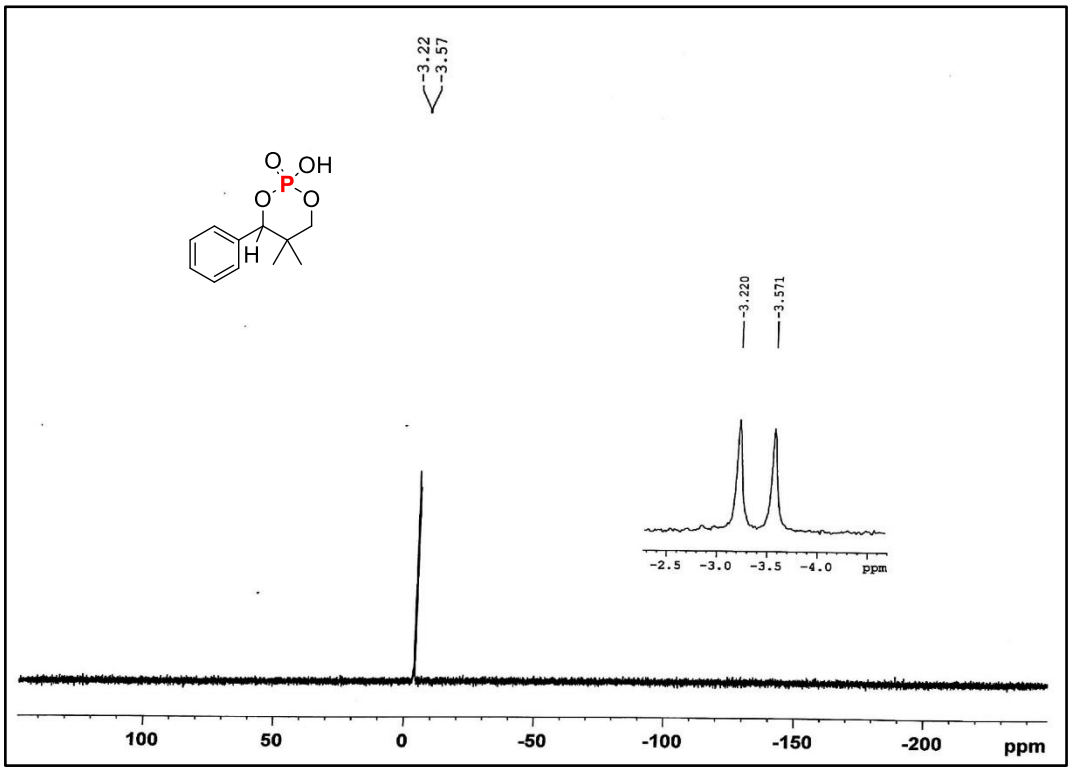

^{31}P NMR Spectra of (**F-I**) with (*R*,*R*)-**17**

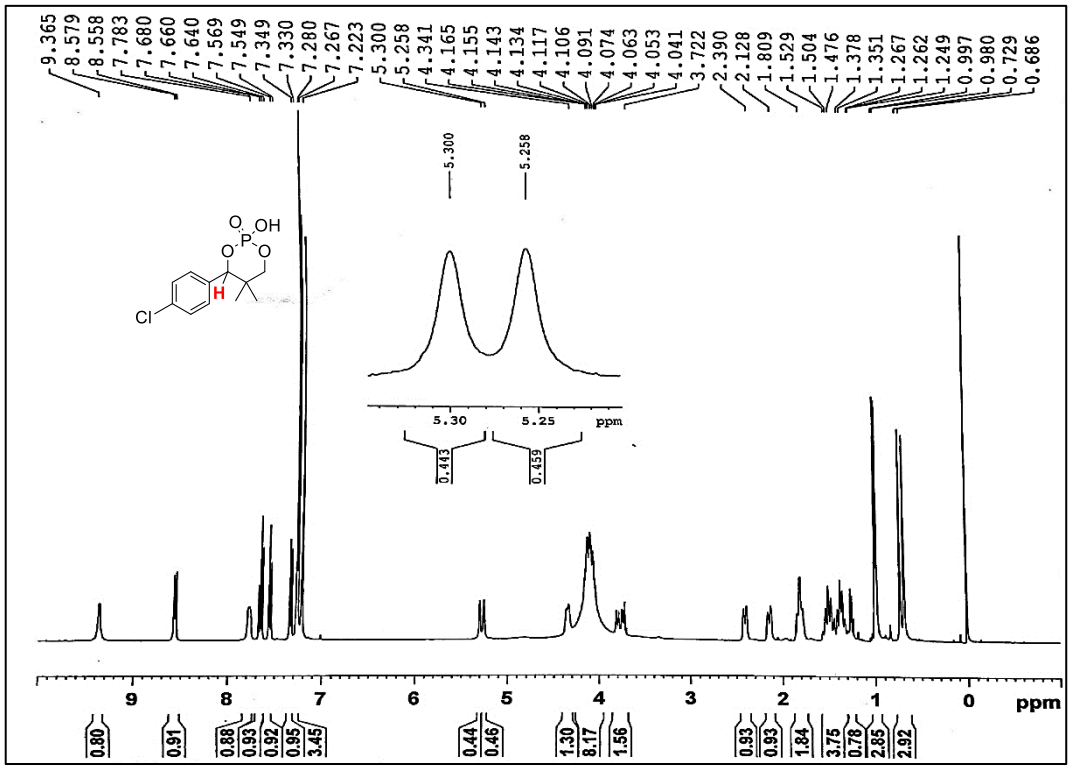

^{1}H NMR Spectra of (**F-II**) with (*R*,*R*)-**17**

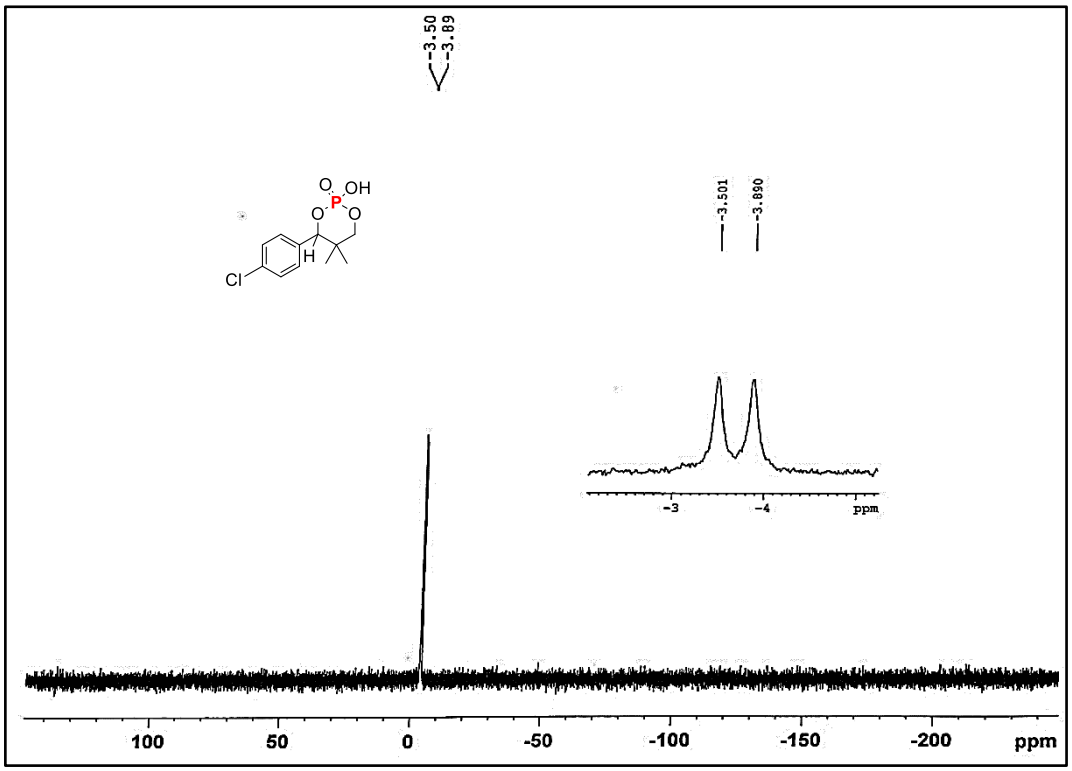

^{31}P NMR Spectra of (**F-I**) with (*R,R*)-**17**

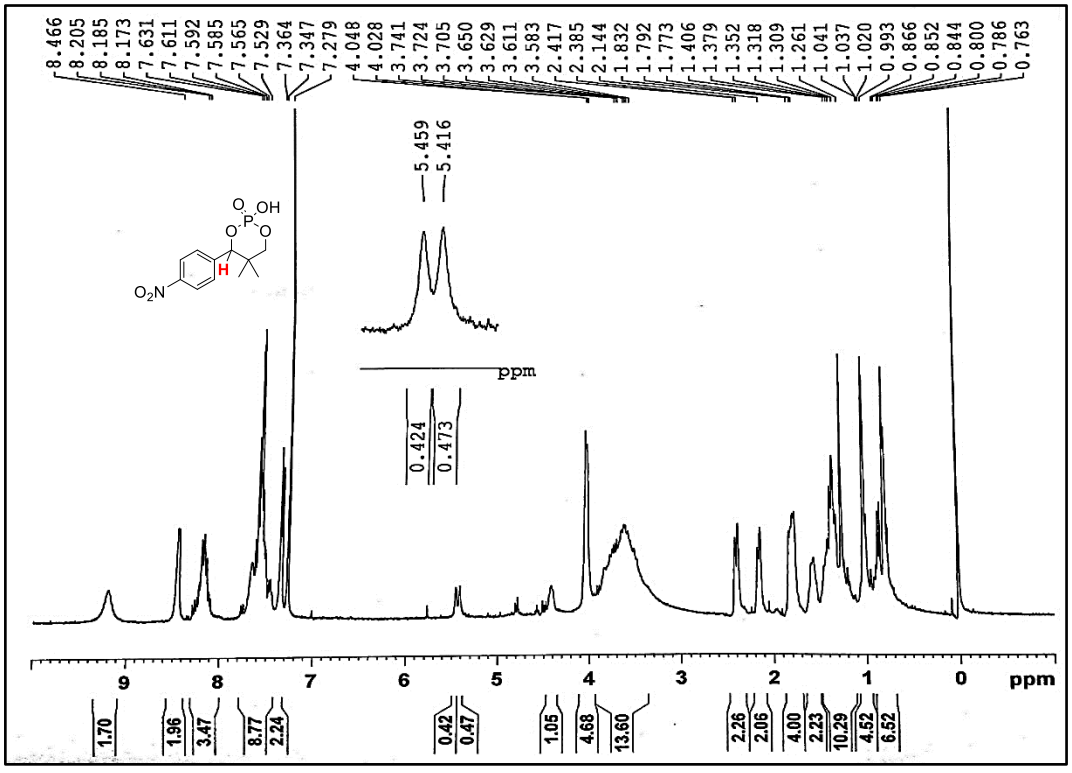

^{1}H NMR Spectra of (**F-III**) with (*R,R*)-**17**

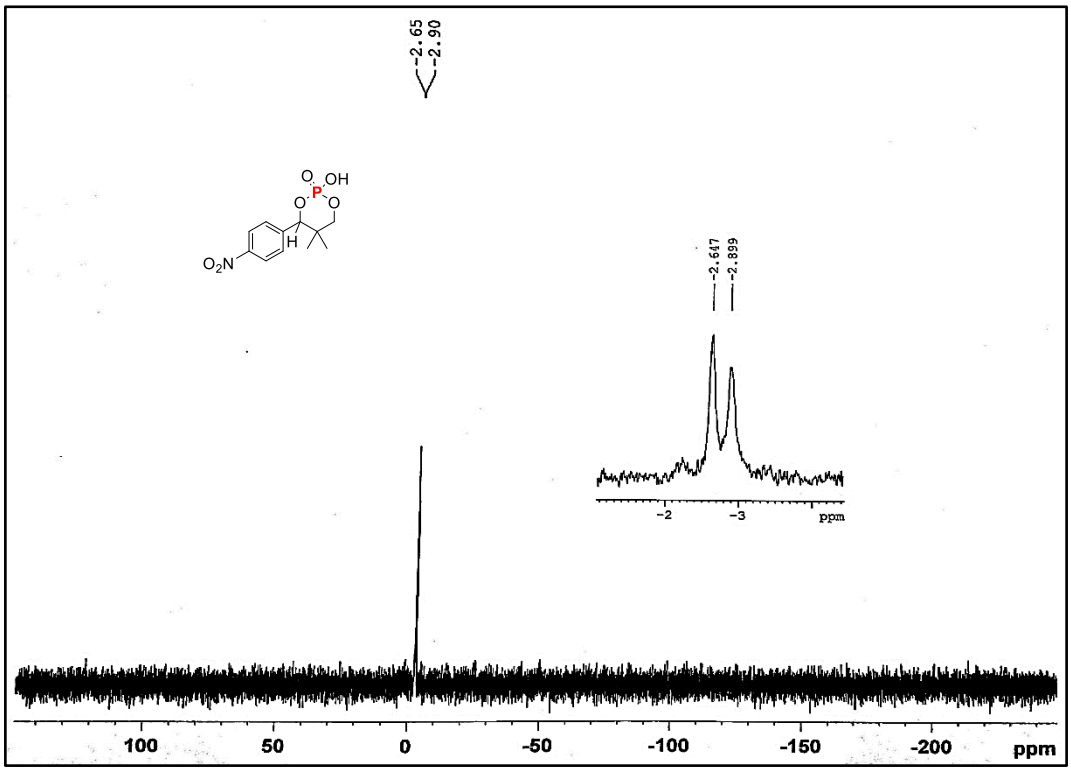

^{31}P NMR Spectra of (**F-III**) with (*R,R*)-**17**

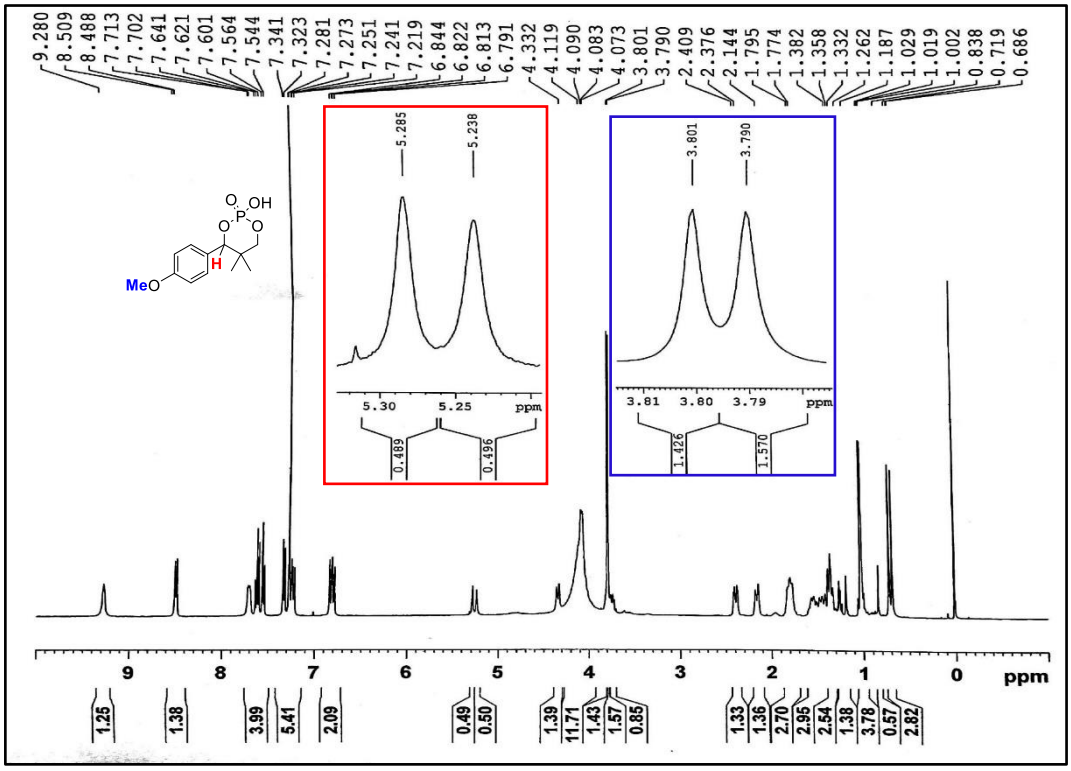

^{1}H NMR Spectra of (**F-IV**) with (*R,R*)-**17**

4.5.3 X-Ray Crystal data

X-ray crystal data for CCDC No 1853115 (*R*,*R*)-**17** and CCDC No 1853116 (*S*,*S*)-**17**

Details	Compound (*R*,*R*)-**17** CCDC-1853115	Compound (*S*,*S*)-**17** CCDC-1853116
Empirical Formula	$C_{15}H_{17}NO_{2.5}$	$C_{15}H_{17}NO_{2.5}$
Formula Weight	504.61	504.61
Temperature	293(2)	293(2)
Wavelength	0.71073A	0.71073A
Crystal system	Orthorhombic	Orthorhombic
Space group	C 222_1	C 222_1
Unit cell dimensions	a = 8.4035(9) Å b = 22.609(2) Å c = 14.0695(18) Å α = 90° β = 90° γ = 90°	a = 8.3581(6) Å b = 22.439(2) Å c = 14.0407(11) Å α = 90° β = 90° γ = 90°
Volume	2673.1	2633.3 (4)
Z	4	4
(Density calculated)	1.2538	1.268
Absorption coefficient(μ)	0.085	0.086
F(000)	1080.5	1072.0
Crystal size	-	-
2θ range for data collection	6.82 to 57.34°	7.58 to140.06°
Reflections collected	8210	3560
Independent reflections	2971[R(int) = 0.0209]	2607[R(int) = 0.0192]
Refinement method	Least Squares minimisation	Least Squares minimization
Data / restraints / Parameters	2971/0/453	2607/0/453
Goodness of fit on F2	1.0419	1.029
Final R indices [I>2sigma(I)]	R1 =0.0396, wR2 = 0.0828	R1 =0.0421, wR2 = 0.091
R indices (all data)	R1 = 0.0531, wR2 = 0.0902	R1 = 0.0584, wR2 = 0.1011
Largest difference peak and hole	0.15/-0.15	0.14/-0.16

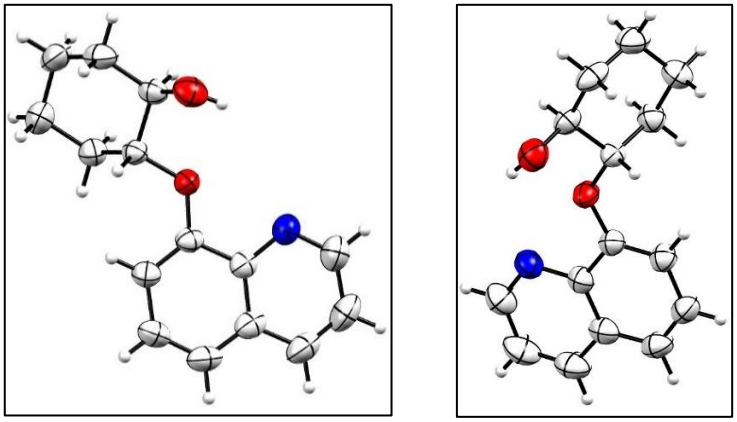

ORTEP diagram of the compound (*R*,*R*)-**17** CCDC-1853115 (left); (*S*,*S*)-**17** CCDC-1853116 (50% probability factor for thermal ellipsoids)

X-ray crystal data for CCDC No 1853111 (*R*,*R*,*R*)-**19**

Details	Compound (*R*,*R*,*R*)-19 CCDC-1853111
Empirical Formula	$C_{25}H_{26}N_2O_4$
Formula Weight	419.48
Temperature	293(2)
Wavelength	0.71073A
Crystal system	Orthorhombic
Space group	P $2_12_12_1$
Unit cell dimensions	a = 8.1390(5) Å b = 15.8253(10) Å c = 17.1850(17) Å α = 90° β = 90° γ = 90°
Volume	2213.5(3)
Z	4
(Density calculated)	1.2587
Absorption coefficient(μ)	0.088
F(000)	888.5
Crystal size	-
2θ range for data collection	6.9 to 57.74°
Reflections collected	13669
Independent reflections	5032[R(int) = 0.0419]
Refinement method	Least Squares minimisation
Data / restraints /Parameters	5032/0/281
Goodness of fit on F2	0.986
Final R indices [I>2sigma(I)]	R1 =0.0546, wR2 = 0.0830
R indices (all data)	R1 = 0.1027, wR2 = 0.0947
Largest difference peak and hole	0.280/-0.30

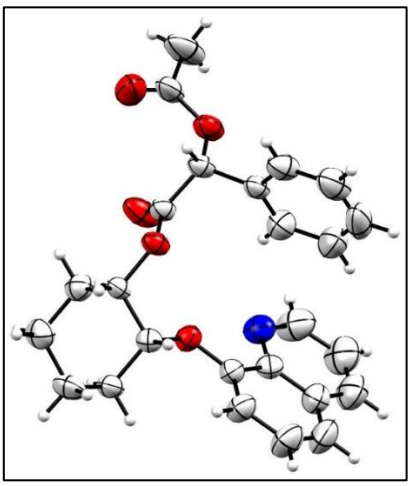

ORTEP diagram of the compound (*R*,*R*,*R*)-**19** CCDC-1853111
(50% probability factor for thermal ellipsoids)

X-ray crystal data for CCDC No 1853111 (*R*,*R*,)-**17**-**(*R*)**-MA

Details	Compound (*R*,*R*)-**17**-(*R*)-MA CCDC-1853113
Empirical Formula	$C_{23}H_{25}NO_5$
Formula Weight	395.44
Temperature	293(2)
Wavelength	0.71073A
Crystal system	Monoclinic
Space group	I2
Unit cell dimensions	a = 10.7133(9) Å b = 12.3487(8) Å c = 15.4466(15) Å $\alpha = 90^o$ $\beta = 98.90^o$ $\gamma = 90^o$
Volume	2018.9(3)
Z	8
(Density calculated)	1.323
Absorption coefficient(μ)	0.092
F(000)	804.0
Crystal size	-
2θ range for data collection	6.92 to 58.08^o
Reflections collected	4426
Independent reflections	3392[R(int) = 0.0419]
Refinement method	Least Squares minimisation
Data / restraints /Parameters	3392/0/281
Goodness of fit on F2	1.016
Final R indices [I>2sigma(I)]	R1 =0.0569, wR2 = 0.1225
R indices (all data)	R1 = 0.0950, wR2 = 0.1495
Largest difference peak and hole	0.17/-0.20

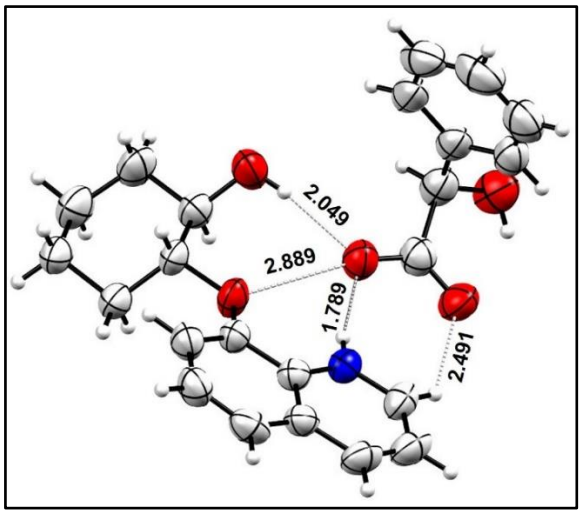

ORTEP diagram of the compound (*R*,*R*,)-**17**-(*R*)-MA
(50% probability factor for thermal ellipsoids) CCDC-1853113

X-ray crystal data for CCDC No (*R*,*R*,)-**23**

Details	Compound (*R*,*R*)-**23** CCDC-1883255
Empirical Formula	$C_{35}H_{39}N_3O_4$
Formula Weight	541.7
Temperature	293(2)
Wavelength	0.71073A
Crystal system	Monoclinic
Space group	$P2_1$
Unit cell dimensions	a = 12.3268(9) Å b = 7.2375(6) Å c = 16.9492(13) Å $\alpha = 90^o$ $\beta = 96.015^o$ $\gamma = 90^o$
Volume	1503.8(2)
Z	2
(Density calculated)	1.1962
Absorption coefficient(μ)	0.079
F(000)	580.3
Crystal size	-
2θ range for data collection	6.54 to 58.02°
Reflections collected	17317
Independent reflections	6857 [R_{int} = 0.0427]
Refinement method	Least Squares minimisation
Data / restraints /Parameters	6857/1/363
Goodness of fit on F2	0.908
Final R indices [I>2sigma(I)]	R_1 = 0.0538, wR_2 = 0.0917
R indices (all data)	R_1 = 0.1061, wR_2 = 0.1047
Largest difference peak and hole	0.31/-0.34

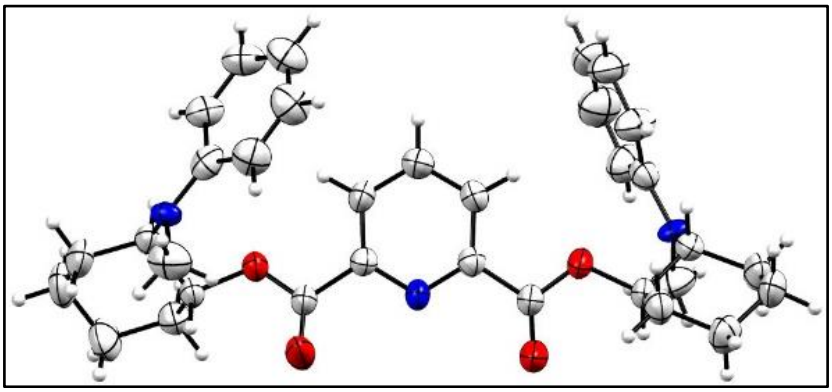

ORTEP diagram of the compound (*R*,*R*,)-**23**
(50% probability factor for thermal ellipsoids) CCDC-1883255

4.5.4 UV and Fluorescence Spectras

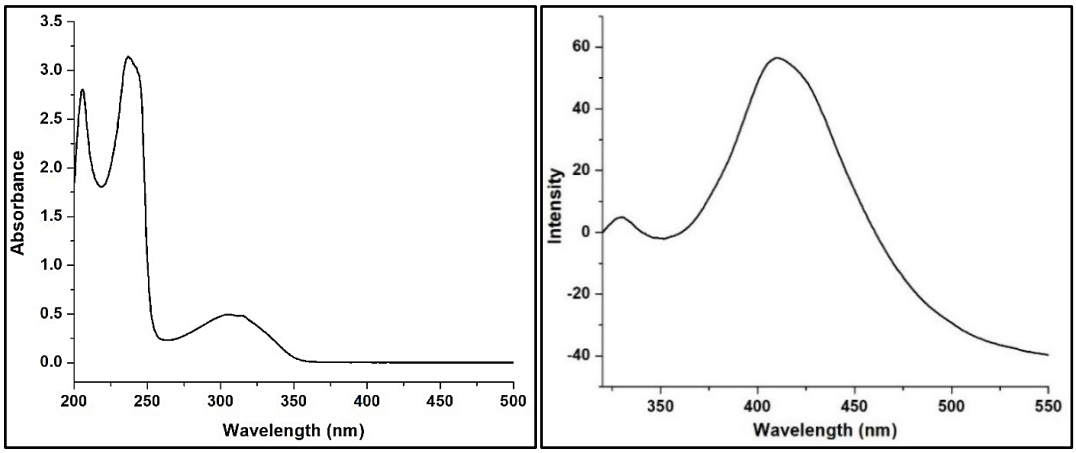

UV-vis Spectra of (*R*,*R*)-**17**(1x10^{-5} M) (left); Fluorescence Spectra of (*R*,*R*)-**17** (1x10^{-5}M)(right)

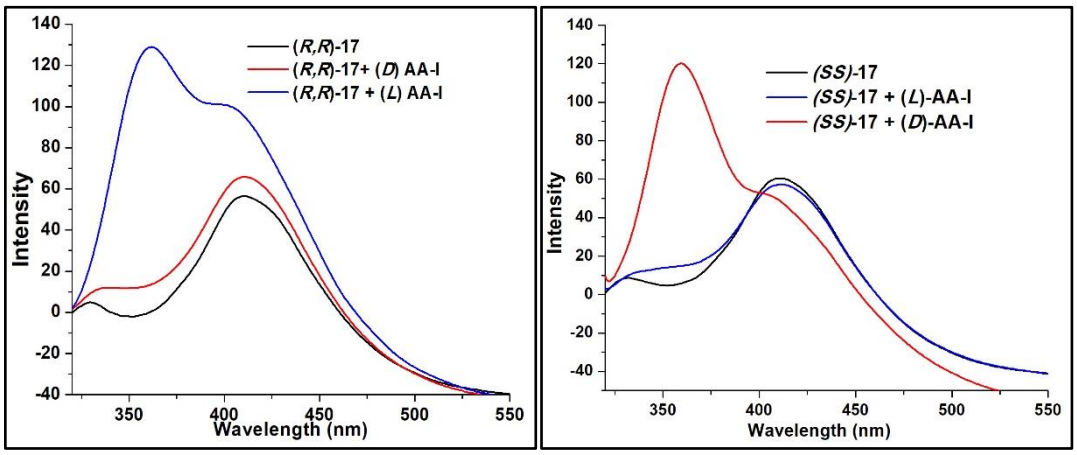

Fluorescence Spectra of **(*R*,*R*)-17** (1 x 10^{-5} M), **(*D*)-AA-I** and **(*L*)-AA-I** (1 x 10^{-3}M) in presence of (*R*,*R*)-**17** in EtOH (λ_{ex} = 300 nm); (left) Fluorescence Spectra of (*S*,*S*)-**17** (1 x10^{-5} M)), **(*D*)-AA-I** and **(*L*)-AA-I** (1 x 10^{-3}M) in presence of (*S*,*S*)-**17** in EtOH (λ_{ex} = 300 nm) (right).

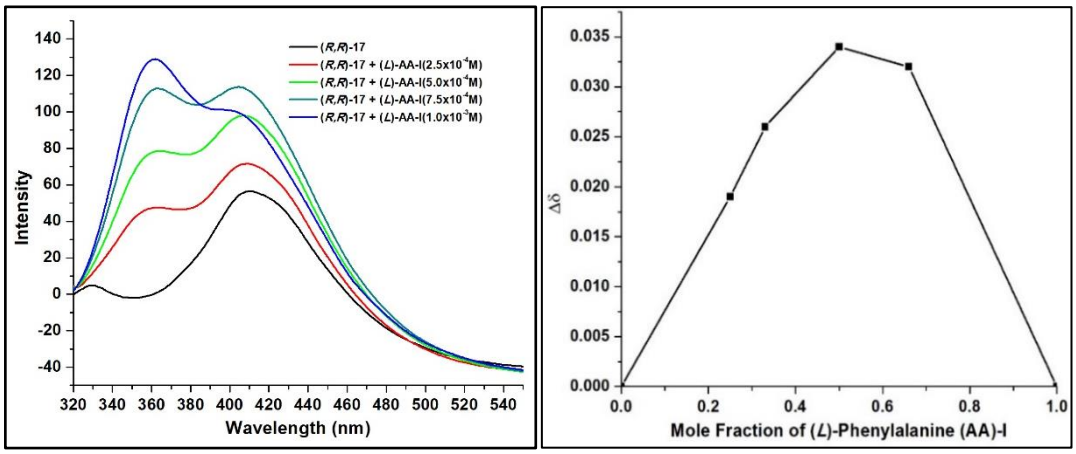

Fluorescence Spectra of (*R*,*R*)-**17** (1 x10^{-5} M) with increasing concentration of **(*L*)-AA-I**; (left) Job's Plot: NMR titration of (*R*,*R*)-17 with **(*L*)-AA-I** (right) in CD_3OD (20 mM conc.) (right).

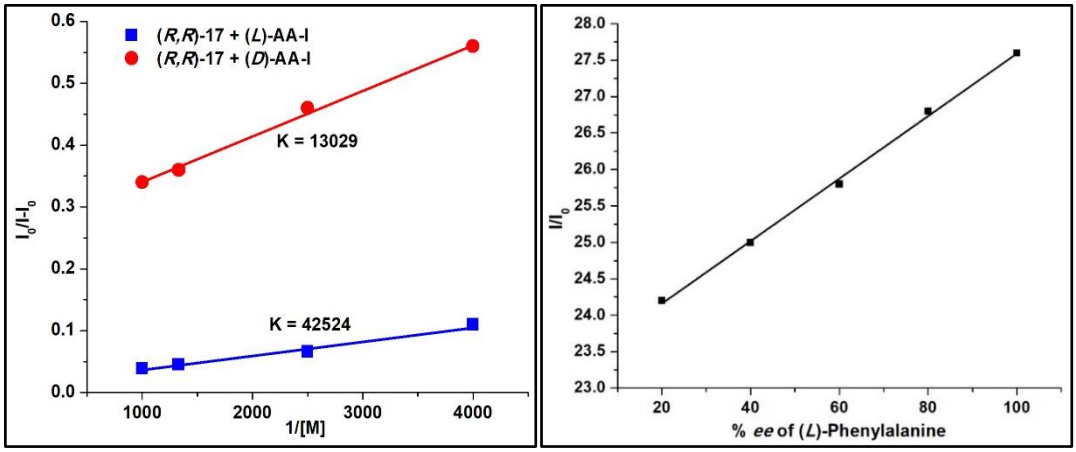

a) Benesi-Hildebrand plot of (*R*,*R*)-**17** (1.0 x 10^{-5} M in EtOH) in the presence of (*D*)- and (*L*)-phenyl alanine (**AA-I**) (left) b) Plot of fluorescence response of (*R*,*R*)-**17** (1.0 x 10^{-5} M in EtOH) in the presence of **AA-I** (1.0 x 10^{-3} M in EtOH) with varying *ee* ratio. (right).

The sensor (*R*,*R*)-**17** when treated with enantiomers of phenylglycine (**AA-II**) exhibited similar response as for **AA-I**. The (*L*)-isomer of phenylglycine showed marked fluorescence enhancement while the other enantiomer showed negligible enhancement.

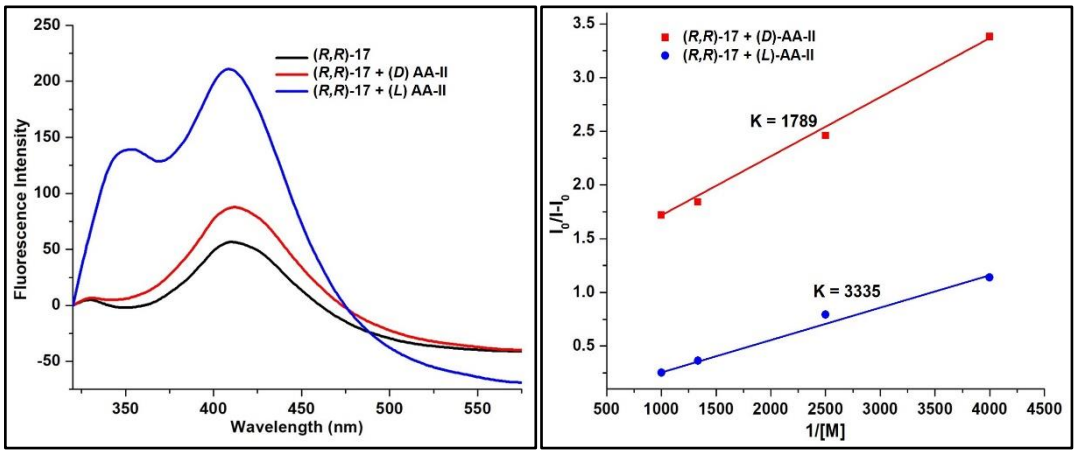

a) Fluorescence Spectra of (*R*,*R*)-**17** (1 x 10^{-5} M), **(*D*)-AA-II** and **(*L*)-AA-II** (1 x 10^{-3} M) in presence of (*R*,*R*)-**17** in EtOH (λ_{ex} = 300 nm); (left) b) Benesi-Hildebrand plot of (*R*,*R*)-**17** (1.0 x 10^{-5} M in EtOH) in the presence of (*D*)- and (*L*)-phenyl glycine (**AA-II**) (right).

The sensor (*R*,*R*)-**17** was then treated with aliphatic amino acid derivative, **AA-III**, where a reverse trend was observed. The (*D*) isomer exhibited greater enhancement on fluorescent signal as compared to (*L*) isomer.

I

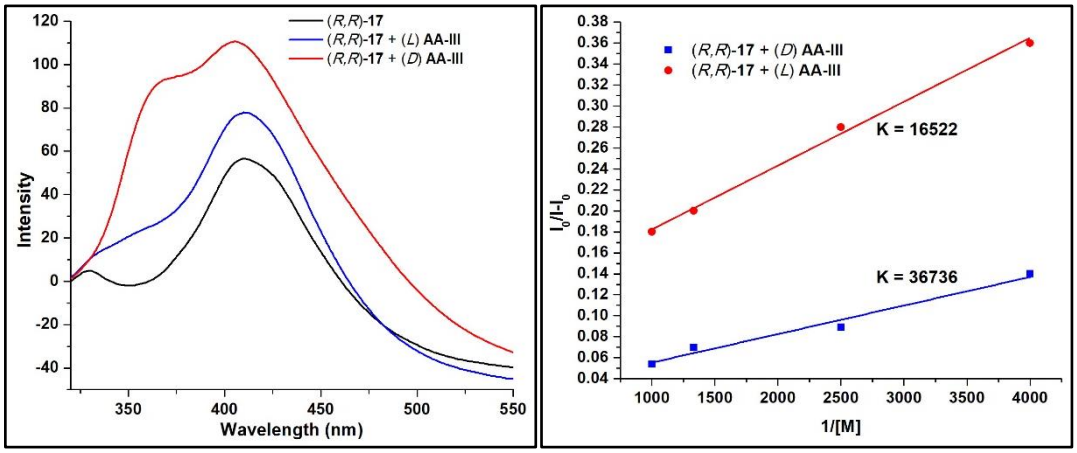

a) Fluorescence Spectra of (*R*,*R*)-**17** (1 x 10^{-5} M), **(*D*)-AA-III** and **(*L*)-AA-III** (1 x 10^{-3} M) in presence of (*R*,*R*)-**17** in EtOH (λ_{ex} = 300 nm); (left) b) Benesi-Hildebrand plot of (*R*,*R*)-**17** (1.0 x 10^{-5} M in EtOH) in the presence of (*D*)- and (*L*)-proline (**AA-III**) (right).

The fluorescence spectra of (R,R)-17 with the enantiomers of valine, showed similar response as for proline. However the enhancement observed in case of valine is much better as compared to proline. The Benesi-Hildebrand also revealed highly enantioselective response.

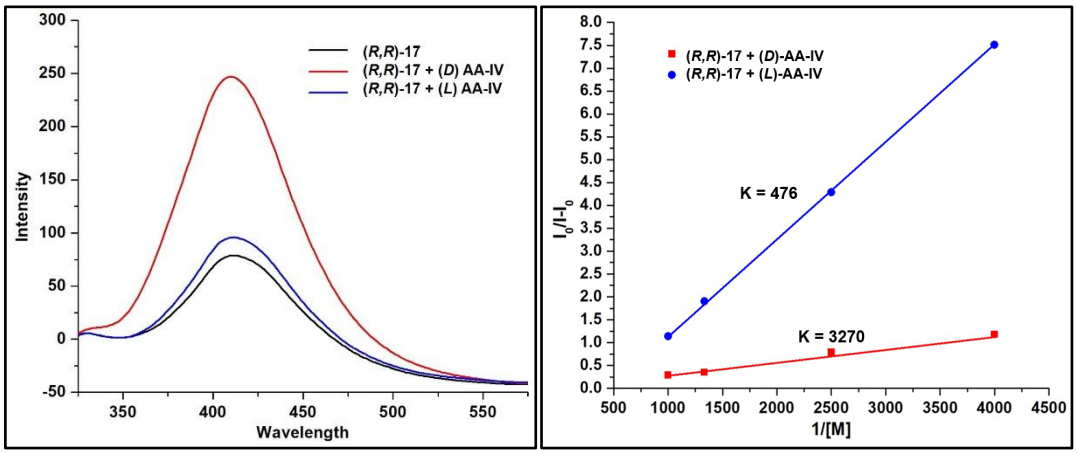

a) Fluorescence Spectra of (*R*,*R*)-**17** (1 x 10^{-5} M), **(*D*)-AA-IV** and **(*L*)-AA-IV** (1 x 10^{-3} M) in presence of (*R*,*R*)-**17** in EtOH (λ_{ex} = 300 nm); (left) b) Benesi-Hildebrand plot of (*R*,*R*)-**17** (1.0 x 10^{-5} M in EtOH) in the presence of (*D*)- and (*L*)-valine (**AA-IV**) (right).

The sensor (*R*,*R*)-17 when treated with dipeptide derivatives showed moderate recognition with increased fluorescence enhancement for (*L*) isomer as compared to (*D*).

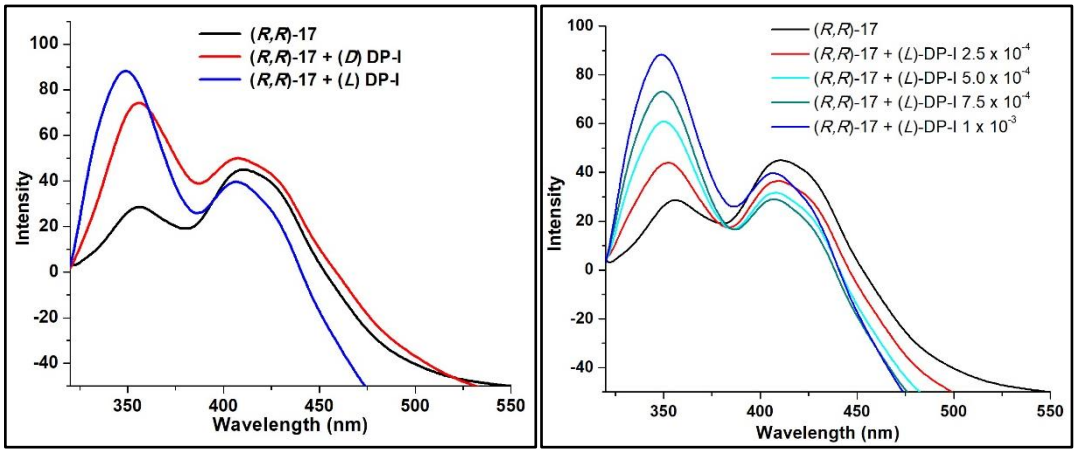

a) Fluorescence Spectra of (*R*,*R*)-**17** (5 x 10^{-6} M), **(*D*)-DP-I** and **(*L*)-DP-I** (1 x 10^{-3}) in presence of (*R*,*R*)-**17** in EtOH (λ_{ex} = 300 nm); (left) b) Fluorescence Spectra of (*R*,*R*)-**17** (1 x 10^{-5} M) with increasing concentration of **(*L*)-DP-I** (right).

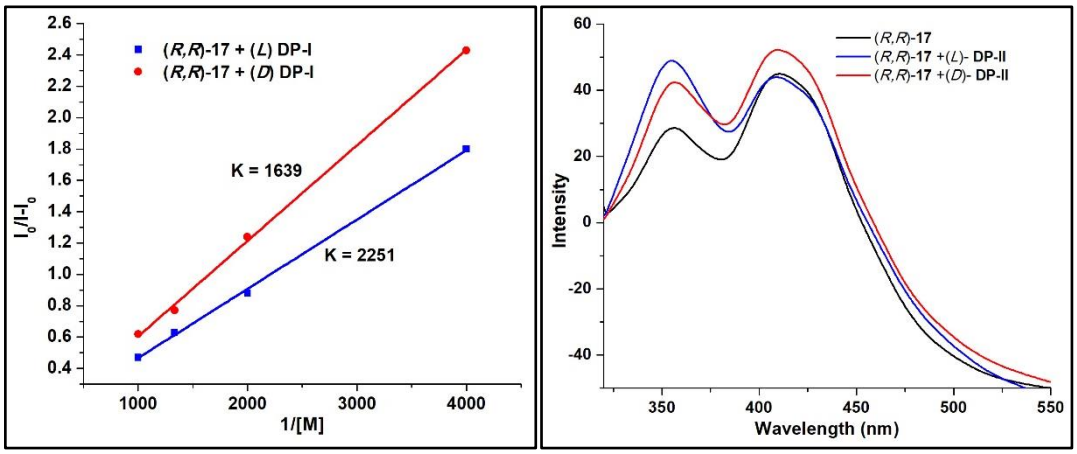

a) Benesi-Hildebrand plot of (*R*,*R*)-**17** (1.0 x 10^{-5} M in EtOH) in the presence of (*D*)- and (*L*)-**DP-I**; (left) b) Fluorescence Spectra of (*R*,*R*)-**17** (5 x 10^{-6} M), **(*D*)-DP-II** and **(*L*)-DP-II** (1 x 10^{-3} M) in presence of (*R*,*R*)-**17** in EtOH (λ_{ex} = 300 nm) (right).

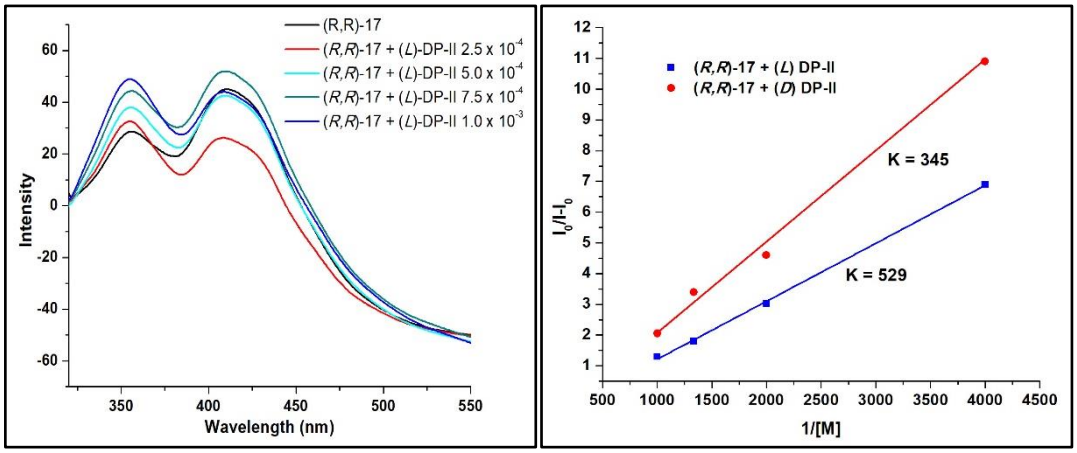

a) Fluorescence Spectra of (*R*,*R*)-**17** (1 x 10^{-5} M) with increasing concentration of **(*L*)-DP-II** (left); b) Benesi-Hildebrand plot of (*R*,*R*)-**17** (1.0 x 10^{-5} M in EtOH) in the presence of (*D*)- and (*L*)-**DP-II**; (right)

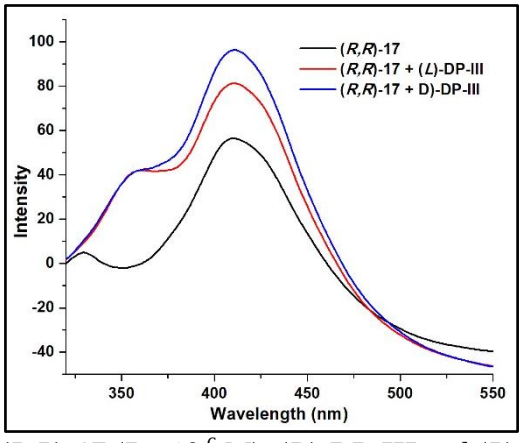

Fluorescence Spectra of (*R*,*R*)-**17** (5 x 10^{-6} M), **(*D*)-DP-III** and **(*L*)-DP-III** (1 x 10^{-3}M) in presence of (*R*,*R*)-**17** in EtOH (λ_{ex} = 300 nm)

4.6 References

1. Pirkle, W.H.; Liu, Y. *J. Chromatogr. A* **1996**, *736*, 31.
2. (a) Guo, J.; Wu, J.; Siuzdak, G.; Finn, M.G. *Angew. Chem.. Int. Ed*. **1999**, *38*, 1755. (b) Reetz, M.T.; Becker, M.H.; Klein, H.-W.; Stockigt, D. *Angew. Chem.. Int. Ed*. **1999**, *38*, 1758. (c) Markert, C.; Pfaltz, A. *Angew. Chem.. Int. Ed*. **2004**, *43*, 2498 (d) Yu, X.; Yao, Z.-P. *Anal. Chim. Acta* **2017**, *968*, 1.
3. (a) Reetz, M.T.; Zonta, A.; Schimossek, K.; Liebeton, K.; Jaeger, K.E. *Angew. Chem., Int. Ed*. **1997**, *36*, 2830. (b) Reetz, M.T.; Becker, M.H.; Kuhling, K.M.; Holzwarth, A. *Angew. Chem., Int. Ed*. **1998**, *37*, 2647.
4. (a) Ding, K.; Shii, A.; Mikami, K. *Angew. Chem.. Int. Ed*. **1999**, *38*, 497. (b) Reetz, M.T.; Kuhling, D.A.; Hinrichs, H.; Belder, D. *Angew. Chem.. Int. Ed*. **2000**, *39*, 3891. (c) Nieto, S.; Dragna, J.M.; Anslyn, E.V. *Chem. Eur. J*. **2010**, *16*, 227. (d) Ghosn, M.W.; Wolf, C. *J. Am. Chem. Soc*. **2009**, *131*, 16360. (e) Schmid, M.G. *J. Chromatogr. A* **2012**, *1267*, 10.
5. Matsushita, M.; Yoshida, K.; Yamamoto, N.; Wirsching, P.; Lerner, R.A.; Janda, K.D. *Angew. Chem., Int. Ed*. **2003**, *42*, 5984.
6. Mccreary, M.D.; Lewis, D.W.; Wernick, D.L.; Whiteside, G.M. *J. Am. Chem. Soc*. **1974**, *96*, 1038.
7. (a) Jacobus, J.; Raban, M.; Mislow, K. *J. Org. Chem*. **1968**, *33*, 1142. (b) Dale, J.A.; Dull, D.L.; Mosher, H.S. *J. Org. Chem*. **1969**, *34*, 2543. (c) Anderson, R.C.; Shapiro, M.J. *J. Org. Chem.* **1984**, *49*, 1304. (d) Alexakis, A.; Chauvin, A.-S.; *Tetrahedron: Asymmetry* **2001**, *12*, 1411. (e) Rodriguez-Escrich, S.; Popa, D.; Jimeno, C.; Vidal-Ferran, A.; Pericas, M.A. *Org. Lett.* **2005**, *7*, 3829. (f) Reiner, T.; Naraschewski, F.N.; Eppinger, J. *Tetrahedron: Asymmetry* **2009**, *20*, 362. (g) Wenzel, T.J.; Chisholm, C.D. *Chirality* **2011**, *23*, 190.
8. (a) Pirkle, W.H. *J. Am. Chem. Soc*. **1966**, *88*, 1837. (b) Fulwood, R.; Parker, D. *J. Chem. Soc., Perkin Trans. 2,* **1994**, 57. (c) Bilz, A.; Stork, T.; Helmchem, G. Tetrahedron: Asymmetry 1997, 8, 3999. (d) Wenzel, T.J.; Amanoo, E.P.; Shariff, S.S.; Aniagyei, S.E. *Tetrahedron: Asymmetry* **2003**, *14*, 3099. (e) Lovely, A.E.; Wenzel, T.J. *J. Org. Chem*. **2006**, *71*, 9178. (f) Yang, X.; Wang, G.; Zhong, C.; Wu, X.; Fu, E. *Tetrahedron: Asymmetry* **2006**, *17*, 916. (g) Ema, T.; Tanida, D.; Sakai, T. *J. Am. Chem. Soc*. **2007**, *129*, 10591. (h) Ma, F.; Ai, L.; Shen, X.; Zhang, C. *Org. Lett*. **2007**, *9*, 125. (i) Peña, C.; Gonzáles-Sabín, J.; Alfonso, I.; Rebolledo, F.; Gotor, V. *Tetrahedron*, **2008**, *64*, 7709. (j) Periasamy, M.; Dalai, M.; Padmaja, M.

J. Chem. Sci., **2010**, *122*, 561. (k) Pal, I.; Chaudhari, S.R.; Suryaprakash, N. *New J. Chem*. **2014**, *38*, 4908. (l) Tanaka, K.; Iwashita, T.; Sasaki, C.; Takahashi, H. *Tetrahedron: Asymmetry* **2014**, *25*, 602.

9. (a) Eelkema, R.; van Delden, R.A.; Feringa, B.L. *Angew. Chem. Int. Ed.* **2004**, *43*, 5013. (c) Zhu, L.; Anslyn, E.V. *J. Am. Chem. Soc.* **2004**, *126*, 3676. (d) Mei, X.; Wolf, C. *Chem. Commun.* **2004**, 2078. (e) Folmer-Andersen, J.F.; Lynch, V.M.; Anslyn, E.V. *J. Am. Chem. Soc*. **2005**, *127*, 7986. (f) Tumambac, G.E.; Wolf, C. *Org. Lett*. **2005**, *7*, 4045. (g) Mei, X.; Wolf, C. *J. Am. Chem. Soc*. **2006**, *128*, 13326. (h) Upadhyay, S.P.; Pissurlenkar, R.R.S.; Coutinho, E.C.; Karnik, A.V. *J. Org. Chem*. **2007**, *72*, 5709. (i) Leung, D.; Anslyn, E.V. *J. Am. Chem. Soc*. **2008**, *130*, 12328.
10. (a) Mei, X.; Wolf, C.; *J. Am. Chem. Soc*. **2004**, *126*, 14736. (b) Li, Z.-B.; Lin, J.; Pu, L. *Angew. Chem*. **2005**, *117*, 1718. (c) Li, Z. -B.; Lin, J.; Sabat, M.; Hyacinth, M.; Pu, L. *J. Org. Chem.* **2007**, *72*, 4905. (d) Costero, A. M.; Colera, M.; Gaviña, P.; Gil, S.; Kubinyi, M.; Pál, K.; Kalláy, M. *Tetrahedron*, **2008**, *64*, 3217. (e) Dhara, K.; Sarkar, K.; Roy, P.; Nandi, M.; Bhaumik, A.; Banerjee, P. *Tetrahedron* **2008**, *64*, 3153. (f) Yang, X.; Liu, X.; Shen, K.; Fu,Y.; Zhang, M.; Zhu, C.; Cheng, Y. *Org. Biomol. Chem.*, **2011**, *9*, 6011. (g) Song, F.; Wei, G.; Wang, L.; Jiao, J.; Cheng, Y.; Zhu, C. *J. Org. Chem.* **2012**, *77*, 4759. (h) Akdeniz, A.; Mosca, L.; Minami, T.; Anzenbacher, P. *Chem. Commun*. **2015**, *51*, 5770. (i) Wang, C.; Wu, E.; Wu, X.; Xu, X.; Zhang, G.; Pu, L. *J. Am. Chem. Soc*. **2015**, *137*, 3747. (j) Akdeniz, A.; Minami, T.; Watanabe, S.; Yokoyama, M.; Ema, T.; Anzenbacher, P. *Chem. Sci*. **2016**, *7*, 2016.
11. (a) Pu, L. *Chem. Rev*. **2004**, *104*, 1687. (b) Pu, L. *Acc. Chem. Res.* **2012**, *45*, 150. (c) Zhang, X.; Yin, J.; Yoon, J. *Chem. Rev*. **2014**, *114*, 4918.
12. Bardez, E.; Devol, I.; Larrey, B.; Valeur, B. J. Phys. Chem. B **1997**, *101*, 7786.
13. Faber, K.; *Biotransformations in organic chemistry*, Springer-Verlag, Berlin, Heidelberg, 6th edn.2011.
14. (a) Jain, N.; Mandal, M.B.; Bedekar, A.V. *Tetrahedron* **2014**, *70*, 4343. (b) Jain, N.; Patel, R.B.; Bedekar, A.V. *RSC Adv*. **2015**, *5*, 45943. (c) Gupta, R.; Gonnade, R.G.; Bedekar, A.V. *J. Org. Chem.* **2016**, *81*, 7384. (d) Jain, N.; Khanvilkar, A.N.; Sahoo, S.; Bedekar, A.V. *Tetrahedron* **2018**, *74*, 68.

15. The carbonyl stretching shifted from 1716 cm^{-1} of **A-I** to 1630 and 1598 cm^{-1} on salt formation with (*R*,*R*)-**1**. Durmaz, M.; Yilmaz, M. Sirit, A. *Org. Biomol. Chem*. **2011**, *9*, 571.
16. Veverka, A.; Nuzum, D.S.; Jolly, J.L. *Ann. Pharmacother*. **2006**, *40*, 1353.
17. (a) Brunel, J.M. *Chem. Rev.* **2005**, *105*, 857. (b) Akiyama, T. *Chem. Rev*. **2007**, *107*, 5744.
18. Takaya, T.; Kishida, Y.; Sakakibara, S. *J. Chromatogr*. **1981**, *215*, 279.
19. (a) He, X.; Cui, X.; Li, M.; Lin, L.; Liu, X.; Feng, X. *Tetrahedron Lett*. **2009**, *50*, 5853. (b) Yang, X.; Shen, K.; Liu, X.; Zhu, C.; Cheng, Y. *Tetrahedron Lett.* **2011**, *52*, 4611. (c) Wang, F.; Nandhakumar, R.; Hu, Y.; Kim, D.; Kim, K.M.; Yoon, J. *J. Org. Chem*. **2013**, *78*, 11571.
20. a) Mei, X.; Wolf, C. *J. Am. Chem. Soc.* **2006**, *128*, 13326. (b) Zhang, Y.; Hu, F.; Wang, B.; Zhang, X.; Liu, C. *Sensors* **2015**, *15*, 10723. (c) Zeng, C.; Zhang, X.; Pu, L. *Chem. Eur. J.* **2017**, *23*, 2432.
21. Lin, J.; Zhang, H. -C.; Pu, L. *Org. Lett.* **2002**, *4*, 3297.
22. Ojida, A.; Sakamoto, T.; Inoue, M.; Fujishima, S.; Lippens, G.; Hamachi, I. *J. Am. Chem. Soc.* **2009**, *131*, 6543.
23. Sekar, G.; Singh, V. K. *J. Org. Chem.*, **1999**, *64*, 287.
24. (a) Yamashita, H. *Chem. Lett.*, **1987**, 525. (b) Yamashita, H. *Bull. Chem. Soc. Jap.*, **1988**, *61*, 1213. (c) Sekar, G.; Kamble, R. M.; Singh, V. K., *Tetrahedron: Asymmetry* **1999**, *10*, 3663.